NORTHWESTERN UNIVERSITY

Sensory Substitution in the Presence of Vision: Providing Joint Speed Feedback to Improve Myoelectric Prosthesis Control and Adaptation

A DISSERTATION

SUBMITTED TO THE GRADUATE SCHOOL

IN PARTIAL FULFILLMENT OF THE REQUIREMENTS

for the degree

DOCTOR OF PHILOSOPHY

Field of Biomedical Engineering

By Eric Joseph Earley

EVANSTON, ILLINOIS

MARCH 2020

Unless otherwise noted, the work contained within this dissertation is licensed under a

Creative Commons Attribution 4.0 International (CC BY 4.0)

license.

© Copyright by Eric J. Earley 2020

Some Rights Reserved

The work contained within Appendix C is adapted from a preprint by

Drs. Dan Blustein and Jon Sensinger.

© Copyright by Dan Blustein 2020

All Rights Reserved

Abstract

Sensory Substitution in the Presence of Vision: Providing Joint Speed Feedback to Improve Myoelectric Prosthesis Control and Adaptation

Eric J. Earley

Maneuvering your limbs requires both accurate commands for how to move, and accurate feedback of their true movements. Conventional prosthetic arms currently lack this sense of proprioceptive feedback, which can make daily tasks difficult without close visual monitoring. Although studies have successfully provided artificial proprioceptive feedback to improve control, this benefit is only consistent when devices are out of view. When sight of the prosthesis is unobstructed, improvements are inconsistent across studies. A potential explanation is that vision may provide more precise proprioceptive information than artificial feedback; thus, artificial feedback may not significantly improve one's understanding of their prosthesis movements if visual feedback is present.

In this thesis, I studied human vision to better understand how well it estimates different aspects of biomimetic movements, such as endpoint and joint speeds in stationary and moving reference frames. Through a series of psychophysics experiments, I found that distal joint speed measured relative to proximal joints (e.g. elbow speed in relation to a moving shoulder) is perceived with high uncertainty. I then developed a sensory substitution system using audio feedback to supplement vision and reduce this joint speed uncertainty. In virtual center-out reaching tasks emulating a myoelectric prosthesis, I demonstrated that non-amputee subjects achieved lower baseline errors when the dynamics of the arm were perturbed if provided joint speed feedback.

These results were more pronounced for transradial amputee subjects, who demonstrated lower reaching errors with audio feedback in the presence and absence of perturbations.

These results suggest that the availability and precision of intact senses is a crucial factor when developing sensory feedback for prosthetic arms. When intact senses are considered alongside other aspects of the task, we may be able to develop reliable sensory feedback systems for prosthesis users to improve proprioception and the ability to complete everyday tasks.

Acknowledgements

Pursuing a PhD has been an incredibly rewarding and fulfilling experience. It is a career that has granted nearly unparalleled freedom and the opportunity to add new insights to the body of collective knowledge. It has allowed me to travel to research conferences throughout the world and meet with some of the smartest people in the field. However, it has also been a difficult journey, one resulting in many long days (especially as I write this!) and sometimes pushing me beyond my limit. There have been several times when I questioned if this was the right path for me. Fortunately, I have found myself surrounded by wonderful people who helped me up and gave me strength. This is not a journey I could have undergone alone, and it would not have been possible without the love and support of so many people who have been a part of my life in one way or another.

Northwestern University hasn't provided a page limit for the acknowledgement section of this thesis, which may have been a mistake on their part. I plan to take full advantage of this oversight.

So get comfortable.

First, thank you to my parents for your unwavering love and dedication throughout my entire life. You have always helped me to do my best and your support as I explored my interests instilled in me my passion for learning. You introduced me to a wide variety of film, music, literature, and more, and kindled my curiosity in the world around me. You were an anchor, always available when I needed you, and I cannot fully express in words my appreciation.

Thank you to my brother for just being an all-around awesome dude. Even when we don't see each other for an entire year, every time we meet up it's as if no time has passed. You have helped me

to push my boundaries and be adventurous in my tastes, and I've become a more well-rounded person as a result. I am extremely grateful for everything you've taught me and for all the weird music recommendations you've given me over the years.

Thank you to my advisor, Dr. Levi Hargrove, for your mentorship and guidance over the years. Working with you has trained me to think critically and to question. You've taught me when to think and plan, and when to act and iterate. You've given me opportunities to explore on my own, to fail, learn, and try again, and I've become a stronger researcher as a result.

Thank you to Drs. Jon Sensinger and Reva Johnson for collaborating with me on this research, and helping to shape it into something that I'm truly proud of. Our meetings together are a highlight of my journey and were irreplaceable in my understanding of what is a complex topic. Your insight has been invaluable, and it has been a great experience working with you.

Thank you to my committee members, Drs. Eric Perreault and Sandro Mussa-Ivaldi, for your valuable feedback on my research. I know my research is also about feedback, which makes it confusing to thank you for your feedback, but… you know what I mean. Your perspectives have been very helpful in understanding my work within the context of the field, and your expertise has been greatly appreciated.

Thank you to all of the students in the Center for Bionic Medicine over the years who have refined my education and helped me work through the roadblocks in my research. Being able to solicit your feedback and bounce ideas off you all has been a huge boon, and I have learned so much from our interactions. Max, Blair, and Nili, in particular – it has been an honor crossing the finish line together with you all!

Thank you to all of the CBM clinicians for teaching me about the patient care side of prosthetics, the engineers for your help with setting up experiments and maintaining our demos, and to all the other members for making my time in the CBM a great experience. You have given me a well-rounded education that I could not have gained from an engineering program alone.

Thank you to the researchers I've met at conferences over the years. Networking with you has undoubtedly enriched my experience during my PhD, and during a time when I wasn't sure if academic research was for me, listening to your passion as you talked about your research inspired me to keep going.

Thank you to everyone who participated in my experiments, which have been described as "the most fun game [they've] ever played." I suspect that sentiment to be hyperbole as admittedly the tasks I was asking you to do were incredibly dull at times. I appreciate you setting aside time to help me during my research and for staying awake during my experiments (aside from the one person who fell asleep – you know who you are).

Thank you to all of the friends I've made at Northwestern who gave me moral support during my PhD. It has been great exploring Chicago, engaging in deep conversation about esoteric topics, and going through the graduate school experience together. I have so many fond memories from these past seven years, and I will be forever grateful for your friendship.

Thank you to my therapist, Darren, for your guidance and coaching over these past few years. From the moment I walked in your door, I knew we were a good fit, and I am thankful for all of the skills you have given me to help me manage my mental health.

Thank you to the Buddhist Temple of Chicago for serving as a sanctuary where I could clear my mind, and thank you to Carlos for leading meditations. Meditation is one of the hardest things I have done, and there is still much to learn, but it is also one of the most valuable skills I can rely on when life seems to move at a mile a minute.

Thank you to Ialel, Lothaar, Rhawen, and Imsh for all of the adventures we went on together. I cherish the fun we had and the camaraderie we forged, but on a personal note it was also a source of personal growth and reflection at a time when I needed it. That wasn't the original intent, but that's what ended up happening, and I'm grateful you were by my side for that journey.

Thank you to everyone I've met and worked with through the Communicating Science Conference. I could not have imagined the impact this organization would have on me when I first attended, and I am extraordinarily fortunate to get to network with so many inspiring and passionate science communicators. You are all doing incredible work, and I am proud to work alongside you.

Finally, thank you to anyone else in my life I might have missed here. Every interaction is an opportunity to make a difference in someone's life, and our interactions have changed my life for the better.

This research was made possible through funding from the National Science Foundation (NSF-NRI 1317379), National Institute of Health (NIH T32 HD07418), and generous philanthropic support of the Regenstein Foundation Center for Bionic Medicine at the Shirley Ryan AbilityLab.

Table of Contents

Summary of Figures

Chapter 1

Chapter 2

Chapter 3

Chapter 4

Appendix A

Appendix B

Appendix C

Summary of Tables

Chapter 1

Chapter 3

Chapter 4

Appendix A

Appendix C

1. Introduction

1.1. Motivation

In preparation for a long and self-referential day of dissertation writing, a man presses his hand against the decorated glass door of his favorite local coffee shop and pushes inwards. The door swings open and elicits an electronic chime to signify the entrance of a customer. He steps inside, taking care to lift his feet higher than normal to avoid tripping on the singular step from the sidewalk to the tiled shop floor. Navigating the twisting and turning queueing, the man approaches the counter and, after a brief and cheerful exchange with the barista, places his order. He reaches into his back pocket, undoes the button holding his wallet in place, and extracts it, opening the leather pouch and sliding a card out from its slot. Deftly rotating the credit card in his fingers, he inserts the electronic chip into the credit card interface. After tipping the barista and illegibly signing what appears to be his name, he removes the card and undoes the sequence of events, returning the wallet to his back pocket. Transaction complete, he sits down at a well-lit table abutting a window and pulls out his laptop. As his fingers follow a pre-programmed pattern, committed to memory, of 16 random non-sequential characters containing at least one lower-case letter, upper-case letter, number, and special character, he accidentally misses one of the keys. Even before fully cognizant of his error, he has hit backspace and continued typing the password. His computer starts up, and he opens his dissertation to resume his work. A few minutes in, a server comes by and sets down a coffee and saucer on the table next to his laptop. The man reaches towards the cup without looking, fingers feeling for the handle before hooking on and bringing the vessel to his face. He briefly admires the artistic flourishes poured through the foam floating atop his beverage before indulging a sip. Hot, strong, with a mild bitterness and pleasant berry notes,

the coffee invigorates him as he sets down the cup on its saucer and continues his work with renewed fervor.

The inattentiveness with which many people perform mundane tasks conceals their hidden complexity. Even the simplest of actions, such as sipping of a cup of coffee, comprises numerous steps, each requiring precise manipulation of bodily joints. In the above example, the man reaches for his coffee while preoccupied with his dissertation. He thus relies on the memory of the coffee's location and maneuvers his hand there, coordinating his elbow and shoulder joints such that his hand hovers just above the table surface. Once his fingertips contact the hot ceramic, his movement adjusts to trace the cup's circumference and wrap around the handle. He lifts the cup and provides just enough force to move the cup closer to him, while simultaneously regulating his movements to prevent the hot coffee from spilling over his laptop, his fingers providing him constant information about the oscillations of the liquid. As the coffee nears his mouth, he estimates the size of the cup and where his hand must be for the rim of the cup to meet his lips. Upon contact, he gently tilts the cup back, ensuring a slow and steady stream of coffee pours over the rim of the cup. He finally returns the cup to a level orientation and sets the cup back down on the saucer, adjusting to the new weight and inertia of the cup in the process. During each step of this simple activity, efferent neurons issue motor commands derived from the central nervous system, and afferent neurons carry sensory stimuli back to the central nervous system, regulating and modulating future motor commands (Bilodeau and Bilodeau, 1961; Jones, 2000). It is this communication loop that permits us to complete tasks with such ease.

Solely commanding muscles and interpreting sensory cues are insufficient to complete this task. The communication loop is accompanied by corresponding internal models. Forward models

accompanying motor control predict how the limb will respond to motor commands, given its current configuration. By comparison, inverse models accompanying sensory cues predict the motor command responsible for the limb's current movement, given its current configuration (Wolpert, Ghahramani and Jordan, 1995). These concurrent processes allow the man to make minute corrections over the course of the task. The table prevents his hands from moving in a straight line from his lap to the cup, so he avoids hitting the edge of the table while ensuring his hand still takes an efficient path. He must form an estimate of the size, weight, and inertia of the cup before picking it up; if, in lifting the object, he discovers there is a discrepancy between his prior mental estimate and its observed properties acquired from his sensory organs, he must form a new mental estimate by combining the prior and observed estimates.

Clearly, disruption of either path in this communication loop impacts limb control. The loss or disruption of motor control can limit function via unintentional muscle synergies, spasticity, tremor, or other movement disorders. Likewise, the loss or disruption of sensory information can result in a greater reliance on visual monitoring or excessive or exaggerated movements and forces. Furthermore, the simultaneous disruption of both paths compounds these challenges; this is the case for those who use prosthetic limbs.

In 2005 in the United States, an estimated 1.6 million people lived with limb loss, and that number is projected to increase to 2.2 million by 2020, and 3.6 million by 2050 (Ziegler-Graham *et al.*, 2008). Based on trends between 1988 and 1996, over 170,000 amputations are performed each year, and another 970 infants are born annually with congenital limb differences (Dillingham, Pezzin and MacKenzie, 2002). Limb loss can restrict opportunities and participation in education, employment, and physical and recreational activities (Gallagher *et al.*, 2011), and many people

with amputations are unable to return to their previous employment (Fernández, Isusi and Gómez, 2000; Burger, Maver and Marinček, 2007; Hebert and Burger, 2016).

Commonly, individuals with limb loss will employ the use of a myoelectric prosthesis to restore missing function. These prostheses are controlled with surface electromyographic (EMG) signals generated by contracting muscles, and have seen clinical use since the 1970s (Feeny and Hagaeus, 1970; Yamada, Niwa and Uchiyama, 1983; Parker and Scott, 1986). Their control ranges in complexity from simple dual-site amplitude control to employing pattern recognition algorithms to enable intuitive control of multiple prosthetic functions using independent contraction patterns (Hudgins, Parker and Scott, 1993; Englehart and Hudgins, 2003; Kuiken *et al.*, 2009; Li, Schultz and Kuiken, 2010; Khushaba *et al.*, 2012). More recent advancements have extended this myoelectric control to include simultaneous movements (Young *et al.*, 2013; Hahne *et al.*, 2014), though these controllers require a lengthy learning period (Kuiken *et al.*, 2016).

Despite their technical superiority to body-powered prostheses, myoelectric prosthesis abandonment remains a prevalent issue (Biddiss and Chau, 2007). Several factors can lead a person with limb loss to abandon a prosthesis, and these factors vary across prosthesis types (Biddiss, Beaton and Chau, 2007). For myoelectric prosthesis users, these factors include weight, cost, lack of fine motor skills and dexterity, and independent control of available movements. However, one major limitation contributing to the abandonment especially of upper-limb myoelectric prostheses is their lack of sensory feedback; these devices may provide an approximation of the missing motor control, but they do nothing on their own to restore the other half of the communication loop.

The reintroduction of sensory feedback into prosthesis design is not a new concept, dating back to the 1960s (Beeker, During and Den Hertog, 1967; Prior *et al.*, 1976; Childress, 1980).

Furthermore, the term “sensory feedback” describes numerous aspects of sensation, including tactile, pressure, vibration, texture, proprioceptive, or kinesthetic sensation; each sensation provides distinct information applicable in a variety of contexts. Though each sensation has its purpose, this thesis focuses on proprioception – knowledge of the position and configuration of the body – and kinesthesia – knowledge of the movement and speed of the body – and their relation to gross limb movements. The method by which this information is conveyed to subjects also differs across studies. Broadly, these approaches can be categorized as direct feedback – direct stimulation of the nerves or brain – or sensory substitution feedback – conveyance of missing sensory information via alternative intact sensory pathways. The latter – which can take the form of vibration, skin stretch, audio cues, or other modalities – is the focus of this thesis.

Sensory substitution is non-invasive and simple to implement, indeed making it a popular choice for prosthetic feedback. Numerous studies have proposed benefits of sensory substitution systems, yet sensory substitution continues to have no commercial presence. One hypothesis to explain this omission stems from the conditions in which sensory feedback is tested. The benefits of sensory feedback are clear and consistent when subjects are blindfolded, and other sources of information transmission from the prosthesis (e.g. motor vibration and sound) are controlled. However, when subjects can see the task and can rely on these incidental sources of feedback, the benefits of sensory substitution become mixed – some studies show a benefit, and some show negligible differences.

A possible explanation for this dichotomy draws on insights from Bayesian sensory integration. In short, when the brain receives a the same information (e.g. proprioception) from two sources (e.g. vision and sensory substitution), it forms a single estimate by combining the redundant

observations in a statistically optimal fashion (Ernst and Banks, 2002). The information source with lower uncertainty is weighted more favorably in this fusion, while observations with greater uncertainty have less influence on the final fused estimate.

To provide an example, consider a man searching for his car in a parking lot. Not remembering where he parked and unable to see his vehicle from a cursory glance, he grabs his car keys and presses the alarm button. From across the parking lot, he hears his car horn and begins moving in that direction, periodically pressing the button to reaffirm his car's location. As he peers down a row of cars, he sees his car's lights flash with the horn and begins walking towards his car. However, now that he can *see* his car, his ability to *hear* his car doesn't appreciably assist him in locating his car. From a Bayesian perspective, the uncertainty with which the man located his car via *sound* was high compared to *sight*. Thus, the sound of his car horn only helped him locate his car when he couldn't see it; once he could see his car, the sound was no longer beneficial (Ghahramani, Wolpert and Jordan, 1997).

Returning to prostheses, our theory was that sensory substitution feedback is perceived with a high degree of uncertainty compared to vision. Thus, the artificial feedback only helps control a prosthesis when one can't see it; once a user can see their prosthesis, the artificial feedback may no longer be beneficial.

For sensory feedback to contribute meaningfully to a user's understanding of prosthesis proprioception and kinesthesia, one of two conditions must be met:

1. The feedback must provide information not available to any other sense

   or

2. The feedback must provide the same information available to other senses, but with appreciably low uncertainty compared to other senses

Vision is a powerful sense, contributing significantly to the execution of reaching tasks (Smyth and Murray Marriott, 1982; Land, Mennie and Rusted, 1999; McCarty *et al.*, 2001). Furthermore, vision is heavily relied upon by prosthesis users, to such an extent that prosthesis user gaze and tracking behaviors differ from non-amputee behavior (Hebert *et al.*, 2019). Thus, developing a sensory feedback system capable of matching the precision of vision is difficult. Though vision can perceive positional information with high precision (Ross, 2003), visual uncertainty is known to be much higher for speed information (Chen *et al.*, 1998). This makes restoring kinesthesia a more appealing candidate for sensory substitution, from a Bayesian perspective, than proprioception.

Although previous studies have quantified visual speed perception, these studies typically involve amorphous moving gratings (Chen *et al.*, 1998) and do not provide a clear picture of the uncertainty associated with biomimetic speeds. For example, how does the perception of the shoulder moving relative to the torso compare to the perception of the elbow moving relative to the already-moving shoulder? Is there a difference between how precisely humans can see angular movement and Cartesian movement? If vision is heavily relied upon by prosthesis users, and our goal is to provide artificial sensory information to augment senses with higher uncertainty, then it is important to identify the conditions under which vision perceives motion with the greatest uncertainty, and to develop an artificial sensory feedback system which augments this perception.

This is the core purpose of this body of work. First, we investigated vision's perception of speed as defined in different biomimetic reference frames. We then developed a sensory substitution system for a single-degree-of-freedom (DoF) myoelectric interface and tested how it affects non-amputee reaching errors and adaptation behaviors during hybrid tasks requiring coordinated biological and myoelectric limb movement. Finally, we tested this system with transradial amputee subjects to investigate how incidental feedback differences between non-amputee and amputee users affect performance and adaptation.

1.2. Background

1.2.1. Human Motor Control, Learning, and Adaptation

With a few exceptions (Eibl-Eibesfeldt, 1973; Thelen, Bradshaw and Ward, 1981), human movement must be learned through an iterative process of trial-and-error. Starting with gross limb movements *in utero* (Hadders-Algra, 2018), we slowly learn the brain commands required to achieve desired movements, and we hone this understanding throughout our lives. As we master simple movements, the door opens to learn complex, coordinated, and precise tasks. We learn to manipulate tools, embodying them as extensions of ourselves. And when presented with a novel task, we pull from our ever-growing repertoire of motor skills to learn these new movements. All of this is encompassed within the field of *motor learning*.

Motor learning, as described by Dr. Daniel Wolpert, "is a consequence of the co-adaptation of the neural machinery and structural anatomy." (Wolpert, Ghahramani and Flanagan, 2001) It is the process by which humans (and, indeed, many animals) learn new motor tasks and refine known motor tasks. We perform an action, compare the resulting movement to our expected movement,

and adjust accordingly to minimize the discrepancy between the two. Consider, as an example, a woman learning to throw darts. Starting out, she has perhaps an elementary understanding of the motions required to propel the dart in the direction of the dartboard, but she has not developed the "muscle memory" to do so. She throws her first dart, and it falls short of the dartboard, landing instead in the floor. From this initial throw, she learns that she needs to throw the dart with more force, and to release it from her fingers more quickly. She takes a second dart and tries again, this time hitting the dartboard. With each throw, she better understands the coordination of muscle contractions required to land the dart near the bullseye.

An important aspect of motor learning is that it requires a knowledge of how the body will react to a series of muscle contractions, and an understanding of the anticipated sensory information. These stored motor memories are often described using the framework of *internal models*, which approximates neural processes with concepts drawn from control literature (Wolpert, Ghahramani and Jordan, 1995; Kawato, 1999). To understand how internal models fit into the human motor control paradigm, consider **Figure 1** below:

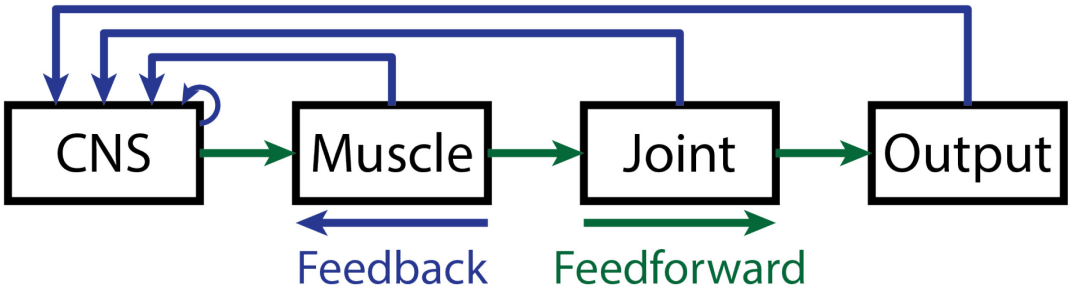

Figure 1. Flowchart of Able-Bodied Human Motor Control.

After deciding on a desired motor output, the brain issues *feedforward* commands (green) which travel from the central nervous system out to the periphery stimulating the muscles, which act upon the joints of the body and ultimately result in some motor output. At each of these descending levels, the body is outfitted with sensors which provide the brain with *feedback* signals (blue) identifying the true activity that the motor commands have elicited, including an *efference copy* within the brain.

There exists a clear communication pathway between the central nervous system (CNS) and the body. When trying to make a limb movement, the brain calls upon a *forward model*, which describes how a motor command issued in a given state (e.g. limb position and velocity) will affect the next limb state. Once a *feedforward* motor command is decided, it propagates from the CNS to the periphery, resulting in movement. Simultaneously, the body's various sensory organs are sending *feedback* signals to the brain, which calls upon an *inverse model* to convert the limb state back into its causal motor command. Each internal model is used to identify discrepancies between what was expected, and what has occurred (Shadmehr and Mussa-Ivaldi, 1994); the forward model compares the actual sensory feedback to the feedback predicted from an efference copy of the command, and the inverse model compares the predicted causal motor command to the actual generated command (Poulet and Hedwig, 2007).

Considering our example above, the woman starts inexperienced in dart throwing and has therefore not yet developed internal models for this task. However, she does have previous experience in

throwing other projectiles – paper airplanes, baseballs, hand axes, and so on – and therefore has other internal models she can use (Wolpert and Kawato, 1998). Though these internal models are initially poor approximations of the motions necessary to throw a dart, each throw updates her internal models, gradually improving her throws. Her brain slowly consolidates these internal model changes when they are not in use, especially as she sleeps (Walker *et al.*, 2002) but even to a lesser extent during the short breaks between rounds (Huang and Shadmehr, 2007; Boenstrup *et al.*, 2019). After several weeks of practice, she finds that dart throwing has become second nature; she has successfully developed an altogether new internal model, one specific to dart throwing.

This example illustrates the concept of *motor learning*, but a second process exists which fine-tunes existing models: *motor adaptation*. It should be noted that the term "motor learning" is often used interchangeably with "motor adaptation", though their processes differ; in this dissertation, the two are distinguished (Bastian, 2008). If motor learning is the long-term development of novel internal models dedicated to specific tasks, motor adaptation is the gradual tuning of an internal model to reduce future errors (Shadmehr and Mussa-Ivaldi, 1994). To demonstrate this concept of motor adaptation, consider a scenario where the woman purchases a new set of metal darts. As she tries them out, she finds her accuracy has taken a hit – these new darts are much heavier than the ones she has practiced with previously. Even though her dart throwing internal model is still valid for this task, she needs to iteratively tune it to the new paradigm of throwing heavier darts. After a few rounds, she's developed a feeling for how to adjust her throws with the heavier darts; she has successfully adapted her dart throwing internal model.

The processes of motor learning and motor adaptation are not mutually exclusive. To the contrary, it is likely that both processes occur even when learning to use a new tool, though the level of

adaptation of existing models is dependent on the stability of the dynamics of the novel tool – gradual changes in a tool's dynamics increases the extent to which one adapts models of the arm, over the development of new models representing the tool (Kluzik *et al.*, 2008).

1.2.2. Bayesian Estimation, Sensory Integration, and Sensorimotor Adaptation

Uncertainty is an inherent part of control systems, and the human motor control system is no exception. Every movement we perform and every observation we make has variability, though this variability is not synonymous with noise (Newell *et al.*, 2006); in fact, movement variability allows for purposeful exploration of the control space and is therefore a crucial component of motor learning (Bernshteĭn, 1967; Dhawale, Smith and Ölveczky, 2017; Sternad, 2018). Furthermore, the amount of motor or sensory uncertainty influences adaptation in a manner described by Bayesian theory (Körding and Wolpert, 2004). Consider once more the woman throwing darts. When first throwing the heavier darts she isn't accustomed to, there is a large amount of uncertainty in her throws; were she blindfolded, she would have a poor estimate of the final landing position of the dart, based solely on her feedforward motor commands. However, she can clearly see that her dart hit low on the board, so she bases her estimate of the dart's location more on her visual feedback than her feedforward motor commands. Now consider an opposite situation where she is throwing her usual darts, but the dartboard is in a dimly lit corner. Just as the dart leaves her fingers, even before she sees where it's landed, she knows that she threw it a bit too high. However, because the poor lighting makes the dartboard difficult to see, it's hard for her to confirm this is the case from visual feedback. Thus, she bases her estimate of the dart's location more on her "gut" (i.e. her forward model) than her visual feedback. The unfamiliar darts is an example of high feedforward uncertainty, and the dim lighting is an example of high feedback

uncertainty. The fusion of these uncertainties can be modeled as a Kalman filter – the final estimate biases more towards the information source with lower uncertainty (Kalman, 1960; Wolpert, Ghahramani and Jordan, 1995).

In much the same way, sensory information is fused together in a statistically optimal fashion; the final sensory estimate will be biased towards the sensory channel with less uncertainty (Ernst and Banks, 2002). Some senses are also subject to Bayesian processes; for example, visual estimates of speed have a statistical prior biased towards nonmovement (Stocker and Simoncelli, 2006). Sensory integration is also not a consistent process, and changes in movement and task can change the relevant priors (Yin *et al.*, 2019), sensory uncertainty (Klever *et al.*, 2019), and the integration weighting (Sober and Sabes, 2005).

Modeling the motor process as a single Kalman filter suggests that increased feedforward uncertainty should result in increased adaptation (Wei and Körding, 2010), so Dr. Reva Johnson built upon a hierarchical Kalman filter model proposed in 2008 (Berniker and Kording, 2008). The first model simulates state control and estimation, and is responsible for merging the state prior with feedback to generate a posterior state estimate [**Figure 2a**]. Furthermore, the discrepancy between feedforward and feedback estimates is used to update the internal model for subsequent movements, according to uncertainty in their control, senses, and internal models (Reva E. Johnson *et al.*, 2017) [**Figure 2b**]. The Kalman gains are updated according to the calculated uncertainty of the internal model, and the rate at which they adapt decreases with increasing feedforward and feedback uncertainties [**Appendix C**].

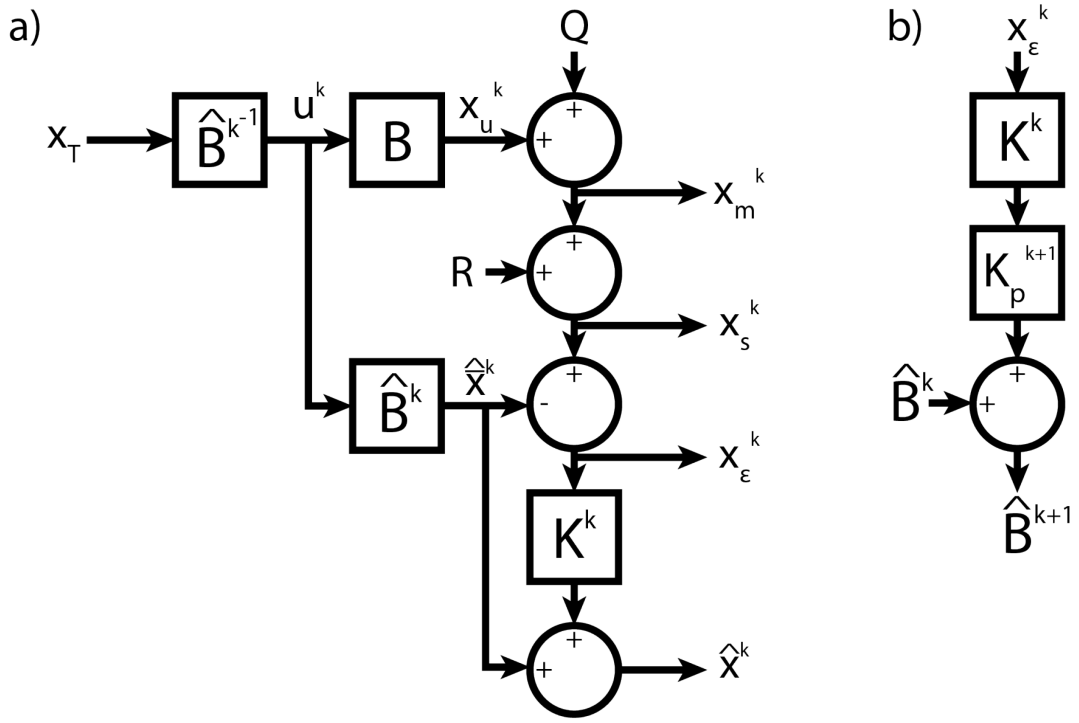

Figure 2. Bayesian Estimation and Sensorimotor Adaptation.

A model for ballistic trial-by-trial sensorimotor adaptation based on hierarchical Kalman filters. (a) State control and estimation. During trial $\boldsymbol{k}$, the target $\boldsymbol{x_T}$ is fed into the inverse model $\widehat{\boldsymbol{B}}^{\boldsymbol{k^{-1}}}$ to generate the command $\boldsymbol{u^k}$. This command generates an intended movement $\boldsymbol{x_u}^{\boldsymbol{k}}$ and an efference copy $\widehat{\hat{\boldsymbol{x}}}^{\boldsymbol{k}}$. The intended movement $\boldsymbol{x_u}^{\boldsymbol{k}}$ is corrupted by process noise $\boldsymbol{Q}$ yielding the measured movement $\boldsymbol{x_m}^{\boldsymbol{k}}$, which is further corrupted by sensory noise $\boldsymbol{R}$ when observing the movement $\boldsymbol{x_s}^{\boldsymbol{k}}$. Subtracting the prior estimated movement $\widehat{\hat{\boldsymbol{x}}}^{\boldsymbol{k}}$ to the observed movement $\boldsymbol{x_s}^{\boldsymbol{k}}$ results in the observation error $\boldsymbol{x_\varepsilon}^{\boldsymbol{k}}$, which is adjusted by a Kalman gain $\boldsymbol{K^k}$ and used to generate the final estimated movement $\widehat{\boldsymbol{x}}^{\boldsymbol{k}}$ (b) Parameter estimation. The observation error $\boldsymbol{x_\varepsilon}^{\boldsymbol{k}}$ is multiplied by the state Kalman gain $\boldsymbol{K^k}$ and the internal model Kalman gain $\boldsymbol{K_p}^{\boldsymbol{k}}$. The resulting value is added to the previous estimate of the internal model $\widehat{\boldsymbol{B}}^{\boldsymbol{k}}$ to yield and updated internal model estimate $\widehat{\boldsymbol{B}}^{\boldsymbol{k+1}}$. See **Appendix C** for the full model.

As a result of the stepwise nature of this hierarchical Kalman filter, it is particularly useful for modeling adaptation during ballistic movements – movements completed faster than reaction time, typically 200-230ms (Schmidt *et al.*, 1979; Franklin *et al.*, 2019). Ballistic reaches are thusly

modeled as a single motor command and a subsequent single error observation, with internal model updates occurring between trials. This sensorimotor adaptation model can also be used for continuous motor control (Reva E. Johnson *et al.*, 2017), though this application is outside of the scope of this thesis.

1.2.3. Motor Control in Myoelectric Prostheses

Robotic prosthetic limbs have existed in some form as early as the 1920s (Schlesinger, 1919), with myoelectric control proposed as a possible control interface in the 1950s (Berger and Huppert, 1952; Battye, Nightingale and Whillis, 1955). In its most basic form, electrical signals are recorded from contracting muscles and filtered. The amplitudes of a pair of signals are then used to proportionally control a single joint of a prosthetic limb (e.g. hand aperture) (Herberts, 1969; Parker and Scott, 1986). Though simple, its straightforward nature has also led this control method to become a popular choice for robotic prostheses (Silcox *et al.*, 1993; Asghari Oskoei and Hu, 2007). However, much information from the EMG signal timeseries is lost when converted into only an amplitude (De Luca, 1979); as such, more advanced pattern recognition algorithms have been proposed to interpret the user's intent for prosthesis control (Hudgins, Parker and Scott, 1993; Englehart and Hudgins, 2003; Hargrove *et al.*, 2007).

This control scheme differs significantly from control of an intact limb. Compare the schematic for able-bodied limb control in **Figure 1** to that of myoelectric prosthesis control in **Figure 3** below:

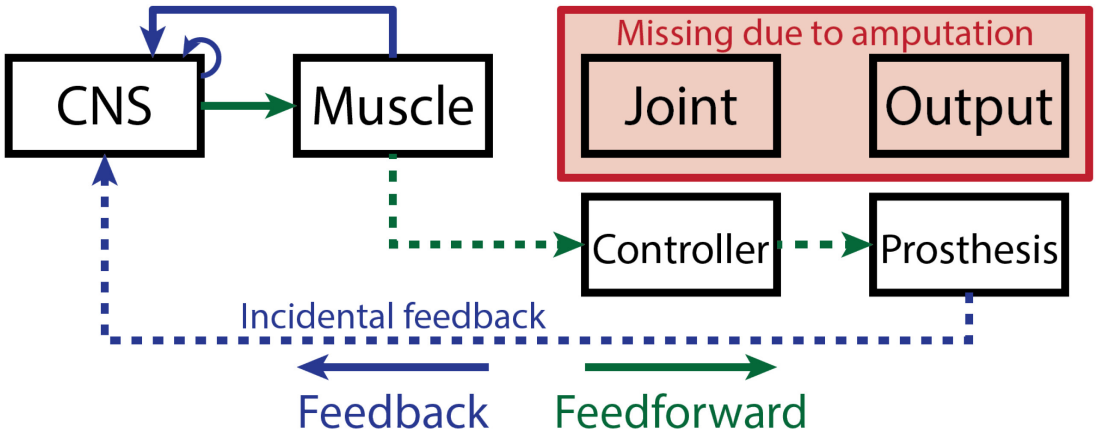

Figure 3. Flowchart of Myoelectric Prosthesis Motor Control.

After amputation, muscles still respond to neural drive, and so the resultant EMG signals are used to direct prosthesis movements. However, the feedback sources originating from the biological limb are now missing, and instead are replaced with incidental feedback including prosthesis motor sounds and vibration, as well as sight of the prosthesis.

Because the motor output is missing due to amputation (or limb difference), a prosthesis is used to provide a facsimile of the intended action. To do this, myoelectric signals are used to communicate intent to a controller, which then decides on the motors to activate in the prosthesis. Without the benefit of years of motor training, however, this new feedforward pathway is indirect and approximate, subject to errors. Furthermore, the biological feedback pathways once originating from the limb currently have no equivalent; instead, sources of feedback as to the current state of the prosthesis are incidental – including sight, sound, vibration, and device weight and inertia. Finally, even the remaining biological feedback – muscle sensors including spindles and Golgi tendon organs – are not unaffected by amputation; absence of the usual agonist-antagonist muscle pairs results in modified activation of these sensors, though recent surgical techniques seek to restore this pairing (Clites *et al.*, 2018).

These changes to the communication loop as depicted in **Figure 3** are inevitably accompanied by changes in motor learning and adaptation behavior [**Section 1.2.1**]. Controlling reaching movements with EMG results in higher errors than with other controllers (Johnson *et al.*, 2014), though these differences are a result of more than simply a reduced signal-to-noise ratio (Reva E Johnson *et al.*, 2017). Rather, simulations using the hierarchical Kalman model shown in **Figure 2** suggest that increased control noise Q will increase internal model uncertainty and reduce adaptation, meaning myoelectric prosthesis users are less likely to over-adapt to random errors arising from large process noise. Likewise, the increase in sensory noise R associated with the loss of biological sensory channels also increases internal model uncertainty and reduces adaptation, meaning myoelectric prosthesis users will adapt more slowly to the errors they observe (Reva E. Johnson *et al.*, 2017) [**Appendix C**].

Clearly, improved adaptation benefits prosthesis users; the ability to adapt to errors more quickly means users have more volition over their control and may need to adjust their prosthesis less often. The hierarchical Kalman model suggests that this can be achieved by either reducing control noise, or by reducing sensory noise. The high degree of uncertainty in incidental feedback and the clear need to reduce this noise is a major motivator behind research and development of artificial sensory feedback for prosthetic limbs.

1.2.4. Multimodal Sensory Feedback

Research into sensory feedback for prosthetic limbs dates back as early as the 1960s, shortly after the introduction of myoelectric prostheses (Beeker, During and Den Hertog, 1967; Prior *et al.*, 1976; Childress, 1980). However, these early efforts were homogenous in motivation, aiming to restore a sense of contact and pressure to the user. Since that time, the term “sensory feedback”

has come to represent a wide variety of techniques and applications, both within and outside of the field of prosthetics, and the body of work has grown exponentially [**Figure 4a**]. To provide a framework by which to categorize the body of literature, I employ two levels of distinction.

First, sensory feedback can be categorized by the *restored sense*. The restored sense is the observed metric – *what* is the user receiving information about? Restored senses can include, but are not limited to: force and pressure, compliance, contact, slip, aperture, proprioception, kinesthesia, prosthesis state, and EMG signal. These senses can be broadly grouped into two categories: proprioceptive, and tactile. *Proprioceptive* senses are those that describe the configuration of the prosthesis – the position, speed, or prosthesis mode (such as differences between grasping states or gait patterns). *Tactile* senses are those that describe interactions between the prosthesis and objects – grasping force, contact, or slippage. Tactile senses, especially contact and grasping force, are the most common and were the earliest to be researched. However, with more surveys of prosthesis users suggesting a strong desire to operate the device without needing to look at it (Cordella *et al.*, 2016), proprioceptive senses are now receiving more research attention.

Second, sensory feedback can be categorized by the *feedback modality*. The feedback modality is information pathway – *how* is the user receiving information? Feedback modalities can include, but are not limited to: vibrotactile, electrotactile, mechanotactile, skin stretch, visual, acoustic, osseoperception, and peripheral nerve stimulation. These modalities can be broadly grouped into two categories: sensory substitution, and direct feedback. *Sensory substitution* is the restoration of one feedback channel via a different channel, or via the same channel in a different location (modality-matched feedback); examples include vibrotactile, skin stretch, or auditory feedback. *Direct feedback* is the restoration of physiologically-analogous sensation – typically accomplished

by activating the nerve in a similar manner to how they would in an intact limb. Examples of direct feedback include peripheral nerve stimulation and illusory movements via tendon vibration. Sensory substitution is by far the most common type of feedback due to its simplicity, whereas direct feedback is generally invasive, limiting the number of studies that can investigate such interventions [**Figure 4b**].

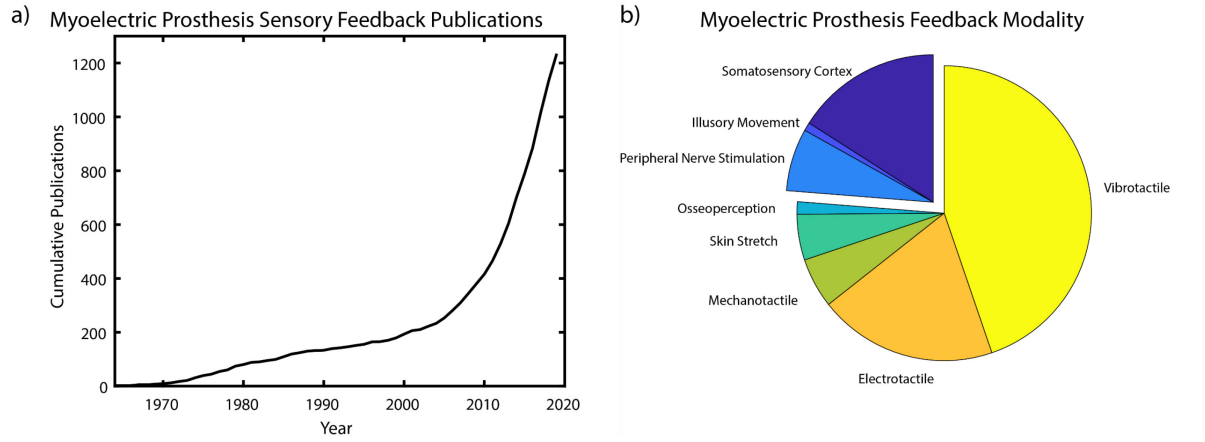

Figure 4: Myoelectric Prosthesis Sensory Feedback Publication Summary.

The term "sensory feedback" has come to represent a wide variety of techniques and applications, and research has gained much traction in recent years. (a) Cumulative publications from the Scopus database containing the terms (1) *feedback*, (2) *myoelectric* or *limb*, and (3) *prosthesis*, *prostheses*, *prosthetic*, or *prosthetics* in the title, abstract, or keywords. The body of research has grown exponentially in the 21st century. (b) Breakdown of feedback modality terms appearing in publications from the Scopus database, in addition to the terms listed above; some publications may contain more than one term, and the sum of publications from this breakdown is less than that of the current total listed in (a). Broken out sections represent direct feedback techniques. Sensory substitution methods make up most of the sensory feedback literature.

These two categories are independent of one another; each type of feedback modality has been used to restore each type of sense. **Table I** summarizes these categories.

Table I: Sensory Feedback Categories.

Sensory feedback can be categorized by restored sense and feedback modality.

Restored Sense		Feedback Modality	
Proprioceptive	**Tactile**	**Sensory Substitution**	**Direct Feedback**
Aperture Proprioception Kinesthesia Prosthesis state EMG	Force Pressure Compliance Contact Slip	Vibrotactile Electrotactile Mechanotactile Skin stretch Visual Acoustic Osseoperception	Peripheral nerve stimulation Illusory movement Somatosensory cortex stimulation

It should be mentioned that several of the restored senses mentioned above are related. For example, although I distinguish kinesthesia and proprioception, the two are physiologically acquired from the same sensory organs, namely muscle spindles, Golgi tendon organs, and skin stretch receptors including the Ruffini corpuscles. Furthermore, knowledge of one can provide an estimate of the other; rate of proprioceptive change yields an estimate of kinesthesia, and integrating kinesthesia across movement time yields an estimate of proprioception. These definitions are differentiated here to more closely match how information may be encoded and conveyed via artificial sensory feedback.

One confounding factor affecting many sensory feedback studies is incidental feedback from the prosthesis, or more specifically the lack thereof in experimental setups [**Figure 3**]. Providing artificial sensory feedback does not remove these incidental feedback sources; to the contrary, these sources fuse in accordance with their uncertainty to create a single estimate of the restored sense [**Section 1.2.2**]. Thus, laboratory settings involving control of virtual limbs, or those involving the obstruction of incidental feedback including blindfolding, noise-cancellation, and

disconnect from the prosthesis, do not effectively simulate day-to-day conditions of user-in-the-loop prosthesis control. Potentially as a result, many such studies show significant benefits from the addition of artificial sensory feedback. This is perhaps unsurprising – how can they not, when the alternative is to have no source of information and to rely solely on the forward model?

When incidental feedback is provided or available to the user, however, these results become mixed. Some studies still do show a benefit of artificial sensory feedback. However, other literature suggests that benefits emerging in laboratory conditions do not persist with incidental feedback available (Antfolk *et al.*, 2013; Markovic, Schweisfurth, Engels, Bentz, *et al.*, 2018). Studies have noted that incidental feedback is sufficient for center-out reaching (Miall *et al.*, 2018), object identification (Cho *et al.*, 2015), grasping force regulation (Saunders and Vijayakumar, 2011; Brown *et al.*, 2015) and simple grasping tasks (Ninu *et al.*, 2014; Markovic *et al.*, 2017; Markovic, Schweisfurth, Engels, Farina, *et al.*, 2018; Raveh, Friedman and Portnoy, 2018), though more complex tasks may still benefit from artificial feedback (Markovic *et al.*, 2017; Markovic, Schweisfurth, Engels, Bentz, *et al.*, 2018).

Furthermore, for multifunction prosthetic hands, the control algorithm used to control the hand can determine what information is available. For example, simultaneous and proportional control of two DoFs provides a direct understanding of the underlying EMG control signal, whereas sequential control of only one DoF at a time obfuscates the magnitude of the control signal for the other DoF. Studies suggest that sequential control allows for superior short-term performance, while simultaneous control allows for stronger internal model generation (Ahmed W Shehata, Scheme and Sensinger, 2018); a follow-up study further suggests that implementing the sequential controller with the feedback from the simultaneous controller combines these advantages (Ahmed

W. Shehata, Scheme and Sensinger, 2018). This clearly illustrates the importance of considering the contributions of incidental feedback when developing artificial sensory feedback systems.

One potential explanation for this phenomenon is the level of uncertainty of the provided feedback, relative to the uncertainty of incidental feedback sources. The most notable source of incidental feedback is vision. When sensory substitution feedback is provided in the presence of vision, the two modalities are integrated according to a weighted sum based on each modality's uncertainty (Kuschel *et al.*, 2010). Visual estimates of position are highly precise, capable of perceiving changes as small as 1% (Ross, 2003). In some cases, vision is more precise than even intact proprioception (van Beers *et al.*, 2002). Thus, providing artificial sensory feedback encoding limb position is unlikely to significantly augment a user's estimate of proprioception unless the uncertainty of the artificial feedback is comparable or superior to that of vision, making the feedback unlikely to meaningfully change a user's performance.

If, instead, the artificial sensory feedback encodes information that is not available via incidental feedback, such as discrete task information (Cipriani *et al.*, 2014; Clemente *et al.*, 2015; Aboseria *et al.*, 2018), or encodes information that incidental feedback only provides with high uncertainty, then it should successfully augment a user's estimate of the restored sense. What remains to be investigated, then, is if this augmented estimate translates to performance improvement.

1.3. Specific Aims

The work presented in this thesis is an extension of the thesis work of Dr. Reva Johnson (Johnson, 2015). In her thesis, she investigated how changes to feedforward and feedback uncertainty affect trial-by-trial adaptation in single-DoF reaching tasks. Her work showed that the mechanisms

underlying adaptation remain unimpaired after amputation, but that increased feedforward and feedback uncertainty deteriorate adaptation capability. It suggests that improving control interfaces and sensory feedback may allow prosthesis users to overcome these setbacks. To this end, this thesis builds off of the outcomes from a pilot study (Earley *et al.*, 2017b, 2017a) and endeavors to address uncertainty in sensory feedback by identifying highly-uncertainty intact feedback and developing a sensory substitution system to augment this intact feedback.

Aim 1: Investigate visual joint speed perception of biomimetic arm motions

Prior studies investigating vision have found that visual perception of speed is poorer than that of position. However, speed must be defined relative to some reference frame, and there exist several definitions that are relevant to biomimetic limb movement. The purpose of this aim was to quantify visual perception of biomimetic speeds to determine the speed with the highest uncertainty, and to subsequently augment with artificial feedback to determine its capacity for improvement.

Aim 2: Evaluate augmented joint speed feedback during non-amputee hybrid physical/myoelectric reaching tasks

Although the previous aim demonstrated the capacity to augment vision with audio feedback in observational tasks, it was not guaranteed that this would translate to an improvement during real-time reaching tasks. The purpose of this aim was to test a joint speed feedback system delivering frequency-modulated audio tones during non-amputee virtual center-out reaching tasks. These reaches involved positional control of the elbow and simultaneous myoelectric control of the wrist, emulating hybrid movements for a trans-radial prosthesis.

Aim 3: Compare non-amputee results to transradial amputee reaching performance and adaptation

Non-amputee subjects have access to incidental feedback that is unavailable to amputee subjects, which may lead to different adaptation behavior and performance while reaching. The purpose of this study was to evaluate transradial amputee performance during a center-out reaching task, and to quantify the effect of joint-speed feedback on steady-state performance and adaptation to a perturbed myoelectric controller.

The rest of this dissertation is organized as follows. **Chapter 2** is an article published in Nature: Scientific Reports addressing Specific Aim 1 (Earley *et al.*, 2018). **Chapter 3** is an unpublished manuscript addressing Specific Aim 2. **Chapter 4** uses the protocol described in the previous chapter to investigate the effects of joint speed feedback for transradial amputee subjects performing center-out reaches, constituting Specific Aim 3. **Chapter 5** concludes this dissertation by summarizing what was learned during this research, limitations of the approaches, and lingering questions that remain to be answered.

Appendix A is based on a conference paper from the IEEE International Conference on Rehabilitation Robotics (Earley *et al.*, 2017b, 2017a); however, additional non-amputee and transhumeral amputee subject data not presented in the conference paper are included in this dissertation. This study is considered pilot work for this thesis, and the outcomes from this study steered the direction of research for **Chapters 2-4. Appendix B** is conference paper from the International Conference of the IEEE Engineering in Medicine and Biology Society detailing a data analysis and simulation approach originally intended for use in Aim 2, but which was ultimately replaced with the methods discussed in **Chapter 3** (Earley and Hargrove, 2019).

Appendix C is a summary of unpublished work by Drs. Daniel Blustein and Jon Sensinger updating the hierarchical Kalman model first proposed in (Reva E. Johnson *et al.*, 2017). It includes simulations describing how changes to free parameters affect the calculated internal model adaptation rate.

2. Joint Speed Discrimination and Augmentation For Prosthesis Feedback

Authors: Eric J. Earley, Reva E. Johnson, Levi J. Hargrove, Jon W. Sensinger

2.1. Abstract

Sensory feedback is critical in fine motor control, learning, and adaptation. However, robotic prosthetic limbs currently lack the feedback segment of the communication loop between user and device. Sensory substitution feedback can close this gap, but sometimes this improvement only persists when users cannot see their prosthesis. suggesting the provided feedback is redundant with vision. Thus, given the choice, users rely on vision over artificial feedback. To effectively augment vision, sensory feedback must provide information that vision cannot provide or provides poorly. Although vision is known to be less precise at estimating speed than position, no work has compared speed precision of biomimetic arm movements. In this study, we investigated the uncertainty of visual speed estimates as defined by different virtual arm movements. We found that uncertainty was greatest for visual estimates of joint speeds, compared to absolute rotational or linear endpoint speeds. Furthermore, this uncertainty increased when the joint reference frame speed varied over time, potentially caused by an overestimation of joint speed. Finally, we demonstrate a joint-based sensory substitution feedback paradigm capable of significantly reducing joint speed uncertainty when paired with vision. Ultimately, this work may lead to improved prosthesis control and capacity for motor learning.

2.2. Introduction

When we move our bodies, a complex communication loop is formed between our brains and our extremities. Our brains send efferent commands to our limbs instructing them to move in a specific way. As our limbs carry out these commands, they also send afferent proprioceptive signals back

to the brain detailing the positions, speeds, and forces of the limb (Jones, 2000). From these afferent signals, modifications to the efferent neural drive can correct movement errors and ensure smooth limb control (Bilodeau and Bilodeau, 1961).

Both communication paths are represented by a corresponding internal model. Forward internal models predict future limb movements taking into account the limb's current configuration and descending signals, while inverse internal models predict the motor command resulting in the limb's current movement (Wolpert, Ghahramani and Jordan, 1995). To develop, adapt, and improve control of the limb over time, these models require knowledge of efferent motor commands (i.e. efference copy) and of the limb's current configuration and movement (i.e. proprioception and kinesthesia). Lack of these proprioceptive signals hampers internal model development and is detrimental to limb control, especially inter-joint coordination (Ghez and Sainburg, 1995; Sainburg *et al.*, 1995). Despite its importance in understanding and correcting limb movement, this sense of proprioception is missing for commercially-available robotic prosthetic limbs.

Sensory feedback remains a research priority for prosthesis users (Cordella *et al.*, 2016). Recent technologies can restore these missing senses via physiologically-analogous stimuli, such as peripheral nerve stimulation (Tan *et al.*, 2014; Schiefer *et al.*, 2016) and vibration-induced illusory kinesthesia (Marasco *et al.*, 2018). However, a more common approach uses sensory substitution, in which information from a missing sensory channel is provided indirectly via a separate, intact sensory channel (Antfolk *et al.*, 2013). Numerous substitution methods have been proposed over the past decades, including vibrotactile (Stanley and Kuchenbecker, 2012; Witteveen *et al.*, 2012; Cipriani *et al.*, 2014; De Nunzio *et al.*, 2017; Krueger *et al.*, 2017), electrotactile (Witteveen *et al.*,

2012), skin stretch (Stanley and Kuchenbecker, 2012), and audio (Mirelman *et al.*, 2011; Ahmed W Shehata, Scheme and Sensinger, 2018; Ahmed W. Shehata, Scheme and Sensinger, 2018) modalities (Schofield *et al.*, 2014). What is often not considered is that prosthesis users are already using a form of sensory substitution: vision. Thus, providing information that is also available to vision may be redundant.

Vision is capable of estimating grasping force similarly to tactile feedback (Ninu *et al.*, 2014), though several grasping force feedback studies still show significant benefit to prosthesis control with vision present. However, many proprioceptive feedback studies are conducted with sight of the prosthesis obscured, and the benefit of proprioceptive feedback often diminishes when subjects can see the prosthesis. During everyday use, prosthesis users visually monitor their device, adopting a distinct gaze pattern. Able-bodied gaze behavior preempts limb movement with eye saccade towards the object of interest (Land, Mennie and Rusted, 1999), but prosthesis user gaze tends to track the movement of their prosthesis until it reaches the target (Sobuh *et al.*, 2014). This visual monitoring serves to replace the missing proprioception.

When sensory substitution feedback is provided in the presence of vision, the two modalities are integrated according to a weighted sum based on each modality's uncertainty (Kuschel *et al.*, 2010). Visual estimates of position are highly precise, capable of perceiving changes as small as 1% (Ross, 2003). In some cases, vision is more precise than even intact proprioception (van Beers *et al.*, 2002). On the other hand, vision estimates speed with a discrimination threshold of 10% (Chen *et al.*, 1998) and a bias towards slower speeds and non-movement (i.e. position) (Stocker and Simoncelli, 2006). For either proprioception or kinesthesia, if artificial feedback can't match visual precision, it will be largely ignored in favor of vision. Thus, providing sensory feedback

about prosthesis speed should yield a greater benefit than prosthesis position. However, there are several definitions of speed relevant to the movement of a limb.

Limb speed can be defined by the coordinate system (linear speed in Cartesian coordinates, angular speed in polar coordinates) and by the reference frame (absolute speed within a global reference frame, relative speed within a joint-based reference frame). Likewise, feedback provided in joint or global reference frames develop internal models differently, resulting in different generalization to intrinsic or extrinsic error sources (Berniker and Kording, 2008). In addition, feedback concerning joint errors is always relevant, but feedback concerning extrinsic errors are only relevant under specific conditions (Berniker and Kording, 2011). Despite the importance of joint feedback on tuning the internal models of upper-limb movement, it is not known how precisely vision can perceive joint speed, and thus how effectively artificial proprioceptive feedback can be integrated into such estimates.

The purpose of this study was to investigate visual joint speed perception of biomimetic arm motions, and to determine if these visual joint speed estimates can be augmented with artificial sensory feedback. Subjects observed a virtual two-link arm, analogous to a top-down view of a shoulder, elbow, and hand. Stimuli differed only in the reference frame of interest, and subjects completed two-alternative forced choice tasks to determine just noticeable difference (JND) thresholds. We also tested how joint speed JND varies due to changes in reference frame speed. Finally, we tested a frequency-modulated audio feedback paradigm to evaluate its ability to augment visual speed discrimination.

2.3. Methods

2.3.1. Subjects

Experiments were approved by the Northwestern University Institutional Review Board. Methods were carried out in accordance with IRB approval. All subjects provided informed consent before beginning each study. Eight subjects participated in the first and second experiments. Based on a power analysis of simulations using these data, four subjects from the second experiment also participated in the third experiment (Eric J. Earley and Johnson, 2018).

2.3.2. Setup

All protocol and data collection were executed using MATLAB R2017b. Subjects sat in front of a 15.5-inch 1920 x 1080 resolution computer monitor at a distance of 24-36 inches. The screen displayed a black two-link system over a uniform white background [**Figure 5**-**Figure 6**]. The arm had link lengths of 5 cm, widths of 5 points (1.8 mm), and endcap diameters of 6 points (2.1 mm).

Each visual stimulus was presented for 2 seconds, with a 1 second pause between stimuli during which only the white background was shown. Animations were presented at 30 frames per second. Subjects were asked to indicate which stimulus moved faster in the dictated reference frame via a pop-up window prompt. Subjects had unimpaired or corrected vision.

2.3.3. Experiments

Three two-alternative forced choice experiments investigated different aspects of visual speed discrimination. During each experiment, two examples of the two-link arm were displayed to subjects in random order. One stimulus always moved at a nominal speed, whereas the other

stimulus differed from the nominal speed by a magnitude determined by an adaptive staircase. The adaptive staircase was defined as:

$$x(n+1) = x(n) - \frac{C}{n_{shift}+1}[z(n) - \phi] \quad (1)$$

where x was the difference in movement speeds between stimuli, C was the starting speed difference, n_{shift} was the number of decision reversals, ϕ was the target JND probability (84%), and z was a Boolean indicator for the subject's decision (z = 1 when correct and z = 0 when incorrect) (Reva E Johnson *et al.*, 2017). Thus, when subjects correctly identified the faster stimulus, the speed difference between stimuli decreased for the next trial. Likewise, if subjects incorrectly selected the slower stimulus, the speed difference between stimuli increased for the next trial.

The JND for each condition was calculated as the final stimulus difference x tested in the adaptive staircase, which converged after 25 decision reversals. The 84% JND has a unique property (Ernst and Banks, 2002) in that it is linearly variable with the uncertainty (i.e. standard deviation) of the underlying estimator:

$$SD = \frac{JND_{84\%}}{\sqrt{2}} \quad (2)$$

Thus, the 84% JND was converted to uncertainty, normalized, and used as the outcome metric for statistical analyses.

2.3.3.1. Experiment 1: Effect of Speed Type

To determine how discrimination differs between categories of movements, three speed types were tested: *absolute speed*, *joint speed*, and *linear speed* [**Figure 5**]. These speed types correspond with different types of proprioceptive feedback that could be provided for prosthetic limbs: speed of a prosthetic joint relative to the torso (*absolute*) or residual limb (*joint*), or speed of the prosthetic end effector (*linear*).

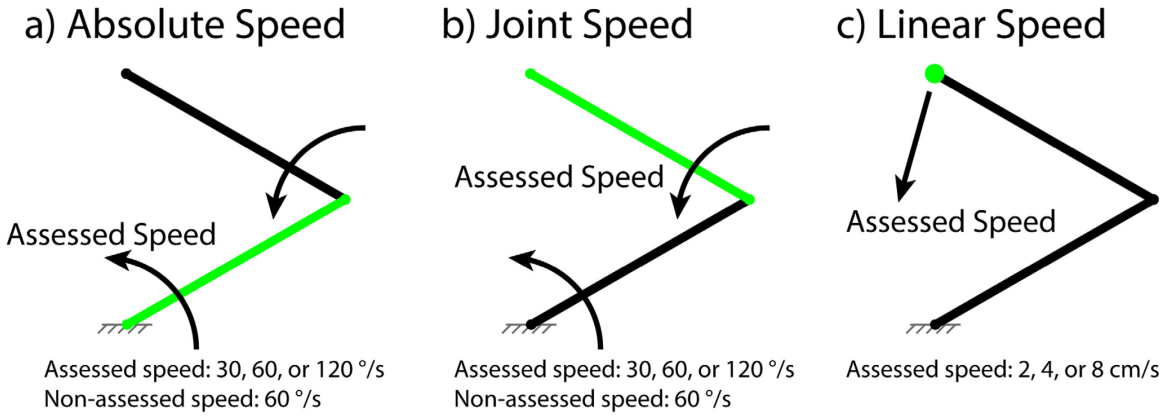

Figure 5. Experiment 1 Setup and Conditions.

Assessed component is highlighted green, while all other components are displayed black. Fixture markings in grey are shown here for clarity but were not displayed during experiments. (a) *Absolute speed* condition. Subjects assessed highlighted proximal link speed in three *speed* conditions: 30, 60, or 120 °/s. Distal link rotated at 60 °/s. (b) *Joint speed* condition. Subjects assessed highlighted distal link speed in three *speed* conditions: 30, 60, or 120 °/s. Proximal link rotated at 60 °/s. (c) *Linear speed* condition. Subjects assessed highlighted endpoint speed in three *speed* conditions: 2, 4, or 8 cm/s. Proximal and distal links were driven by endpoint position.

Absolute speed refers to rotational movement relative to a global, static reference frame. In this condition, the proximal link moved at a nominal speed of either 30, 60, or 120 °/s counter-clockwise (CCW) for one stimulus, and a speed determined by the adaptive staircase in equation (1) for the other stimulus, starting at $C = 50\%$. The distal link moved at a nominal speed of 60 °/s

CCW and accelerated and decelerated randomly but equally for both stimuli; thus, the movement profile was not constant, but was identical for both stimuli [**Figure 5a**].

Joint speed refers to rotational movement relative to a dynamic reference frame, in this case the proximal link. In this condition, the proximal link moved at a nominal speed of 60 °/s CCW and accelerated and decelerated randomly but equally for both stimuli; thus, the movement profile was not constant, but was identical for both stimuli. The distal link moved at a nominal speed of either 30, 60, or 120 °/s CCW for one stimulus, and a speed determined by the adaptive staircase in (1) for the other stimulus, starting at C = 50% [**Figure 5b**].

The random acceleration and deceleration on the proximal link during the *joint speed* condition was implemented to prevent subjects observing absolute speed to estimate joint speed of the distal link by varying the speed of the reference frame. The random acceleration and deceleration on the distal link during the *absolute speed* condition was implemented to match the *joint speed* condition, even though it likely had no effect on estimates.

Linear speed refers to movement in a straight line relative to a static Cartesian reference frame. In this condition, the linkage endpoint moved along a straight path at a constant speed of either 2, 4, or 8 cm/s for one stimulus, and a speed determined by the adaptive staircase in equation (1) for the other stimulus, starting at C = 50%. The links were driven by inverse kinematics to follow the endpoint [**Figure 5c**].

Thus, a total of 9 conditions were tested: 3 speed types, with 3 tested speeds each. Starting positions were randomized for all trials. For *absolute* and *joint speed* trials, the distal link was prevented from crossing the proximal link during movement; invalid starting positions were resampled until

conditions were met. Proximal and distal link speeds were bounded between 0 and 180 °/s, preventing clockwise movement and invalid starting positions due to resampling. For *linear speed* trials, the starting position and movement direction were resampled if the endpoint trajectory exceeded the range of the linkage, or if the endpoint didn't move CCW relative to the origin. The proximal link, distal link, or endpoint were highlighted according to the tested condition.

Statistical analyses performed in RStudio (RStudio, Inc., version 1.1.447) quantified main and interaction effects of the speed type and the observed nominal speed. A Shapiro-Wilk test confirmed normality of the data. A general linear model took the form:

$$SD \sim \beta_0 + speed + type + speed\ x\ type \quad (3)$$

where *speed* was coded as a continuous independent variable in units of octaves (0 at slowest speed, 2 at fastest), and *type* was coded as a categorical independent variable. Because the interaction term was found to be significant, a simple main effects analysis was performed for *speed* (Kutner, 2005). Corrections for 6 comparisons were made via a Bonferroni correction factor.

2.3.3.2. Experiment 2: Effect of Reference Frame Speed Shift

While the first experiment provided an estimate of *joint speed* perception, it only did so at one reference frame speed. Although results showed a higher uncertainty for *joint speed* observations than for *absolute* or *linear speed* observations, it did not shed any light on possible interaction between changes to the reference frame speed and visual uncertainty. Further, one concern from the first experiment was that during *joint speed* conditions, subjects could conceivably identify the faster joint speed of two stimuli by observing either the joint speed or the absolute rotational speed of the distal link. This ambiguity left open the possibility that the higher uncertainty was due to

observing a faster *absolute speed*, rather than due to the *joint speed* nature of the observation itself. We therefore developed a second experiment to determine how joint speed discrimination differs due to changes in reference frame speed. This experiment investigates visual perception of a prosthetic limb while the residual limb is moving non-uniformly. In this experiment, three reference frame conditions were tested. The proximal link rotated at 60 °/s CCW for one stimulus, and a shifted speed of 60, 85, or 120 °/s CCW for the other stimulus; these speeds correspond with an increase of 0, ½, or 1 octave above 60 °/s, respectively. The distal link rotated at 30, 60, or 120 °/s CCW for one stimulus, and a speed determined by the adaptive staircase in equation (1) for the other stimulus, starting at C = 50%. Thus, a total of 9 conditions were tested: 3 reference frame speed shifts, with 3 distal link speeds each [**Figure 6**]. Each link was highlighted green at the joint, with a highlight length of 2 cm.

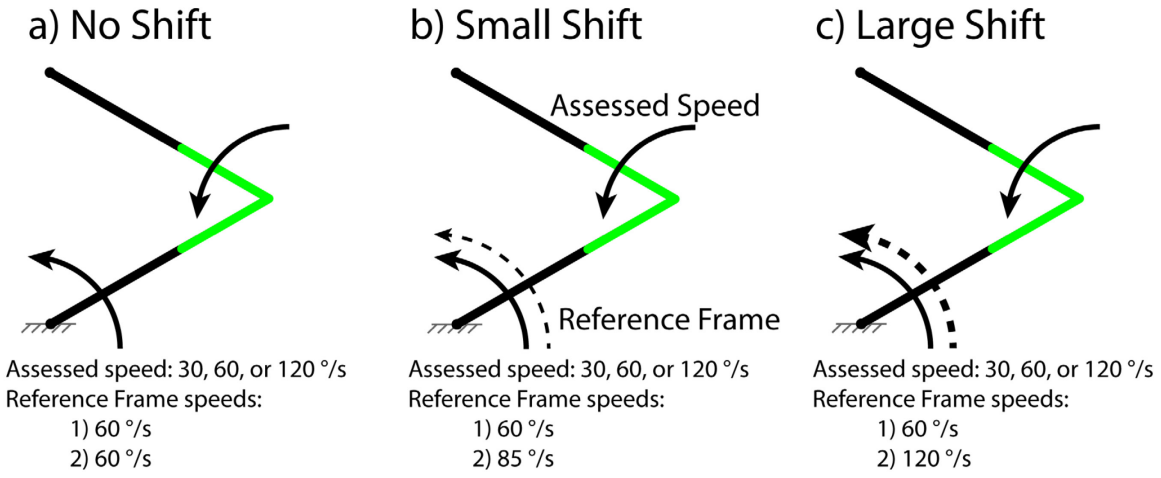

Figure 6. Experiment 2 Setup and Conditions.

For each *shift* condition, subjects assessed highlighted joint speed in three *speed* conditions: 30, 60, or 120 °/s. Fixture markings in grey are shown here for clarity but were not displayed during experiments. (a) *No shift* condition. Reference frame rotated at 60 °/s. (b) *Small shift* condition. Reference frame rotated at 60 °/s in one stimulus, and 85 °/s in the other stimulus (c) *Large shift* condition. Reference frame rotated at 60 °/s in one stimulus, and 120 °/s in the other stimulus.

Statistical analyses were performed to quantify how reference frame speed shift magnitude affects uncertainty. A Shapiro-Wilk test confirmed normality of the data. A multiple linear regression model took the form:

$$SD \sim \beta_0 + speed + shift + speed\ x\ shift \quad (4)$$

where *speed* and *shift* were coded as continuous independent variables. The interaction term was used to determine if *shift* magnitude impacts uncertainty differently at different *speeds*. The interaction term was not found to be significant (B = 0.0002, $t(68)$ = 0.304, p = 0.762), thus the term was removed and the reduced model was reanalyzed (Kutner, 2005).

After inspecting the data, post-hoc analyses tested the pairs of stimuli subjects choose incorrectly. There were two possible stimulus pairs: one where the speed shift of the reference frame aligns with the faster of the two stimuli, and one where the speed shift occurs with the slower of the two stimuli. The former pair might be considered an easier choice – the correct answer with the faster distal link happens to be the stimulus with the faster proximal link – while the latter pair might be considered a more difficult choice – the correct answer with the faster distal link is the stimulus with the slower proximal link. Therefore, we wanted to determine if *speed* or *shift* impacted the rate of errors due to unaligned stimulus changes (the difficult choice). If there was no impact, subjects should make roughly the same number of errors during aligned pairs and unaligned pairs.

Post-hoc statistical analyses were performed using a multiple linear regression model taking the form:

$$Rate \sim \beta_0 + speed + shift + speed\ x\ shift \quad (5)$$

where *speed* and *shift* were coded as continuous independent variables. A Shapiro-Wilk test confirmed normality of the data. The interaction term was not found to be significant (B = 0.280, $t(44)$ = 1.098, p = 0.278), thus the term was removed and the reduced model was reanalyzed (Kutner, 2005).

2.3.3.3. Experiment 3: Effect of Audio Feedback

To determine if joint speed estimates could be improved with supplementary feedback, the *no shift* conditions from the second experiment were repeated. Subjects were provided frequency-modulated audio feedback matching the joint speed of stimuli according to the following equation:

$$f(\omega) = f_{min} \cdot 2^{\frac{\omega}{V_{step}}} \tag{6}$$

where f_{min} was the minimum frequency which was provided when joint speed was zero, and V_{step} was the speed increase required to increase the audio feedback pitch by one octave. For this study, f_{min} was set to 220 Hz (A_3), and V_{step} was set to 60 °/s. Audio signals were generated and output with a sampling frequency of 48 kHz. Subjects wore noise-cancelling headphones, and audio was played at a moderate volume. Based on pilot studies, the starting difference C between joint speeds was set at 10% to allow the adaptive staircase to converge more smoothly.

Statistical analyses were performed using a general linear model taking the form:

$$SD \sim \beta_0 + speed + feedback + speed\ x\ feedback \tag{7}$$

where *speed* was coded as a continuous independent variable and *feedback* was coded as a categorical independent variable. A Shapiro-Wilk test confirmed normality of the data. The purpose of this model was to determine if *vision + audio improved joint speed discrimination*

beyond vision. The interaction term determined if the benefit of audio feedback was partially dependent on distal link speed, or if benefit was global. A main effects analysis compared *vision* and *vision + audio*. Because the interaction term was significant, and a simple main effects analysis was performed for *speed* (Kutner, 2005). Corrections for 3 comparisons were made via a Bonferroni correction factor.

2.4. Results

2.4.1. Experiment 1: Effect of Speed Type

The purpose of Experiment 1 was to investigate how visual speed uncertainty differed between *absolute*, *joint*, and *linear* speed types. In addition, comparing uncertainty across a range of speeds revealed the degree to which uncertainty of each speed type is speed-invariant.

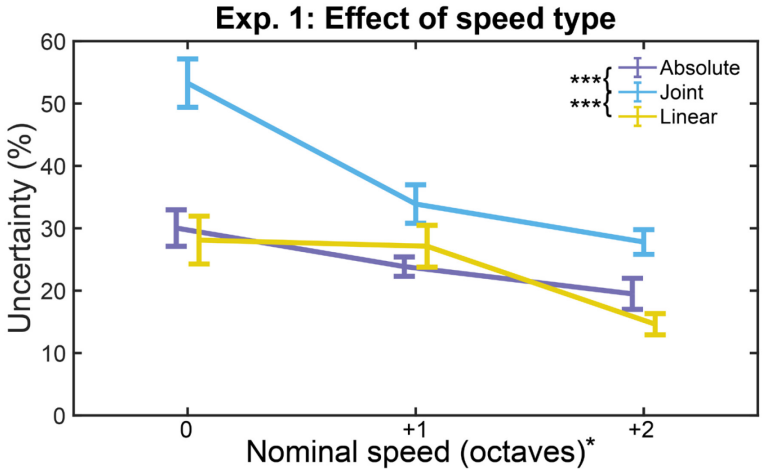

Figure 7. Effect of Speed Type.

Uncertainty generally decreases with increasing stimulus speed. Joint speed discrimination is worse than either absolute or linear speed, especially at slow nominal speeds. Error bars show standard error of the mean (SEM). (*) $p < 0.05$, (***) $p < 0.001$

Main effect analysis revealed higher uncertainty for *Joint speed* than either *Absolute* ($t(36.34) = 4.26$, $p = 0.0008$, $d = 1.23$) or *Linear* speeds ($t(42.79) = 4.24$, $p = 0.0007$, $d = 1.22$). *Absolute* and *Linear* speeds were not significantly different ($t(42.63) = 0.44$, $p > 0.999$, $d = 0.128$) [**Figure 7**]. Thus, our results suggest vision is most uncertain about *joint speed* observations, and therefore augmenting joint speed with artificial sensory feedback should yield the greatest improvement in precision.

Uncertainty decreased with increasing *speed* for *absolute* ($B = -0.053$, $t(22) = 3.18$, $p = 0.026$), *linear* ($B = -0.067$, $t(22) = 2.99$, $p = 0.041$), and *joint* ($B = -0.127$, $t(22) = 5.59$, $p < 0.0001$) speed types. Significant interaction between *speed* and *type* ($F_{4,66} = 3.60$, $p = 0.033$, $\eta^2_{partial} = 0.098$) suggests that this decrease in uncertainty at higher speeds differs between speed types. This interaction is likely due to the large increase in uncertainty for *joint speed* at low speeds. In the slowest *joint speed* condition, the assessed joint speed was half as fast as the reference frame speed. Therefore, most of the absolute speed of the distal link was contributed by the proximal link movement, possibly obfuscating the joint speed.

Our results suggest greater uncertainty for visual estimates of joint speed, compared to absolute speed, for biomimetic motions. However, these results alone cannot tell us if this greater uncertainty is due to poorer precision of joint speed estimates, or if subjects were estimating the faster absolute speed of the distal link. To remove the confounding factor of being able to estimate joint speed using either method, we followed up with Experiment 2.

2.4.2. Experiment 2: Effect of Reference Frame Speed Shift

Experiment 2 expands upon the *joint speed* results from Experiment 1 by exploring the effect of reference frame speed *shift* on joint *speed* uncertainty. Thus, subjects were unable to make joint speed estimates by observing only the absolute speed of the distal link and were required to consider the speed of the proximal link serving as the moving reference frame.

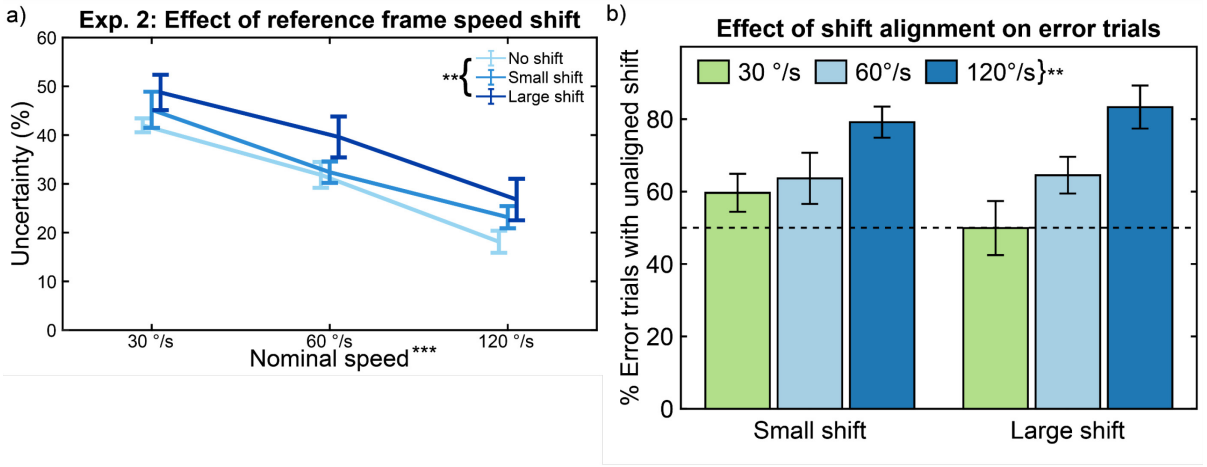

Figure 8. Effect of Reference Frame Speed Shift.

(a) Psychophysics results show that increased proximal link speed shift led to increased uncertainty. Error bars show SEM. (b) Shift and increasing joint speed results in an overestimation in joint speed, as shown by an increase in error rate of unaligned trials. The dashed horizontal line indicates the ideal ratio of aligned- to unaligned trials. Error bars show SEM. (**) $p < 0.01$, (***) $p < 0.001$

Main effects analysis showed that both *speed* (B = -0.0024, $t(69) = 9.02$, $p < 0.0001$) and *shift* (B = 0.0773, $t(69) = 3.12$, $p = 0.0026$) significantly affected uncertainty [**Figure 8a**]. The change in uncertainty associated with changing joint speed confirms the results from Experiment 1 showing similar trends. Additionally, the increase in uncertainty resulting from increased reference frame speed shifts suggests that vision cannot completely filter out reference frame movement during

joint speed observations and provides further evidence that joint speed estimates are more uncertain than absolute speed estimates.

Post-hoc analyses investigated if either *speed* or *shift* affected the proportion of incorrect stimulus selections where the selected joint speed was slower, but the reference frame moved faster, than the correct stimulus. This rate increased significantly during trials with higher joint *speed* (B = 0.293, $t(45) = 4.59$, $p < 0.0001$), but was not affected by *shift* magnitude (B = -3.120, $t(45) = 0.33$, $p = 0.746$) [**Figure 8b**]. This result provides further evidence that vision cannot completely ignore reference frame movement during joint speed observations; instead, reference frame movement may result in an overestimation of, especially, faster joint speeds.

Our results suggest vision cannot completely account for the effect of a moving reference frame when making joint speed estimates, and that a moving reference frame may result in overestimation of the joint speed. Having shown that uncertainty of visual joint speed estimates is greater than absolute speed estimates, we move on to Experiment 3 to determine if vision can be augmented with artificial sensory feedback.

2.4.3. Experiment 3: Effect of Augmentation

Experiment 3 served as a proof-of-concept to show that visual perception of joint speed could be significantly improved with audio feedback. The procedure for Experiment 3 was the same as that for Experiment 2, but subjects wore noise-canceling headphones playing frequency-modulated audio feedback proportional to the speed of the distal joint (i.e. joint speed). Subjects combined visual and auditory cues to arrive at a single joint speed estimate. Main effects analysis revealed

significant improvement in uncertainty with audio feedback, over vision alone ($t(11.06) = 8.14$, $p < 0.0001$, $d = 3.32$), providing clear evidence of visual augmentation [**Figure 9**].

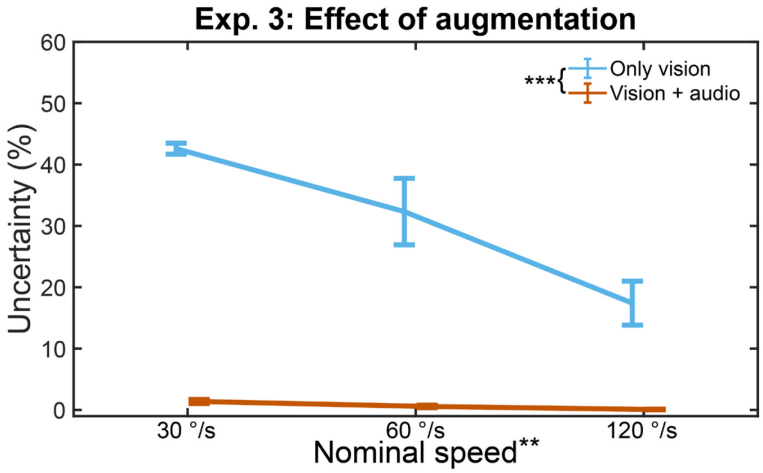

Figure 9. Effect of Augmentation.

Visual perception of joint speed is dependent on speed, but audio feedback perception of joint speed is largely speed invariant. Error bars show SEM. (**) $p < 0.01$, (***) $p < 0.001$

Simple main effects analysis revealed speed-varying uncertainty for both *vision* ($B = -0.0028$, $t(10) = 4.93$, $p = 0.0018$) and *vision + audio* ($B = -0.0001$, $t(10) = 3.86$, $p = 0.0094$). In addition, interaction between *feedback* and *speed* ($F_{1,23} = 21.85$, $p = 0.0001$, $\eta^2_{partial} = 0.522$) suggests these main effects differ between conditions, particularly that joint speed perception with *vision + audio* is more speed-invariant than joint speed perception with only *vision*. Overall, our results suggest our audio feedback paradigm is sufficient to augment vision when estimating joint speed.

2.5. Discussion

In this study, we investigated visual speed perception of biomimetic arm motions to gain insights for providing sensory feedback for prosthetic limbs. In the first experiment, our results showed that discrimination of linear or absolute speed is between 20% and 30%, whereas discrimination

of joint speed is between 30% and 60% [**Figure 7**]. In the context of providing feedback for prosthetic limbs, our results suggest that providing joint speed feedback will yield the largest improvement to artificial kinesthesia when users are also able to see the prosthesis.

In the second experiment, our results revealed that variations in the speed of the reference frame reduced discriminatory ability of joint speed observations [**Figure 8a**]. In post-hoc analyses, we also determined that subjects became more likely to perceive a slower joint speed in a faster reference frame as a faster joint speed, resulting in more incorrect selections [**Figure 8b**]. This may suggest a multiplicative effect of reference frame speed on joint speed perception. While we found no significant interaction effect between *joint speed* and *shift*, interaction between the two may have plateaued below the magnitudes tested. It is possible that this multiplicative effect arises at smaller reference frame speed shift magnitudes, but further experiments would be required to show this effect. In the context of providing feedback for prosthetic limbs, this second experiment provides evidence that visual joint speed perception is more variable when moving within a time-varying reference frame, such as a prosthetic hand and wrist moving relative to a user's biological shoulder and elbow. As such, providing joint speed feedback should be most beneficial during tasks requiring coordinated synchronous movement of both robotic and biological joints.

In the third experiment, we showed that visual joint speed estimates can be successfully supplemented with artificial sensory feedback. We provided subjects with frequency-modulated audio cues encoding the speed of the distal link. By playing this joint speed feedback alongside the visual stimuli, joint speed discrimination was reduced below 1%. Additionally, whereas visual discriminatory power varied across nominal speeds, joint speed discrimination was largely invariant with joint speed changes when audio feedback was provided [**Figure 9**]. This experiment

was conducted with no shift to the proximal link speed, the condition with the greatest visual joint speed perception. Because audio feedback is dependent solely on joint speed, proximal link speed shifts which negatively affect visual perception would have no effect on audio perception. Thus, joint speed feedback would provide greater benefits during tasks requiring inter-joint coordination.

Taken together, these results suggest joint speed audio feedback may improve the sense of kinesthesia for prosthesis users, even when the prosthetic limb is still visible and especially while the residual limb is in motion. This strengthened sensory feedback should, in turn, strengthen internal models associated with reaching tasks, resulting in improved motor learning and control (Wolpert, Ghahramani and Jordan, 1995). These benefits may extend beyond prosthetic limbs to include other applications such as robot teleoperated tasks.

Because sensory feedback is merged inversely proportional to each modality's uncertainty (Kuschel *et al.*, 2010), sensory feedback encoding position will likely not significantly augment proprioception of a prosthetic limb unless it matches or exceeds vision's 1% uncertainty (Ross, 2003) or encodes information in a novel way, such as tactile sensation (Schiefer *et al.*, 2016; De Nunzio *et al.*, 2017) or discrete events in grasping (Cipriani *et al.*, 2014). However, our study suggests that sensory feedback encoding prosthetic joint speed may more significantly augment kinesthesia of a prosthetic limb due to higher uncertainty in visual estimates of limb joint speed. Additionally, sensory feedback provided for intrinsic joint coordinates should always be relevant to limb control, as opposed to feedback provided in extrinsic coordinates, which may only be conditionally relevant (Berniker and Kording, 2011). This persistent relevance would ensure greater generalizability to novel tasks during motor learning with a prosthetic limb (Berniker and

Kording, 2008). Finally, joint speed in this context is synonymous with the robotic motor command; thus, no additional sensors are required to encode joint speed for prosthesis feedback.

The major limitation of our work is that all speed estimates were made in a controlled environment: only the two-arm link was shown on screen over a uniform white background, and subjects wore noise-canceling headphones during audio feedback trials. Subjects were exposed to neither the distractions nor divided attention that occur with daily prosthesis use. Additionally, subjects were not asked to control the simulated limb while assessing joint speed, and subjects were able to devote their full attention to visual estimates. Thus, showing that the audio feedback *can* be incorporated into speed estimates does not necessarily mean that the information *will* be incorporated meaningfully during user-in-the-loop control tasks. Prosthesis users typically visually track their prosthesis while in use until they reach an object of interest, at which point visual attention is shared between the object and the prosthesis end effector (Sobuh *et al.*, 2014), but there is no guarantee that prosthesis users with sensory feedback would revert to able-bodied eye gaze behavior (Land, Mennie and Rusted, 1999). To address this limitation, future real-time experiments will determine the added benefit of joint feedback during reaching tasks.

A limitation of Experiment 2 is that only positive reference frame shifts were tested [**Figure 6**]. The purpose of this experiment was to remove the possibility that subjects were approximating joint speed by estimating absolute speed of the distal link. Shifts slowing down the reference frame would make it easier for subjects to approximate joint speed with absolute speed estimates, so we opted to only test shifts increasing the reference frame speed. To more rigorously quantify psychophysical measures and the effect of reference frame shifts as a confounding factor, a fully-

blocked design with different nominal reference frame speeds, joint speeds, and shift magnitudes and directions would be required.

In this study, audio feedback only provided joint speed information for a single degree of freedom. However, it is unknown how well users will understand feedback presented simultaneously for multiple degrees of freedom. Subjective feedback during a previous study revealed subjects found it difficult to understand amplitude-modulated audio feedback for a two-degree-of-freedom virtual limb (Earley *et al.*, 2017b), though other studies have demonstrated subjects are capable of understanding frequency-modulated audio feedback for two degrees of freedom (Ahmed W. Shehata, Scheme and Sensinger, 2018). Another option is to provide feedback through a different modality, such as vibrotactile, and encode active degree of freedom via stimulus location. Further psychophysical experiments would be necessary to characterize the discriminatory power of simultaneous feedback.

Audio feedback has been shown to strengthen a user's internal model and improve their myoelectric prosthesis control performance (Ahmed W. Shehata, Scheme and Sensinger, 2018), however audio feedback may not be viable for daily use. Many myoelectric prosthesis users exploit sound and vibrations from the motors as a proxy for proprioceptive information (Childress, 1980; Ninu *et al.*, 2014), but this motor noise may also diminish the perceived cosmesis of the limb. Additionally, audio feedback may interfere with activities of daily living requiring unobstructed hearing, such as traveling and conversing with others. Other feedback modalities may be implemented during daily use with fewer obstructions; however, audio feedback provides a best-case scenario for augmenting joint speed discrimination. Pitch discrimination within a standard piano range (27.5 Hz – 4.2 kHz) is well below 1% (Wier, Jesteadt and Green, 1977). By contrast,

our results suggest visual speed discrimination of 20% or more, though previous research has suggested as low as 10% (Chen *et al.*, 1998). Although audio frequency was easily scaled to augment visual joint speed discrimination, other feedback modalities may not have the working range and psychophysical precision to significantly augment visual estimates.

Various methods have been proposed to restore physiologically-analogous sensations. Implanted peripheral nerve cuff electrodes can provide natural touch perception with stable sensory maps (Tan *et al.*, 2014), restoring a sense of grasping force which improves functional task performance (Schiefer *et al.*, 2016). Sensation of limb motion has also been restored through vibration-induced illusory kinesthesia, resulting in improved prosthesis movement control and agency over these movements (Marasco *et al.*, 2018). Though these methods do not rely on sensory substitution to restore physiological kinesthesia, they still must be comparable to the discriminatory power of vision to integrate reliably. Future work will develop a framework to computationally determine the minimum feedback range required for artificial sensory feedback to improve biological observations.

2.6. Conclusions

Lack of sensory feedback is a major limitation for modern prosthetic limbs. It is important to not only develop artificial sensory feedback for these limbs, but also to strive for feedback that is more than situationally beneficial. To this end, we investigated human visual perception of arm motion to determine its strengths and, particularly, weaknesses. Our work suggests that vision is most uncertain about joint speed observations, and that it is possible to improve these estimates with artificial sensory feedback. Because this feedback improves joint speed perception even in the presence of vision, we anticipate our proposed feedback system improving myoelectric prosthesis

control in a variety of daily tasks, ultimately leading to an improved sense of independence and quality of life for upper-limb prosthesis users.

2.7. Data Availability

MATLAB protocol and data analysis code, formatted data files, and R statistical analysis code are freely available for download on the Open Science Framework (E.J. Earley and Johnson, 2018). Additional data are available upon request.

3. Artificial Joint Speed Feedback for Non-Amputee Myoelectric Prosthesis Control

Authors: Eric J. Earley, Reva E. Johnson, Levi J. Hargrove, Jon W. Sensinger

3.1. Abstract

Accurate control of our limbs requires both biological feedforward and feedback signals. For prosthetic arms, feedforward control is commonly accomplished by recording myoelectric signals from the residual limb to predict the user's intent. However, commercial prostheses often lack any feedback signals. Previous feedback studies have demonstrated inconsistent results when artificial feedback was provided in the presence of vision. We hypothesized that negligible benefits in past studies may have been due to artificial feedback with low precision compared to vision, which results in heavy reliance on vision during reaching tasks. In this study, we test an artificial sensory feedback system providing joint speed information and how it impacts ballistic reach performance and adaptation to self- and perturbation-generated errors. We found reduced reaching errors during steady-state reaches in both Cartesian and joint reference frames, and modest improvement in overall reaching errors after perturbed control, but other aspects of reaching behavior are unaffected. These results provide insights into the relevant determinants of artificial sensory feedback, which may further development of myoelectric prosthetic limbs.

3.2. Background

Our bodies rely on bi-directional communication between our brains and our limbs for coordinated movement. Descending motor commands and ascending feedback travel via the nerves in our extremities (Jones, 2000). Sensory feedback encode several aspects of body state, the most important of which during gross limb control is proprioception, which guides the brain to make minute corrections during movements in a process called motor adaptation (Bilodeau and

Bilodeau, 1961). Concurrently, the brain develops and refines internal models of the motor commands required to produce desired limb movements (Wolpert, Ghahramani and Jordan, 1995). Lack of this feedback results in a drastic decrease in coordinated control over the limb (Sainburg *et al.*, 1995).

It is no surprise, then, that the lack of proprioceptive feedback is a major limitation for robotic prosthetic arms (Cordella *et al.*, 2016). A commonly-researched method of restoring this missing branch of the communication loop is through sensory substitution (Antfolk *et al.*, 2013). Proprioceptive information such as limb position or speed are communicated to the user indirectly using separate sensory channels including vibration (Stanley and Kuchenbecker, 2012; Witteveen *et al.*, 2012; Cipriani *et al.*, 2014; De Nunzio *et al.*, 2017; Krueger *et al.*, 2017) and audio (Mirelman *et al.*, 2011; Ahmed W Shehata, Scheme and Sensinger, 2018; Ahmed W. Shehata, Scheme and Sensinger, 2018) cues. However, although studies typically show improved limb control with sight of the prosthesis obscured, these benefits do not always translate to tasks where the prosthesis is visible – some studies demonstrate improvement (Graczyk, Resnik, *et al.*, 2018; Marasco *et al.*, 2018; Markovic, Schweisfurth, Engels, Farina, *et al.*, 2018; Christie *et al.*, 2019), while others show no change (Cipriani *et al.*, 2008; Brown *et al.*, 2015; Witteveen, Rietman and Veltink, 2015; Christie *et al.*, 2019).

Recent research suggests that the success or failure of artificial sensory feedback to confer improvements to prosthesis control is dependent on several connected factors, including the complexity of the task and the precision of feedforward internal models (Markovic, Schweisfurth, Engels, Bentz, *et al.*, 2018). As feedforward internal models improve, tasks can be completed while relying less on feedback to make corrections. However, appropriately developing this

feedforward controller requires accurate sensory feedback. One unexplored factor which may affect both the achieved benefit from artificial feedback and the speed of developing a feedforward controller is that of sensory fusion (Körding and Wolpert, 2004).

When a single measurement (e.g. limb kinematics) can be observed simultaneously from two sources (e.g. vision and proprioception), the final estimated measurement is weighted according to each source's uncertainty (Ernst and Banks, 2002; Hillis *et al.*, 2002). Thus, because vision is often significantly more precise than the modality used for sensory substitution, these redundant proprioceptive cues may be ignored in favor of vision. This phenomenon suggests that the benefit conferred by sensory substitution is dependent on its level of uncertainty compared to vision – negligible benefit with higher uncertainty, marginal benefit with approximately equivalent uncertainty, and significant benefit with lower uncertainty.

Prior research suggests that vision has very low uncertainty when estimating position (van Beers *et al.*, 2002; Ross, 2003), but higher uncertainty when estimating speed (Chen *et al.*, 1998; Stocker and Simoncelli, 2006). In our previous study, we used psychophysics techniques to measure speed perception in vision and showed that visual estimates of joint speed are poorest when compared to absolute angular or linear speeds. Furthermore, we developed an audio feedback paradigm capable of providing prosthetic limb joint speed more precisely than vision (Earley *et al.*, 2018). Although we have demonstrated the capacity to augment vision with audio feedback in observational tasks, we have yet to investigate the effects of audio feedback during real-time reaching tasks.

The purpose of this study is to evaluate augmented joint speed feedback's ability to reduce reaching errors and improve the rate of adaptation during reaching tasks. Subjects performed ballistic center-out reaches requiring coordinated movement of a positional- and myoelectric-controlled

limb. We measured trial-by-trial adaptation to self-generated errors during steady-state reaches to determine the strength of the generated internal model. We also measured the adaptation rate across several trials immediately post-perturbation to understand the speed at which internal models update to changing system parameters.

3.3. Methods

3.3.1. Subjects

16 right hand-dominant, non-amputee subjects participated in this study, which was approved by the Northwestern University Institutional Review Board. The number of subjects was determined via power analysis to detect a large effect size ($f = 0.4$) with significance level $\alpha = 0.05$, power $(1-\beta) = 0.80$, and up to 12 planned comparisons with Bonferroni corrections. All subjects provided informed consent before starting the study.

3.3.2. Experimental Setup

Subjects participated in two experimental sessions: one session with no audio feedback, and one session with frequency-modulated joint speed audio feedback. The order of these sessions was randomized across subjects using balanced block randomization.

Subjects sat in front of a computer monitor and placed their right arms in a wrist brace. The wrist brace was supported by a ball bearing cart on a table adjusted so the subject's shoulder was abducted to 90°. The ball bearing cart allowed the brace to move freely across the surface of the table. A blanket was draped over the table to reduce noise from the ball bearings during movement.

Two Delsys Bagnoli electromyographic (EMG) sensors were placed over the flexor and extensor compartments of the forearm. The reference electrode was placed over the olecranon. EMG signals

were high-pass filtered at 0.1Hz, positive-rectified, and low-pass filtered at 5Hz using 2nd order Butterworth filters. A Biometrics twin-axis electrogoniometer was secured to the upper and lower arm to measure the elbow flexion angle. Goniometer signals were low-pass filtered at 5Hz using a 2nd order Butterworth filter. Data were acquired at 1000Hz and, after filtering, downsampled to 100Hz.

Subjects used the goniometer and their EMG signals to control a virtual two-link arm with 10cm lengths. Goniometer measurements controlled the position of the proximal link, and EMG measurements controlled the velocity of the distal link; wrist extension drove the link clockwise, and wrist flexion drove the link counterclockwise. [**Figure 10a**].

The virtual arm started with the proximal link vertical (at 90°) and the distal link creating a 30° angle from the proximal link [black link, **Figure 10b**]. Throughout the experiment, targets appeared in one of four locations corresponding to limb positions relative to the home position: +60° and -60° from the neutral proximal link position, and -45° and -90° from the neutral distal link position [green crosses, **Figure 10b**].

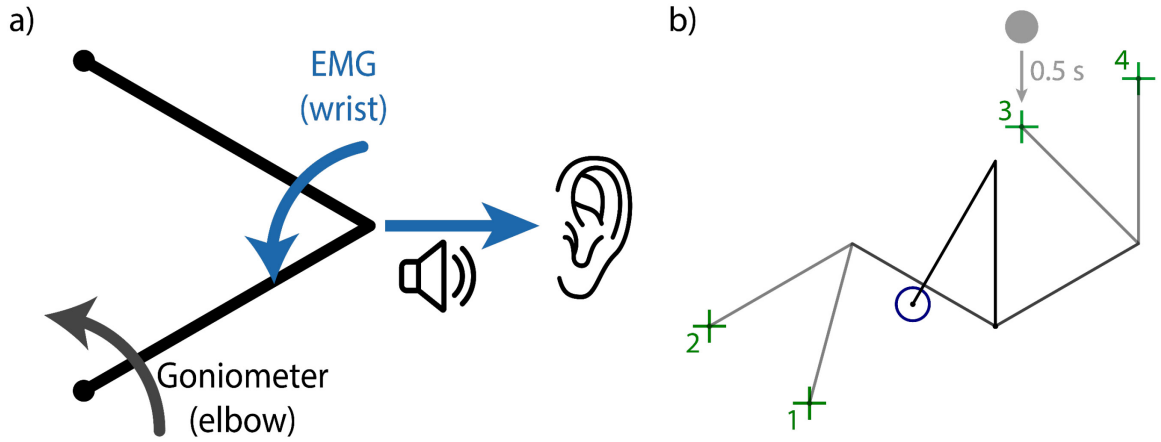

Figure 10. Center-Out Reaching Experiment Setup.

(a) Goniometer controls the proximal link, EMG controls the distal link. Distal link speed is used for frequency-modulated audio feedback. (b) Subjects perform center-out reaches with the virtual limb (black), starting from the home circle (blue) and reaching for one of four targets (green). Before each reach, a grey ball would appear above the target. When the limb endpoint left the home circle, the ball began to drop, centering on the target after half a second, signifying the end of the trial.

Subjects controlled the virtual arm to perform ballistic center-out reaches. A ball was shown above each target and dropped at a constant speed when the cursor left the home circle [blue circle, **Figure 10b**]. The ball aligned with the center of the target at 0.5 seconds; subjects were instructed to reach towards the target, stopping when the ball reached the target (Schmidt *et al.*, 1979).

If the proximal or distal link were moving faster than 45°/s, the ball was colored red to indicate the failed end condition. Otherwise, if the cursor was inside of the target at the end of the trial, the ball was colored green to indicate a successful trial.

3.3.3. Audio Feedback

During both experimental sessions, subjects wore noise-canceling headphones (Bose QuietComfort 35 II). During the *No Feedback* session, no sounds were played. During the

Feedback session, frequency-modulated joint speed audio feedback was provided according to the following equation:

$$f = f_{min} * 2^{\frac{\omega}{V_{step}}} \quad (8)$$

where ω is the angular speed of the distal link, f_{min} is the minimum desired frequency (220 Hz), and V_{step} is the angular velocity increase that would result in a one-octave increase in pitch (60°/s). No sound played while the distal link was not moving. Audio feedback was provided during the entire session, including during training.

3.3.4. Familiarization

To learn to control the virtual arm, subjects completed 80 training center-out reaches [**Figure 11a**]. The first 40 trials had a specified reaching order (four sets of 10 reaches towards each target), and the second 40 trials had a balanced and randomized reaching order (10 reaches total towards each target).

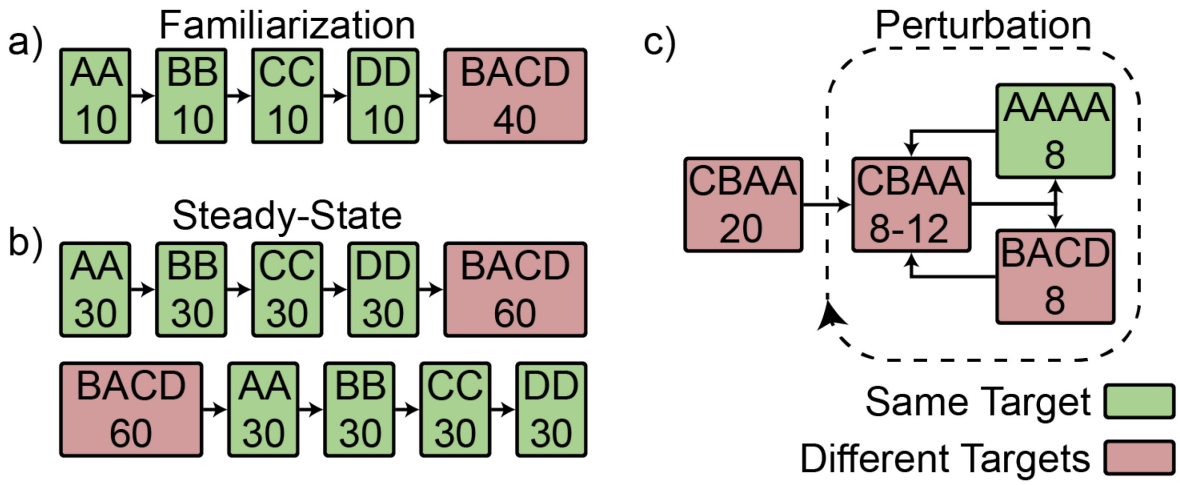

Figure 11. Non-Amputee Experimental Protocol.

Subjects completed the experimental protocol twice – once with and once without audio feedback. The order of the *feedback* and *no feedback* sessions was randomized across subjects. (a) Familiarization involved a total of 80 reaches: four sets of 10 reaches towards each target, and 40 reaches towards targets in balanced random order. (b) The steady-state block involved a total of 180 reaches: four sets of 30 reaches towards each target, and 60 reaches towards targets in balanced random order. The order of same- or different-target groupings was randomized across subjects and consistent between subject visits. (c) The Perturbation block started with 20 reaches towards targets in random order. After these baseline trials, subjects did cycles of 8-12 reaches towards targets in random order, followed by either 8 reaches towards the same target, or 8 reaches towards targets in balanced random order. The order of these cycles was randomized across subjects and consistent between subject visits.

3.3.5. Steady-State Block

To test trial-by-trial adaptation to self-generated errors, subjects completed 180 center-out reaches separated into one set of 60 and one set of 120 [**Figure 11b**]. The order of these sets was randomized across subjects using balanced block randomization.

During the set of 60 trials, subjects reached towards targets in a balanced and randomized order. During the set of 120 trials, subjects completed four sets of 30 reaches towards each target. For

each set, expanding window optimization separated initial trials from steady-state trials (Blustein *et al.*, 2018).

To determine if subjects moved the proximal and distal links simultaneously during reaches, we calculated the simultaneity of steady-state reaches *post-hoc*. Simultaneity for each trial was calculated as the time where both proximal and distal link speeds are greater than 15°/s, as proportion of the reach time where at least one link speed was greater than 15°/s. These were averaged across steady-state trials for each subject, then compared between feedback conditions and between target order using the following model:

$$y \sim subject + feedback + target + feedback\ x\ target \tag{9}$$

where *subject* was coded as a categorical random variable and *feedback* and *target* were coded as categorical independent variables. Holm-Bonferroni corrections were made for 10 total planned comparisons across all steady-state block analyses.

Trial-by-trial adaptation is defined as the amount of correction from one trial to the next, given the amount of error on the first trial:

$$\Delta_{Error}(t+1) = a * Error(t) + \Delta_0 \tag{10}$$

where a is the adaptation rate and Δ_0 is the y-intercept, or the correction elicited when the previous trial has no error. While the y-intercept holds little real-world import in describing adaptation behavior, the x-intercept b describes the bias during reaches, or the error which elicits no correction:

$$b = \frac{-\Delta_0}{a} \tag{11}$$

Because of limb angle constraints, each position in the Cartesian reaching space can only be achieved with a single joint configuration. Thus, there exists a one-to-one mapping of Cartesian coordinates to joint configuration.

This one-to-one mapping allowed us to calculate trial-by-trial adaptation for the elbow and wrist joint angle deviations from the required angles needed to attain the target. The adaptation rate a and the bias b were compared between feedback conditions and between target order using the following model:

$$y \sim subject + feedback + target + feedback\ x\ target \quad (12)$$

where *subject* is coded as a categorical random variable and *feedback* and *target* are coded as categorical independent variables. Holm-Bonferroni corrections were made for the number of terms in each steady-state block model.

If reaches are drawn from a Gaussian distribution, traditional trial-by-trial analysis biases towards higher adaptation rates (Blustein *et al.*, 2018). To account for this, we ran a secondary *post-hoc* trial-by-trial analysis using a computational motor control approach. This approach models steady-state adaptation behavior using a hierarchical Kalman filter paradigm to simulate state and internal model parameter estimation, providing an unbiased estimate of true adaptation behavior (Reva E. Johnson *et al.*, 2017) [**Appendix C**]. Because this analysis requires a stationary target, we only performed this analysis on steady-state reaches towards the same target.

3.3.6. Perturbation Block

To test the speed of adaptation to external perturbations to the control system, subjects completed 20 practice trials followed by 24 sets of perturbation trials. During each set, subjects started by

making 8-12 unperturbed reaches towards random targets. The system was then perturbed by doubling the EMG gain, increasing the speed of the distal link and making accurate control more difficult. Subjects then made 8 reaches with the perturbed dynamics. These sets of 8 reaches fell into two categories: towards the *same target*, or towards *different targets*. Each category was tested in 12 sets of the perturbation trials [**Figure 11c**]. The order of these sets was determined randomly.

Perturbation adaptation of the Euclidean distance between the cursor and the target was estimated using an exponential decay model (Burge, Ernst and Banks, 2008; Huang *et al.*, 2011; Canaveral *et al.*, 2017):

$$y = \alpha e^{-\lambda t} + \epsilon_{\infty} \tag{13}$$

where t is the number of trials after perturbation onset, α is the gain indicating the immediate increase in error upon perturbation, and λ is the decay rate indicating the speed at which the error converges to the baseline error ε_{∞}.

To fit all three parameters for each *feedback* and *target* condition simultaneously, we used a hierarchical nonlinear mixed effects model. The top-level model was defined as the exponential decay model above. The gain α, decay rate λ, and baseline error ε_{∞} were each fit with the second-level model:

$$y \sim \beta_0 + subject + feedback + target + feedback\ x\ target \tag{14}$$

where *subject* was coded as a categorical random variable and *feedback* and *target* were coded as categorical independent variables.

3.4. Results

3.4.1. Steady-State Block

Steady-state reaches provide insight into how subjects coordinate positional- and myoelectric-controlled joints during reaching tasks, and may be used to quantify compensatory movements in one joint arising from errors or poor control in the other. No significant interactions were found (p_{min} = 0.923), so interaction terms were removed and the models were rerun. Joint speed feedback showed weak evidence of lower endpoint (B = -0.183, $t(61)$ = 1.595, p = 0.187) and wrist errors (B = -1.154, $t(61)$ = 1.740, p = 0.177), but no difference in elbow angle errors (B = -0.272, $t(61)$ = 0.542, p = 0.590). Reaches towards different targets also showed some evidence of higher endpoint errors (B = 0.197, $t(61)$ = 1.714, p = 0.187), elbow errors (B = 1.270, $t(61)$ = 2.532, p = 0.030) , and wrist errors (B = 0.781, $t(61)$ = 1.178, p = 0.245). **Figure 12** shows the errors in Euclidean (**a, d**) and joint (**b-c, e-f**) spaces.

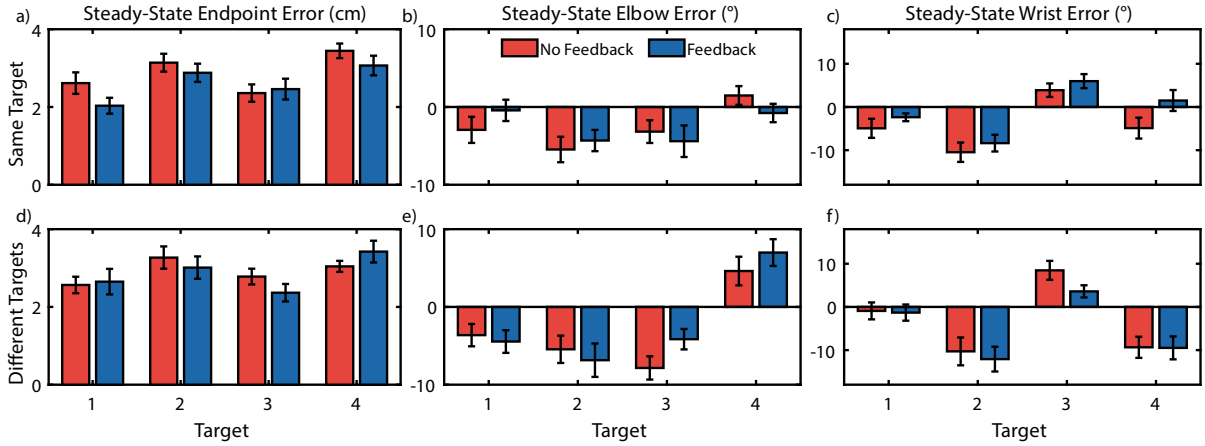

Figure 12. Non-Amputee Endpoint and Joint Angle Errors.

Endpoint and joint angle errors vary moderately by target, but present no consistent differences between feedback conditions, nor between reaches towards same or different targets. Error bars indicate standard error of the mean (a-c) Errors while reaching towards the same target for endpoint (a), elbow (b), and wrist (c). (d-f) Errors while reaching towards different targets for endpoint (d), elbow (e), and wrist (f).

Simultaneity is shown in **Figure 13**. The averaged speed traces shown in **Figure 13a-b** show no significant differences between reaching patterns for feedback or target conditions. The velocity profiles of the elbow appear symmetric, whereas the peak velocity of the wrist appears to occur earlier in the reach and decays more slowly. There are also higher wrist speeds for Targets 2 and 4, which correspond with the targets requiring greater wrist movement to achieve.

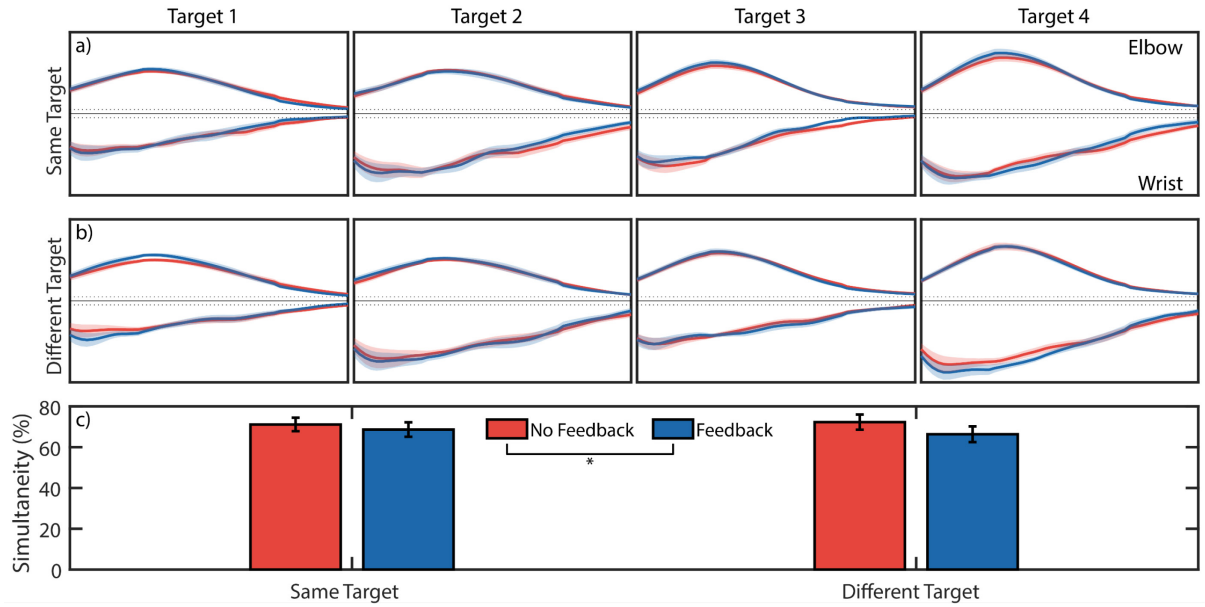

Figure 13. Non-Amputee Reaching Simultaneity.

(a-b) Average and standard error of speed traces during steady-state reaches towards the same target (a) or different targets (b) for the elbow (top) and wrist (bottom) show generally consistent reaching profiles regardless of target. The earlier peak speed and asymmetric speed profile for wrist speed, compared to elbow speed, suggests wrist movement preempts elbow movement. Dashed lines indicate minimum speed threshold. (c) Simultaneity during steady-state reaches suggests lower simultaneity with feedback than without, but no differences between target conditions. Error bars indicate standard error of the mean. (*) indicates $p < 0.05$.

There was no significant interaction between *feedback* and *target* ($p = 0.667$), so the interaction term was removed and the model rerun (Kutner, 2005). We found significantly lower simultaneity with feedback than without ($B = -0.040$, $t(61) = 2.822$, $p = 0.014$), which may be caused by ending wrist movements sooner during reaches [**Figure 13a-b**]. We found no significant differences between target conditions ($B = -0.006$, $t(61) = 0.447$, $p = 0.657$).

Trial-by-trial adaptation fit coefficients showed no differences in adaptation bias, but consistently lower adaptation rate when reaching towards different targets, compared to reaching towards the same target, for both the goniometer-controlled elbow and EMG-controlled wrist [**Figure 14**].

There were no significant interactions between *feedback* and *target* for elbow bias or rate (p_{min} = 0.592), so the interaction terms were removed and the models rerun (Kutner, 2005). Elbow bias was reduced when provided *feedback* (B = -0.163, $t(61)$ = 1.516, p = 0.136) and increased when reaching towards different *targets* (B = 0.228, $t(61)$ = 2.119, p = 0.079). We found a significant difference in elbow rate between *target* conditions (B = -0.188, $t(61)$ = 6.866, $p < 0.001$), but not *feedback* conditions (B = -0.033, $t(61)$ = 1.225, p = 0.227).

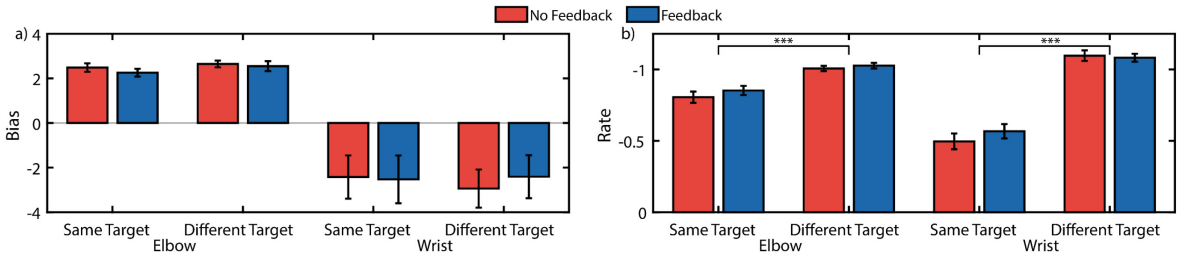

Figure 14. Non-Amputee Trial-by-Trial Adaptation Analysis.

Trial-by-trial adaptation coefficients suggests the elbow overreaches to compensate for an underreaching wrist, but shows no change in trial-by-trial adaptation between feedback conditions. (a) Trial-by-trial adaptation bias (b) Trial-by-trial adaptation rate. (***) indicates $p < 0.001$.

There were no significant interactions between *feedback* and *target* for wrist bias or rate (p_{min} = 0.509), so the interaction terms were removed and the models rerun (Kutner, 2005). There were no significant differences in wrist bias between *feedback* (B = 0.213, $t(61)$ = 0.380, $p > 0.999$) or *target* conditions (B = -0.199, $t(61)$ = 0.357, $p > 0.999$). We found a significant difference in wrist rate between *target* conditions (B = -0.558, $t(61)$ = 12.809, $p < 0.001$), but not *feedback* conditions (B = -0.028, $t(61)$ = 0.652, p = 0.518).

To supplement our traditional trial-by-trial analysis, we ran a secondary analysis using the Control Bottleneck Index (CBI), a computational motor control approach [**Appendix C**]. Interestingly, we

found that joint speed feedback may improve steady-state adaptation of the positional elbow movements (B = 0.178, $t(62)$ = 1.592, p = 0.122), but did not significantly affect adaptation rate of myoelectric wrist movements (B = -0.091, $t(62)$ = 1.006, p = 0.322) [**Figure 15**]. Analyzing the control noise (Q) revealed a no significant differences for elbow (B = -5.120, $t(62)$ = 1.371, p = 0.190) or wrist (B = 1.295, $t(62)$ = 0.063, p = 0.951) control.

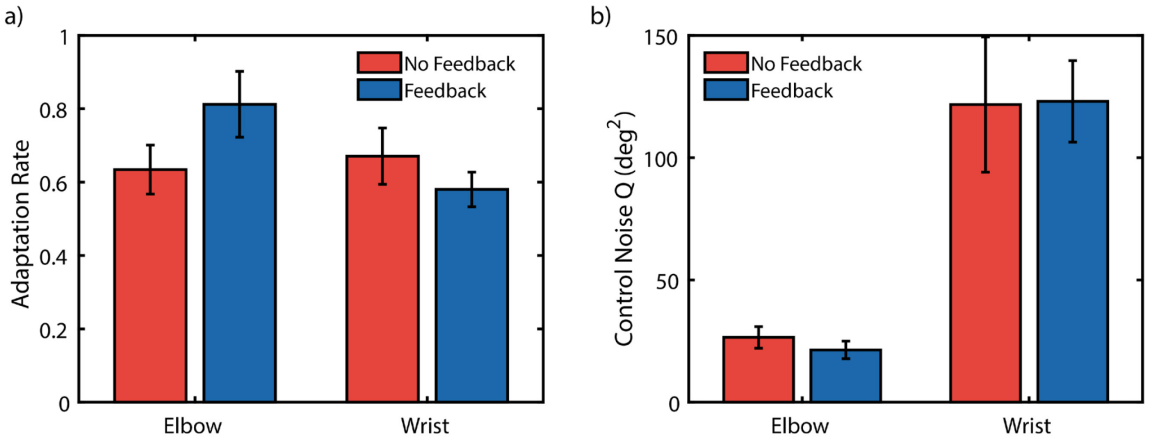

Figure 15. Non-Amputee Control Bottleneck Index Analysis.

A secondary trial-by-trial analysis using computational motor control approach found that (a) joint-speed feedback improved adaptation of positional elbow movements, but also reduced adaptation of myoelectric wrist movements, and (b) that control noise was significantly higher for the myoelectric controlled wrist than the positional controlled elbow.

These results taken together suggest that adaptation to self-generated errors was lower when relying solely on a generalized motor program (*different targets*) compared to target-specific motor plans (*same targets*), but that joint speed feedback did not affect trial-by-trial adaptation behavior.

3.4.2. Perturbation Block

Perturbing reaches during ballistic movements creates a window through which we can measure adaptation to novel conditions. By measuring the initial and final errors after perturbing system

control and calculating the rate at which one decays to the other, it is possible to gain insight into how quickly the sensorimotor system responds and adapts to novel conditions. **Figure 16a-b** shows target error during perturbed reaches. Our results suggest that joint speed feedback may lower the overall error rate after perturbations. However, we found no significant differences in other aspects of adaptation behavior, including initial error increase upon sudden perturbation and adaptation rate.

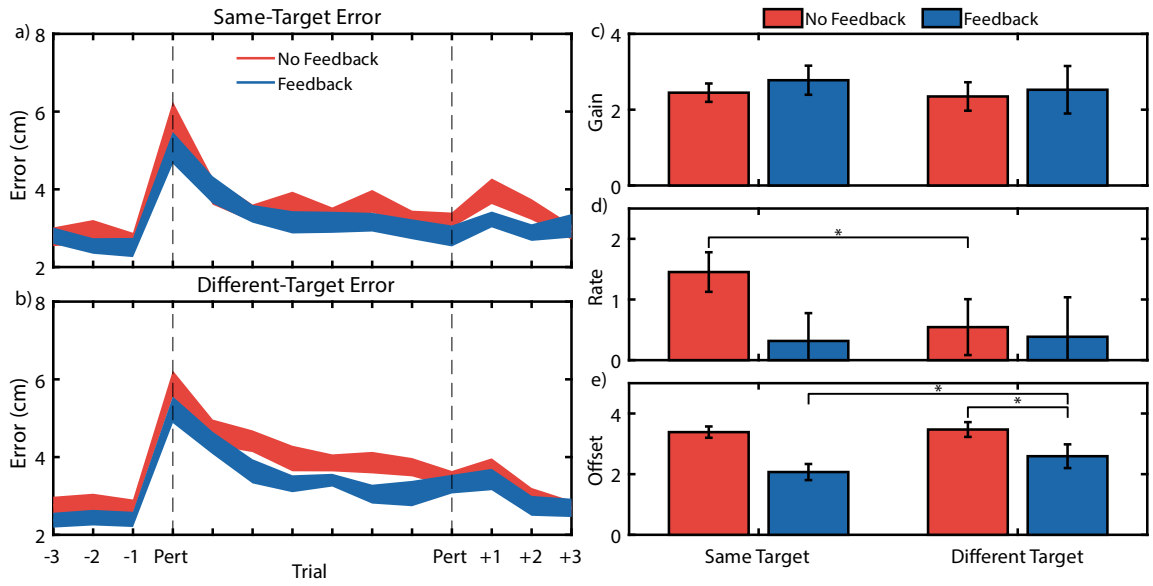

Figure 16. Non-Amputee Perturbation Adaptation.

Average error trace during perturbation block shows that feedback reduces errors during perturbation but does not change adaptation rate. (a-b) Error traces during perturbed reaches towards the same target (a) and different targets (b). (c-e) Hierarchical nonlinear mixed effects model exponential decay coefficients for the gain (c), rate (d), and offset (e). (*) indicates confidence intervals not containing 0.

A hierarchical nonlinear mixed effects model fit exponential decay coefficients to these data. **Figure 16c-e** shows these resulting coefficients. There was significant interaction between *feedback* and *target* conditions for the decay rate ($B = 0.977$, $CI = [0.038, 1.916]$). Thus, we ran a

subsequent simple main effects model for each factor at each level of the other factor (Kutner, 2005). **Table II** summarizes these results.

Table II. Non-Amputee Perturbation Block Simple Main Effects

Simple main effects analysis of exponential decay coefficients extracted from the hierarchical nonlinear mixed effects model. 95% confidence intervals shown are Holm-Bonferroni corrected for 12 planned comparisons. Greyed comparisons indicate confidence intervals not containing 0.

Parameter	Effect of *Feedback*						Effect of *Target*					
	Same Target			Different Target			No Feedback			Feedback		
	B	CI		B	CI		B	CI		B	CI	
Gain	-0.340	-1.091	0.410	-0.062	-0.742	0.617	-0.022	-0.703	0.660	-0.208	-0.900	0.484
Rate	-0.292	-1.081	0.496	-0.019	-0.176	0.138	**-1.005**	**-2.001**	**-0.008**	0.107	-0.373	0.252
Offset	-0.337	-0.692	0.019	**-0.558**	**-0.986**	**-0.130**	-0.008	-0.387	0.371	**0.422**	**0.038**	**0.806**

Of note is that *gain* did not differ significantly across any condition, confirming that behavior of the first perturbation reach is consistent across conditions as should be the case for ballistic reaches. Furthermore, the *offset* was lower with feedback while reaching towards either the *same* (B = -0.337, CI = [-0.704, 0.030]) or *different targets* (B = -0.558, CI = [-0.987, -0.129]), suggesting a lower overall baseline error at the end of the perturbation block. A trend of lower adaptation rate during reaches towards *different targets* was observed with *no feedback* (B = -1.005, CI = [-2.023, 0.012]). It should be noted that the effects B shown in **Table II** may not necessarily match up with those seen in **Figure 16c-e**; the figure shows results of the full hierarchical nonlinear mixed effects model including interaction terms, whereas the table presents results from the subsequent simple main effects models.

An analysis of the first and last perturbation trials echoes these results. We found that providing joint speed feedback significantly reduced the initial error upon sudden perturbation (B = -0.727,

$t(61) = 2.757$, $p = 0.017$), and may have reduced the final error achieved on the last trial ($B = -0.268$, $t(61) = 1.500$, $p = 0.141$).

3.5. Discussion

In this study, we investigated human performance of ballistic center-out reaches requiring simultaneous control of positional- and myoelectric-controlled joints, in a manner analogous to myoelectric prosthesis control. Our results confirmed that such reaches were indeed possible, despite initial subject difficulty. We also evaluated how joint speed feedback affects human adaptation to self-generated and externally-generated errors during ballistic reaching tasks. During steady-state reaches, errors were generally reduced in both Cartesian and joint-based reference frames with joint speed feedback available [**Figure 12**]. Analyzing trial-by-trial adaptation behavior, there was a slight reduction in compensatory elbow bias with feedback [**Figure 14a**]. Furthermore, adaptation rate was higher when reaching towards different targets than when reaching towards the same target [**Figure 14b]**, suggesting subjects adapt to self-generated errors more slowly when relying solely on generalized internal models. This is in line with previous research which has shown prior reaches affect the path of future reaches (van der Wel *et al.*, 2007) and the exploitation of path redundancy (Ranganathan and Newell, 2010). However, joint speed feedback did not significantly affect trial-by-trial adaptation rate or adaptation bias for biological (elbow) or myoelectric-controlled (wrist) joints. A secondary trial-by-trial adaptation analysis confirmed this, finding no changes in adaptation rates [**Figure 15a**] nor control noise [**Figure 15b**].

During perturbation reaches, subjects were able to adapt their reaches to a gain perturbation of the wrist controller and consequently reduce their reaching errors. Subjects achieved a lower baseline error at the end of perturbation blocks and that errors immediately following perturbation were

lower when provided joint speed feedback [**Figure 16**]. However, the adaptation rate did not differ significantly.

Investigating differences in motor control necessitates separating feedforward and feedback segments of reach; thus, ballistic movement is typically enforced, such that reaches are completed before visual or proprioceptive feedback can be used to adjust the reach trajectory. Furthermore, a typical task paradigm used to test motor control is the center-out reaching task (Pine *et al.*, 1996); for arm reaches, this task requires coordinating shoulder and elbow movements to maneuver a cursor towards a target. However, completing such a reach with a prosthetic limb is unique in that it requires simultaneous control of the robotic limb and the residual joints. To our knowledge, no prior study has investigated this type of hybrid biological/robotic ballistic reaching task.

The difference in trial-by-trial adaptation bias suggests that underreaching of the wrist was compensated for by slight overreaching of the elbow. One possible explanation for this behavior is the higher variability in the myoelectric control of that joint; to minimize Euclidean distance error between the limb endpoint and the target, subjects underreached with the wrist to reduce variability and compensated by overreaching with the elbow, which exhibits more consistent control.

One limitation of the trial-by-trial adaptation analysis is that the results describe a biased measure of the true adaptation to self-generated errors (Blustein *et al.*, 2018). We partially accounted for this by only quantifying trial-by-trial adaptation on trials which had achieved steady-state error, however our estimates are still biased. The presence of control noise during a reaching trial obfuscates the true intended response to the previous trial's reach error. In simulations for reaching behavior using a hierarchical Kalman filter model (Reva E. Johnson *et al.*, 2017), we found that

differences in underlying adaptation behavior could still be detected using traditional trial-by-trial adaptation techniques, but that control noise biases the calculated adaptation rates towards a slope of -1 (in other words, perfect adaptation). Thus, traditional trial-by-trial adaptation techniques can only reliably detect larger effect sizes. To address this bias in traditional trial-by-trial adaptation analysis, we ran a secondary analysis using a computer motor control approach. This approach models reach behavior and tuning on the internal model via a hierarchical Kalman filter paradigm (Reva E. Johnson *et al.*, 2017). Our results were unexpected – we determined that joint-speed feedback had improved adaptation for positional elbow movements, but had also worsened adaptation for myoelectric wrist movements. One possible explanation for this divergent behavior is the difference in control noise between the elbow and the wrist. Our analysis showed that the control noise for the myoelectric-controlled wrist was several times higher than the control noise for the position-controlled elbow, and that noise did not differ between *feedback* conditions.

This outcome falls in line with the difference in adaptation bias from the traditional trial-by-trial analysis, suggesting the elbow was used to compensate for wrist errors. The subjects' goal during our center-out reaching task was to minimize the distance between linkage endpoint and target center. If elbow control is deemed "more reliable" (i.e. has lower control noise) than wrist control, subjects may have used the elbow more heavily to correct for errors. Although the joint-speed feedback provided information solely about wrist movements, this information may have been used to better guide the elbow to make corrective adjustments during steady-state reaches.

Exponential decay is a useful model for describing motor adaptation to perturbations, as each parameter quantifies a different aspect of the reaching behavior over time (Burge, Ernst and Banks, 2008; Huang *et al.*, 2011; Canaveral *et al.*, 2017). *Offset* describes the error rate that reaches

converge to following many trials, *Gain* describes the initial jump in error at the onset of the perturbation compared to the *Offset*, and *Rate* describes how quickly error falls from the initial error to the *offset* value. However, one limitation of this model is that it cannot account for error values which fall below the *Offset* due to inherent reach variability. Thus, when fitting an exponential decay model to a small subset of data, such as reaches from a single subject, the model may choose unrealistic values to most closely match the limited data available.

The most common occurrence of this model fitting error was when the variability of reaches during the last 7 trials overshadowed the average improvement during these same trials. When this happens, the model achieves a best fit by passing through the y-intercept (*gain*), then immediately converging to the steady-state error (*offset*), which results in an extremely high decay *rate*. One way to address this is to constrain the model with a lower *offset* estimate (for example, by assuming that the steady-state error following perturbation will be due only to reach variability and removing the effect of reach bias (Earley and Hargrove, 2019) [**Appendix B**]. However, the hierarchical non-linear mixed-effects model circumvents this issue by using a large amount of data and simultaneously fitting the three parameters across all conditions while still allowing for individual subject variability via random effects.

The uncharacteristically high adaptation rate observed for reaches towards the *same target* with *no feedback* warrants additional attention [**Figure 16d**]. On average, while reaching towards the *same target*, errors were higher on the first perturbation trial with *no feedback* available. However, the errors are about the same by the second trial, suggesting larger improvement with no feedback. Furthermore, this behavior is not seen when reaching towards *different targets*. One potential explanation of this behavior is that it is an artifact of the duration of our ballistic movements. In

typical center-out reaching studies, ballistic movements are defined on the order of 200ms or less (Schmidt *et al.*, 1979). However, to accommodate the myoelectric control used in this study, we defined our threshold of ballistic movement as 500ms, which could be long enough for subjects to react to changes. Mean auditory simple reaction times are between 140-160 ms, and mean visual simple reaction times are between 180-200 ms (Welford, 1980); choice reaction times are longer, but differences between modalities remain the same (Sanders, 2013). It is possible that the difference in reaction times between audio feedback and vision-only conditions (*feedback* vs. *no feedback*) were great enough to allow for error correction during the reach with *feedback*, which is suggested by the lower initial error rates. This drastic observed increase in error during *no feedback* conditions combined with the ability to rely on a target-specific motor plan during the *same target* condition may explain the uncharacteristically high adaptation rate.

Artificial sensory feedback for prosthetic limbs is a frequent research topic, but their results vary widely. Studies that block vision and hearing consistently demonstrate the benefits of artificial sensory feedback, whereas study outcomes with these senses available become inconsistent (Markovic, Schweisfurth, Engels, Bentz, *et al.*, 2018). In this study, we investigated whether providing proprioceptive information not interpreted precisely via these intact sensory modalities was a factor in determining the benefit of artificial sensory feedback. Using a Bayesian sensory integration framework, we developed an audio feedback paradigm to provide joint speed cues, a measurement not well estimated by vision.

We found limited improvement in reducing error after sudden controller perturbations, but no improvements reducing average errors or adaptation behavior to self-generated errors. This does not, however, mean that Bayesian sensory integration can provide no insight into creating

beneficial sensory feedback. The determinants of sensory feedback improvement are complex and intertwined. To fit the constraints of ballistic reaching, our tasks were simple center-out reaches. However, recent studies suggest that the benefits of feedback are more pronounced when provided during complex tasks necessitating complex prosthesis coordination (Saunders and Vijayakumar, 2011; Markovic, Schweisfurth, Engels, Bentz, *et al.*, 2018). After practice, subjects may have developed a sufficiently strong internal model for the simple reaches, negating the benefits of feedback.

An alternative explanation for our outcomes is the increased presence of tactile and proprioceptive cues from our intact-limb subjects. Wrist flexion and extension contractions were isometric, but the wrist brace exerted antagonistic forces during these contractions. Thus, it is possible our artificial sensory feedback system was integrating with not only vision, but also the magnitude of this restrictive force. Our results remain valid for the purposes of teleoperated robotics including industrial machinery and surgical robots, however further investigation is required for myoelectric prosthesis applications. Future studies will include trans-radial amputee subjects to control for this additional source of indirect proprioceptive feedback.

3.6. Conclusions

Proprioception and kinesthesia are crucial senses for human limb control, and are currently lacking in modern prosthetic limbs. We developed an artificial sensory feedback system to improve the sense of joint speed and tested its effectiveness on improving control and adaptation to novel conditions. Our results suggest improvement in reaching performance during steady-state and following a perturbation, but negligible differences in adaptation behavior. This suggests that for simple ballistic reaching tasks, feedforward control of a myoelectric limb and visual cues are

sufficient when coordinating movement with a biological limb. However, the effect of joint speed feedback during complex coordinated tasks, and its interaction with other determinants of sensory feedback improvement, remain to be investigated. We anticipate future studies will refine our knowledge of how to successfully implement artificial sensory feedback, leading to improved control for prosthesis user's robotic limbs.

4. Artificial Joint Speed Feedback for Transradial Amputee Myoelectric Control

4.1. Abstract

The human body uses a communication loop that is currently not available for prosthetic limbs. Currently, myoelectric prostheses are a popular choice for restoring motor capability, but they lack feedback to the user about the movements of the device, feedback analogous to kinesthesia in the intact limb. The outcomes of studies providing artificial sensory feedback are often dependent on the availability of incidental feedback. When subjects are blindfolded and disconnected from the prosthesis, artificial sensory feedback consistently improves control; however, when subjects wear a prosthesis and can see the task, benefits deteriorate or become inconsistent. We theorized that providing artificial sensory feedback about prosthesis speed, which cannot be precisely estimated via vision, would improve the learning and control of a myoelectric prosthesis. In this study, we test a joint-speed feedback system with transradial amputee subjects to evaluate how it improves myoelectric center-out reaching performance and adaptation to self-generated and perturbation-generated errors. Our results showed that this feedback lowers reaching errors and control noise during steady-state reaches, and may reduce final errors after perturbation. These outcomes suggest that the benefit of joint speed feedback may be dependent on the complexity of the myoelectric control, task, and how feedback is communicated back to the user.

4.2. Background

For individuals living with upper limb loss or difference, myoelectric prostheses have the potential to restore functionality and independence. Significant advancements have been made on myoelectric control methods for these prostheses, but sensory feedback is still a missing component from commercial prostheses. Sensory feedback is one of the most commonly requested

features of state-of-the-art prostheses (Cordella *et al.*, 2016), and is critical to able-bodied limb control (Miall *et al.*, 2018). Consequently, artificial sensory feedback has received much attention over the past decade (Antfolk *et al.*, 2013; Stephens-Fripp, Alici and Mutlu, 2018). Typically, this takes the form of sensory substitution feedback, where the information provided from missing sensory organs is communicated to the user via an alternative method such as vibrotactile (Stanley and Kuchenbecker, 2012; Witteveen *et al.*, 2012; Cipriani *et al.*, 2014; De Nunzio *et al.*, 2017; Krueger *et al.*, 2017) or auditory stimuli (Mirelman *et al.*, 2011; Ahmed W. Shehata, Scheme and Sensinger, 2018).

Despite this attention, sensory feedback has not yet been made commercially available for prostheses. This may be related in part to the experimental conditions in which these systems are tested. Frequently, artificial feedback is tested with subjects blindfolded and not connected to the prosthesis. Although these studies consistently show the benefit of sensory feedback, they omit the incidental sources of feedback that prosthesis users rely on every day, sources including vision and prosthesis vibration. This incidental feedback often serves the same purpose as the artificial feedback being tested, and studies have shown this incidental feedback is sufficient for some tasks (Markovic, Schweisfurth, Engels, Farina, *et al.*, 2018). Therefore, when artificial feedback is tested *alongside* incidental feedback, results become inconsistent – some studies suggest discernable benefits of artificial feedback (Marasco *et al.*, 2018; Markovic, Schweisfurth, Engels, Bentz, *et al.*, 2018; Schiefer *et al.*, 2018; Christie *et al.*, 2019), while others show no change (Cipriani *et al.*, 2008; Brown *et al.*, 2015; Witteveen, Rietman and Veltink, 2015; Christie *et al.*, 2019).

One theory explaining this dichotomy stems from the degree of precision of each feedback source. When we receive the same information from multiple sources, we merge them in accordance with

their uncertainty – sources with less uncertainty are favored over those with greater uncertainty (Ernst and Banks, 2002; Hillis *et al.*, 2002). Therefore, if incidental feedback (particularly vision) is more precise than the artificial feedback being tested, the tested feedback may not meaningfully improve the users understanding of their prosthesis movements.

In our previous research, we explicitly considered the uncertainty of incidental visual feedback and provided non-amputee subjects with joint speed feedback (Earley *et al.*, 2018). In these studies, we found that joint speed feedback reduced reaching errors after a perturbation to a 1 degree-of-freedom (DoF) myoelectric controller [**Chapter 3**]. However, proprioceptive organs including muscle spindles and Golgi tendon organs are activated differently in an amputated limb than they are in intact limb; agonist-antagonist muscles pairs stimulate these organs during movement, but this pairing is generally absent from amputated limbs. In addition, because our non-amputee subjects performed isometric contractions for myoelectric control, resistive forces applied by the arm brace provide a secondary channel of indirect kinesthesia. Therefore, non-amputee subjects may still have access to sources of incidental feedback not available to people with amputations.

The purpose of this study was to extend the methods of our previous research to investigate the effect of joint speed feedback on prosthesis control and adaptation to errors during reaching. Transradial amputee subjects controlled a virtual 1-DoF myoelectric limb and completed center-out reaching tasks under steady-state and perturbed dynamics conditions. We quantified control by measuring trial-by-trial adaptation to self-generated and perturbation-generated errors to learn how quickly myoelectric control users can update their understanding of the dynamics and adjust accordingly.

4.3. Methods

4.3.1. Subjects

6 transradial amputee subjects participated in this study, which was approved by the Northwestern University Institutional Review Board [**Table III**]. All subjects provided informed consent before starting the study.

Table III. Transradial Amputee Subject Demographics

Subject ID	Sex	Age	Side of Amputation	Years since Amputation	Cause of Amputation
TR1	M	71	R	32	Trauma
TR2	M	33	L	5	Trauma
TR3	M	28	R	10	Trauma
TR4	M	56	R	40	Trauma
TR5	F	60	R	6	Cancer
TR6	M	65	L	6	Trauma

4.3.2. Experimental Protocol: Hybrid Physical/Myoelectric Reaches

Subjects participated in three lab visits: one practice session and one experimental session each with and without audio feedback. The order of the two experimental sessions was randomized across subjects. Details of the experimental protocol are described in **Section 3.3**; the protocol is described in brief and differences are pointed out below.

Subjects sat in front of a computer monitor displaying a virtual arm [**Figure 10a**]. A Biometrics twin-axis electrogoniometer was attached to the upper and lower arm to measure the elbow flexion angle. Goniometer signals were low-pass filtered at 5 Hz with a 2nd order Butterworth filter. Two Delsys Bagnoli electromyographic (EMG) sensors measured EMG signals from wrist flexor and

extensor sites on the residual limb, as determined via voluntary muscle contraction and palpation, and the reference electrode was placed over the olecranon or on the clavicle. EMG signals were high-pass filtered at 0.1 Hz, positive-rectified, and low-pass filtered at 5 Hz using a 2^{nd} order Butterworth filter. Data were acquired at 1000 Hz and downsampled to 100 Hz after filtering.

Subjects used the goniometer and EMG signals to control the virtual arm as described in **Section 3.3.2**. The task was mirrored horizontally for left-side amputee subjects to align the movement of the virtual arm with the subject's arm. Audio feedback was provided as described in **Section 3.3.3**.

To allow subjects ample time to understand the controller, a practice session preceded the two experimental sessions. During the practice session, subjects learned to control the virtual arm through unstructured exploration, untimed targeted reaches, and **Familiarization**, all performed without audio feedback [**Figure 17a**]. To prevent fatiguing during experimental blocks, sections were shortened and repeated with breaks between blocks. Subjects completed two **Steady-State Blocks** of 100 reaches each – four sets of 15 reaches towards each target, and 40 reaches towards targets in balanced random order [**Figure 17b**] – and two **Perturbation Blocks** of 8 perturbation sets each – one towards each target, for both the *same target* and *different target* conditions [**Figure 17c**].

The hierarchical nonlinear mixed effects model described in **Section 3.3.6** was intended to analyze data from the perturbation block. However, this method was not viable due to the variability of reaches; thus, an exponential decay function was fit separately for each subject, for each condition, and the coefficients from these models were compared [**Appendix A**].

During all statistical tests, Holm-Bonferroni corrections were made for the number of terms in each model.

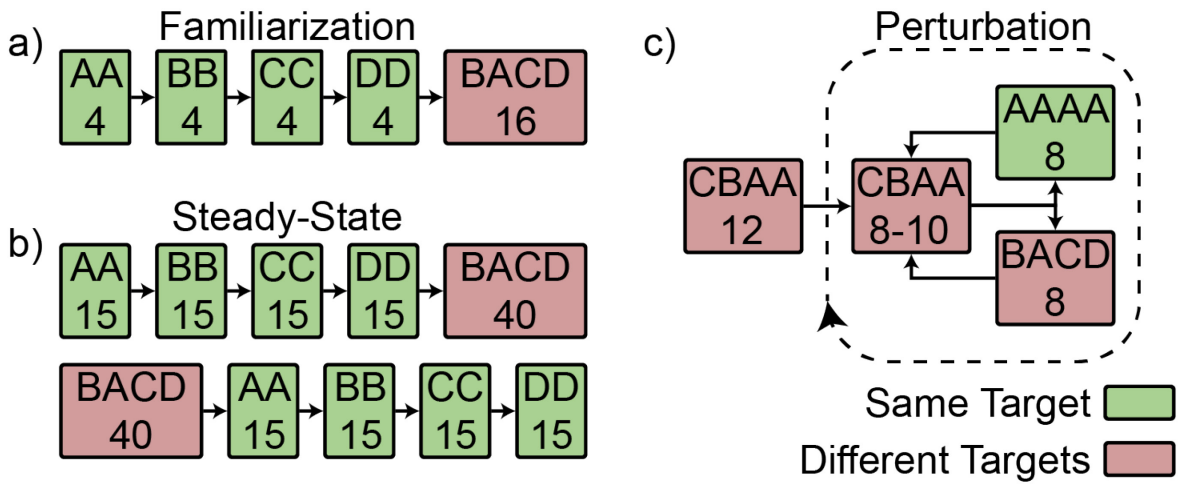

Figure 17. Transradial Amputee Experimental Protocol.

Subjects completed the experimental protocol twice – once with and once without audio feedback. The order of the *feedback* and *no feedback* sessions was randomized across subjects. (a) Familiarization involved a total of 32 reaches: four sets of 4 reaches towards each target, and 16 reaches towards targets in balanced random order. (b) The steady-state block involved a total of 100 reaches: four sets of 15 reaches towards each target, and 40 reaches towards targets in balanced random order. The order of same- or different-target groupings was randomized across subjects and consistent between subject visits. (c) The Perturbation block started with 12 reaches towards targets in random order. After these baseline trials, subjects did cycles of 8-10 reaches towards targets in random order, followed by either 8 reaches towards the same target, or 8 reaches towards targets in balanced random order. The order of these cycles was randomized across subjects and consistent between subject visits.

4.4. Results

4.4.1. Steady-State Block

Steady-state reaches indicate how amputee subjects coordinate their biological elbow movement with their myoelectric control during reaching, and comparing errors in joint space, instead of Euclidean space, may provide insight into compensatory strategies.

No significant interaction effects were found between *feedback* and *target* ($p_{min} > 0.999$), so these terms were removed and the models rerun. Steady-state reaches with feedback resulted in lower endpoint errors ($B = -1.065$, $t(21) = 2.505$, $p = 0.047$) [**Figure 18a,d**] and lower wrist angle errors [**Figure 18c,f**] ($B = -6.746$, $t(21) = 3.496$, $p = 0.006$). Elbow angle errors [**Figure 18b,e**] showed no significant difference between feedback conditions ($B = -1.475$, $t(21) = 1.115$, $p = 0.563$). No differences were found between target conditions for endpoint error ($B = -0.99$, $t(21) = 0.232$, $p = 0.819$), elbow ($B = -1.008$, $t(21) = 0.762$, $p = 0.563$), or wrist ($B = -1.066$, $t(21) = 0.552$, $p > 0.999$).

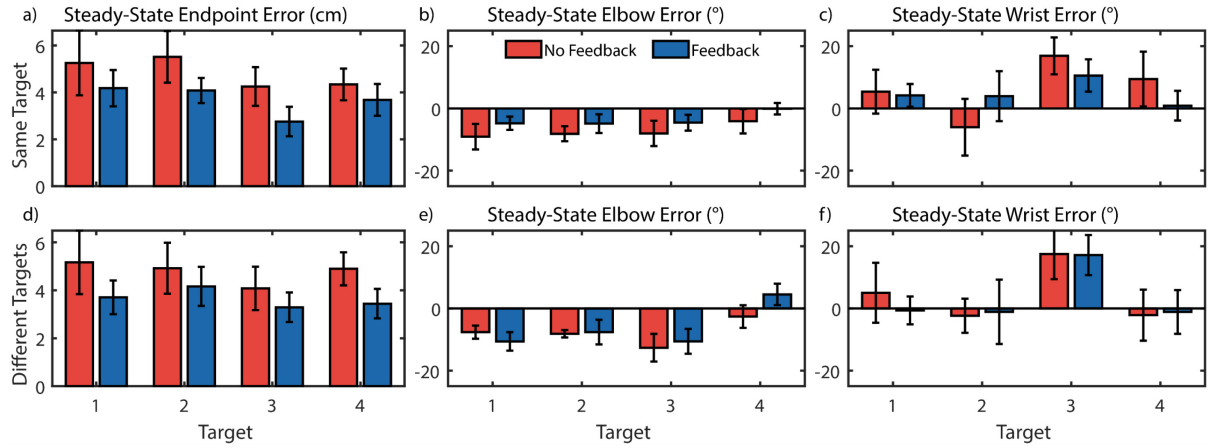

Figure 18. Transradial Amputee Endpoint and Joint Angle Errors.

Endpoint and joint angle errors vary moderately by target, but endpoint errors are consistently lower with feedback. Error bars indicate standard error of the mean (a-c) Errors while reaching towards the same target for endpoint (a), elbow (b), and wrist (c). (d-f) Errors while reaching towards different targets for endpoint (d), elbow (e), and wrist (f).

Figure 19 shows the results of traditional trial-by-trial adaptation analysis of steady-state trials. No significant interactions were found ($p_{min} = 0.690$), so these terms were removed and the models rerun. Steady-state reaches with feedback showed evidence for lower adaptation bias than reaches without feedback for the goniometer-controlled elbow ($B = -1.117$, $t(21) = 2.790$, $p = 0.026$) and

EMG-controlled wrist (B = 3.142, $t(21)$ = 2.380, p = 0.060). No differences were found between target conditions for elbow (B = 0.336, $t(21)$ = 0.839, p 0.414) or wrist bias (B = -1.250, $t(21)$ = 0.947, p = 0.358) [**Figure 19a**].

Adaptation rate was lower when reaching towards the same target for both goniometer-controlled elbow (B = -0.227, $t(21)$ = 5.617, $p < 0.001$) and EMG-controlled wrist (B = -0.260, $t(21)$ = 3.128, p = 0.010), but did not differ between feedback conditions for either elbow (B = 0.032, $t(21)$ = 0.799, p = 0.436) or wrist (B = -0.022, $t(21)$ = 0.265, p = 0.794) [**Figure 19b**].

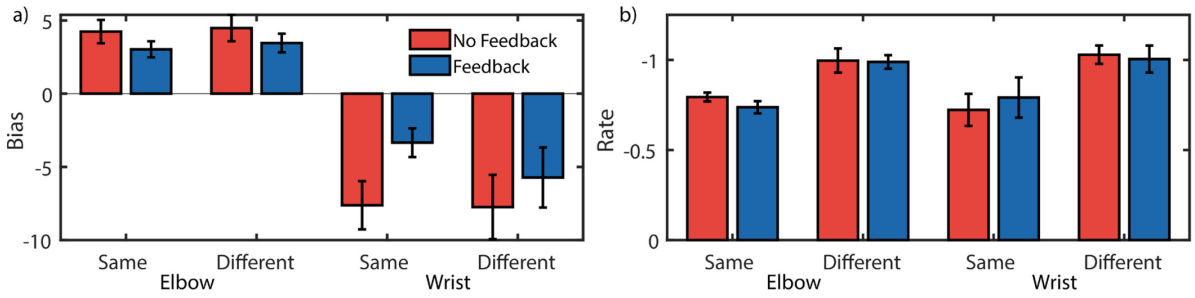

Figure 19. Transradial Amputee Trial-by-Trial Adaptation Analysis.

Trial-by-trial adaptation coefficients suggests the elbow overreaches to compensate for an underreaching wrist, but shows no change in trial-by-trial adaptation between feedback conditions. (a) Trial-by-trial adaptation bias (b) Trial-by-trial adaptation rate.

A secondary analysis using a computational motor control approach supplemented the traditional trial-by-trial adaptation analysis [**Figure 20**]. Compared to able-bodied subjects, who showed minor improved elbow adaptation with feedback, we found no difference in goniometer-controlled elbow adaptation for transradial amputee subjects (B = -0.069, $t(22)$ = 0.213, p = 0.839). However, we did find lower EMG-controlled wrist adaptation with audio feedback provided (B = -0.323,

t(22) = 3.018, *p* = 0.013) [**Figure 20a**]. Although we saw no difference in control noise with able-bodied subjects, with transradial amputee subjects we generally saw reduction in wrist control noise with feedback provided (*B* = -97.876, *t(22)* = 1.363, *p* = 0.231), though we saw no difference in elbow control noise (*B* = -10.308, *t(22)* = 0.518, *p* = 0.627) [**Figure 20b**]. This high control noise may partially explain the high adaptation rate shown in **Figure 20a**.

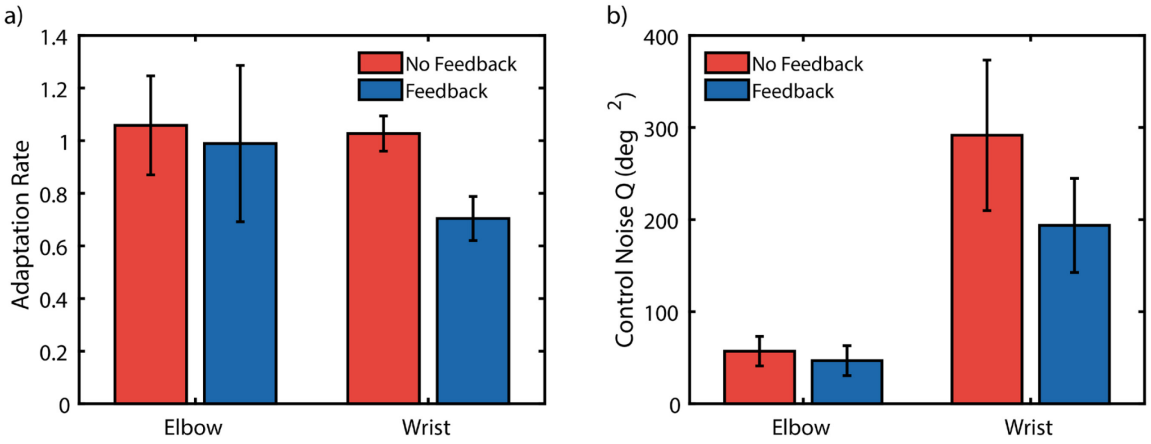

Figure 20. Transradial Amputee Control Bottleneck Index Analysis.

A secondary trial-by-trial analysis using computational motor control approach found that joint-speed feedback improved adaptation of positional elbow movements, but also reduced adaptation of myoelectric wrist movements. (a) No differences in goniometer-controlled elbow adaptation were detected, but the method determined lower adaptation in the EMG-controlled wrist with audio feedback provided. (b) Calculated control noise suggests that significantly higher control noise permeates the EMG-controlled wrist with no audio feedback. This increased control noise increases internal model uncertainty and reduces adaptation at steady-state.

4.4.2. Perturbation Block

In contrast to steady-state trials, perturbation trials test the ability for a person making reaches to adjust to suddenly changing task conditions, such as an abrupt change to the controller. **Figure 21** shows the averaged subject responses to perturbation trials. The hierarchical nonlinear mixed

effects model described in **Section 3.3.6** was unable to run, likely due to insufficient and noisy data, thus individual exponential decay models were fit to each subject's data for each condition, and the resulting coefficients were compared. However, no significant factors were uncovered from these statistical models ($p_{min} = 0.532$).

Post-hoc models were also run on initial and final errors, as well as total achieved improvement across perturbation trials. No significant interaction effects were found between *feedback* and *target* ($p_{min} = 0.474$), so the terms were removed and the models rerun.

Initial errors were not affected by feedback condition ($B = -0.186$, $t(21) = 0.255$, $p > 0.999$) or target ($B = 0.056$, $t(21) = 0.076$, $p > 0.999$). Final errors were also not affected by feedback condition ($B = -0.939$, $t(21) = 1.421$, $p = 0.349$) or target ($B = 0.267$, $t(21) = 0.404$, $p = 0.692$). When final errors were subtracted from initial errors to determine the total improvement across the eight perturbation trials, this improvement was also found to not be affected by feedback condition ($B = 0.753$, $t(21) = 1.106$, $p = 0.563$) or target ($B = -0.211$, $t(21) = 0.310$, $p = 0.759$).

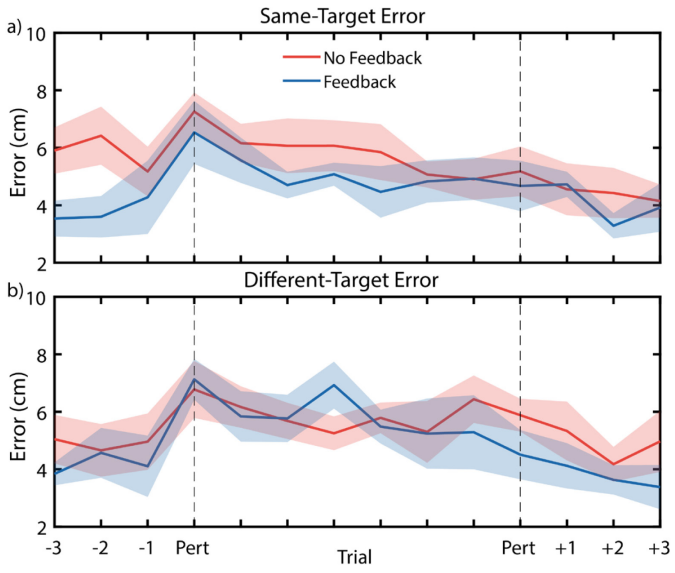

Figure 21. Transradial Amputee Perturbation Adaptation.

Average error trace during perturbation block shows that feedback reduces errors during perturbation but does not change adaptation rate. (a-b) Error traces during perturbed reaches towards the same target (a) and different targets (b).

These results taken together suggest that joint speed feedback may improve the general accuracy of reaches [**Figure 18**], result in less compensatory movement bias [**Figure 19**], lower control noise [**Figure 20b**], and may reduce the final reaching error after perturbation [**Figure 21**].

4.5. Discussion

This study expanded upon our previous work by investigating transradial amputee performance during center-out reaching tasks. These tasks require coordination of elbow angle and wrist EMG to complete the reach. Our results provide some insight into how artificial joint speed feedback may be used to improve control of a myoelectric prosthesis.

We found evidence that subjects were able to reduce their average reaching errors when provided audio feedback encoding the joint speed of a myoelectric limb [**Figure 18**]. We also found

evidence suggesting the feedback may help prosthesis users reduce compensatory movement bias [**Figure 19**] and control noise [**Figure 20**], but may also reduce steady-state adaptation. However, no significant differences were found between feedback conditions for adaptation behavior after abrupt perturbations to the controller.

These results contrast our pilot study in which we investigated adaptation to perturbation-generated errors during virtual reaches with a 2-DoF EMG-controlled limb [**Appendix A**]. In the current study, the joint speed of the distal link, controlled by EMG, was encoded as a single channel of frequency-modulated audio feedback. In the pilot study, there were two degrees of freedom controlled via EMG; rather than encoding each speed as a separate channel of frequency-modulated audio feedback, which we were concerned would be difficult to differentiate, we amplitude-modulated two audio channels, each at a different frequency. Subjects used two pairs of EMG channels to control the speed of a proximal and distal link as they reached towards targets, during which control was perturbed and we measured adaptation using an exponential decay model. In our pilot study, high variability in reaching error obfuscated general trends, yielding fully inconclusive results. This variability may have been due to large control uncertainty, the complexity of the task, or a combination of these factors. Another potential explanation for the inconclusive results is the difference in audio feedback. Subjective feedback from both non-amputee and transhumeral amputee subjects suggests that they were not able to distinguish the two independent amplitudes encoding the speeds; instead, the total amplitude of the combined channels provided only an indirect estimate of the movement of the virtual limb as a whole. Additionally, human hearing perceives changes in frequency with more precision than changes in intensity (Jesteadt, Wier and Green, 1977; Wier, Jesteadt and Green, 1977). Thus, joint speed feedback

provided via amplitude-modulated audio may have higher uncertainty than the same feedback provided via frequency-modulated audio.

Analyses in our current study were limited by the analysis methods available and the data collected for each. Our protocol required subjects to reach for several targets arranged throughout the reaching space, which ensured reaching performance wasn't localized to any one particular region. However, this also required splitting up reaches into smaller blocks of consistent reaches to prevent subject fatigue. As a result, adaptation models for self-generated errors were fit on relatively small amounts of data; this was especially the case for the CBI analysis. Furthermore, the CBI analysis requires a stationary target, thus reaches towards changing targets had to be omitted from this analysis. Analyzing self-generated error adaptation using two different methods allowed us to partially account for the limited data and build a fuller picture of adaptation behavior at steady-state.

The hierarchical model used in **Chapter 3** requires sufficient data to fit all parameters across all included perturbation conditions. Although the intent was to use the same model in this study, the smaller number of subjects prevented this model from fitting. In its place, we took an approach previously used in our pilot study [**Appendix A**]. In this approach, an individual exponential decay model is fit to each subject, for each condition. The coefficients from these models were then analyzed using a linear mixed effects model. To supplement this analysis, post-hoc comparisons were made on the initial and final errors achieved during perturbation trials. However, no significant differences were found during perturbation trials, whereas differences were found for non-amputee reaches. This interestingly contrasts steady-state reaches, which showed differences for transradial amputee adaptation and control noise not seen with non-amputee subjects.

One possible explanation for the inconclusive transradial amputee results during perturbation trials stems from the heightened control noise. Myoelectric control noise for transradial amputees was nearly double that of non-amputee subjects. It is possible that this increased control noise led to increased internal model uncertainty, decreasing the capacity to adapt to perturbations. Simulations of steady-state reaches using CBI techniques support this theory, suggesting that increased control noise increases internal model uncertainty and decreases adaptation rate [**Appendix C**, **Figure 32**]. These trends may extend to adaptation behavior after control system perturbation.

The outcomes from the CBI techniques also warrant additional attention. The reduction in adaptation rate of the EMG-controlled wrist internal model is opposite of what is expected from reduced wrist noise. A possible explanation is that the high EMG control noise for transradial amputees, more than double than that of non-amputees at times, was more substantial than effects of volitional adaptation, which may have influenced the internal model adaptation rate as calculated using CBI techniques. It should be reiterated that CBI analyses were conducted on relatively small amounts of data, which may disproportionately affect the variability or biases of calculated internal model adaptation rate.

The findings in this study corroborate those in a recent study on the clinical relevance of artificial feedback (Markovic, Schweisfurth, Engels, Bentz, *et al.*, 2018). They conclude that the benefit of sensory feedback depends on the complexity of the task and the proficiency of the feedforward control. Our study involves a simple task – center-out reaching – made complicated by the control scheme. In our experiment with trans-radial amputees, we show that improved feedback can reduce the control noise, thereby improving feedforward control. However, our pilot study with trans-humeral amputees used a more difficult control scheme, and the high control noise made control

(and adaptation) difficult. As a result, no clear differences were seen between feedback conditions. This outcome suggests a need to test artificial sensory feedback systems with amputee patients of different levels to determine how beneficial feedback is to each population. Additionally, developing a more complete understanding of the determinants of benefit for prosthesis feedback can help researchers predict how different tasks and amputation levels will respond to prosthesis feedback, expediting and improving the clinical impact of artificial sensory feedback.

5. Concluding Remarks

5.1. Summary of Findings

The purpose of this thesis was to develop an artificial sensory feedback system for upper-limb prostheses that is beneficial to users, even in the presence of incidental feedback including vision. To do this, I pursued three aims. In the first aim, I tested visual perception of biomimetic speeds to identify highly-uncertainty estimates which may benefit most from sensory feedback (**Chapter 2**). This study quantified the precision by which vision perceives biomimetic speeds. Our takeaways from this study are:

- Joint speed has higher uncertainty than absolute rotational or endpoint speeds
- Reference frame speed variation impairs visual perception of joint speed
- There may be a multiplicative effect of reference frame speed on joint speed perception
- Frequency-modulated audio feedback encoding joint speed can significantly improve joint speed perception

In the second aim, I provided frequency-modulated joint speed feedback while non-amputee subjects completed ballistic center-out reaches using a combination of limb position and myoelectric control (**Chapter 3**). During this task, I quantified adaptation to self-generated and perturbation-generated errors. Our takeaways from this study are:

- Steady-state errors were reduced in Cartesian and joint-based reference frames with feedback
- Compensatory elbow bias was reduced with feedback during steady-state reaches
- Steady-state adaptation was lower when repeatedly reaching towards the same target, compared to changing targets

- Initial and final errors after perturbation may be lower when joint speed feedback is provided
- Joint speed feedback had no effect on adaptation behavior after perturbation

In the final aim, I recruited amputee subjects to participate in the protocol outlined in Aim 2. Amputee subjects use different incidental feedback than non-amputee subjects controlling a myoelectric prosthesis, thus this study compares the outcomes from non-amputee subjects with those from amputee subjects (**Chapter 4**). Our takeaways from this study are:

- Transradial amputee steady-state reaches with feedback had lower endpoint and wrist errors than without feedback
- Transradial amputee steady-state reaches with feedback showed lower adaptation bias than reaches without feedback for the goniometer-controlled elbow and EMG-controlled wrist
- Transradial amputee control noise was significantly higher for the myoelectric-controlled wrist than the biological elbow, and this control noise was generally reduced for the wrist when provided joint speed feedback
- After perturbation, no differences were found between feedback conditions for transradial amputee subjects

In this discussion, I will elaborate upon my findings and their clinical and scientific implications for upper-limb myoelectric prostheses, address the limitations of my research, and comment on possible future directions for the field.

5.2. Scientific and Clinical Implications

Myoelectric prosthetic limbs hold the potential to provide significant benefit to individuals with upper-limb loss or difference, and may help restore lost functionality and independence for this

population. Advanced multifunction myoelectric prostheses are now commercially available, yet prosthesis rejection remains a major issue. Several surveys have listed sensory feedback as one of the major missing features of modern upper-limb prostheses, resulting in prosthesis abandonment. However, no sensory feedback system has yet become commercially available. Furthermore, the prior literature on sensory feedback is not consistent; especially when vision is available to subjects, some studies show a benefit while others do not (Antfolk *et al.*, 2013). The hypothesis for this thesis was that the precision of incidental feedback prosthesis users relied upon in place of natural feedback was a key determiner of the conferred benefit for artificial sensory feedback. Said differently, if incidental feedback is already very precise in estimating some aspect of proprioception, providing additional artificial feedback may only be meaningfully beneficial if it, too, is very precise. Otherwise, when the two sources of information are fused, the incidental feedback estimate will be favored over the artificial feedback, and no significant change will be observed. Thus, we decided to take a novel approach to developing artificial sensory feedback for prosthetic limbs: first consider the incidental feedback available to prosthesis users, then design a system around its limitations.

At the outset of this research, the intention was for the capstone of the thesis to be a clinically-viable sensory feedback system – one that can be packaged into a commercial or research prosthesis. We started with audio feedback not because we intended it to be used as the final feedback in a clinical device, but because it provided a best-case proof-of-concept with which to test our feedback. When, during early experiments, we found inconclusive results (**Appendix A**), we pivoted on our original research plan to instead investigate potential reasons why our results did not match our hypothesis. With this pivot came a change in project scope; we now sought to

understand was going on “underneath the hood” (so to speak) when users are observing movement and fusing feedback during reaching tasks. We had two theories as to the inconclusive results for our first study:

1. Joint speed is perceived with less uncertainty than we thought, and therefore providing the same information does not improve joint speed estimates
2. Joint speed estimates are highly uncertain, but supplemental feedback does not demonstrably improve control

Our psychophysics study (**Chapter 2**) provided evidence against the first theory; joint speed is indeed visually perceived with a high degree of uncertainty. We also showed that visual perception of joint speed could be significantly augments with audio feedback. Thus, remained our second theory: that we are augmenting joint speed perception but that it doesn’t improve reaching or adaptation behavior. We used frequency-modulated feedback, which audition perceives with greater discrimination, to provide a single channel of joint-speed feedback, which we believed would make the information easier to understand. We also changed the task from two myoelectric-controlled joints to just one, with elbow position being used to control the other (**Chapter 3**). This hybrid control system combining positional and myoelectric control closely emulates how these prostheses are controlled in daily life and is, to our knowledge, the first instance of such a control system being used in an adaptation study for prosthetic limbs. This unique control scheme allowed for investigation of not just how sensory feedback affects myoelectric control, but also how the same feedback affects compensatory movements in the elbow.

Indeed, our data showed some surprising results: audio feedback encoding myoelectric joint speed slightly improved positional adaptation of the elbow, but did not affect myoelectric adaptation of

the wrist. This outcome may be explained by the nonlinear relationship between the controls (joint speed affecting joint angle) and the task objective (minimize Euclidean distance between the arm endpoint and the target). We expected subjects to adjust their wrist movements to better reach towards the target, however subjects appear to have found it easier to use their elbow, which had lower control noise, to modulate the reach, and the wrist relied more on purely feedforward control. Furthermore, because of the nonlinear relationship between controls and endpoint position, the optimal reach may not be one that perfectly reaches the target, but instead may strategically aim adjacent to the target so as to reduce variability in endpoint error. We recommend that future studies investigating motor learning and motor adaptation with prosthetic limbs consider movements in joint space to capture these reaching strategies.

Although some statistically significant ($p < 0.05$) differences were found between feedback conditions, effect sizes may not translate to clinical benefit. One possible explanation for the small effects found during this research is that the feedback provided (joint speed) did not match the goal of the task (endpoint position matching); in other words, the feedback variable was not critical for the task being performed. This serves to illustrate the trade-off between the applicability of the artificial feedback provided, and the generalizability of the feedback to provide benefit in various scenarios. The best feedback for this task, for example, likely directly encodes the angle error between the distal link and the required limb configuration. However, this type of feedback would require environmental knowledge (the location of the target), and would be unhelpful outside of this limited scope. Teleceptive sensing technologies including vision systems may help to broaden the applicability of this type of feedback (Krausz and Hargrove, 2019), but benefits may still be limited to a narrow selection of tasks.

It is possible that restoring proprioception, instead of kinesthesia, of the EMG-controlled joint may present a balance between task-critical and task-agnostic feedback. Users could learn to identify the feedback stimulus associated with a target and use that information to guide reaching behavior and adaptation. However, if feedback is provided constantly, perception of the artificial feedback may attenuate after prolonged exposure (Graczyk, Delhaye, *et al.*, 2018), in a manner similar to how one may "tune out" the droning hum of an air conditioner or radiator unit in a building. Discrete – instead of continuous – feedback may help to alleviate this attenuation and ensure stimuli are not being ignored (Cipriani *et al.*, 2014). One method to implement proprioceptive feedback in a discrete manner would be to speed-gate the feedback – provide feedback while joint position is changing, but remove it after a period of non-movement. This would provide information about the position of the joint (the feedback stimulus) as well as the speed (the presence vs. absence of feedback), while minimizing risks of sensory attenuation.

In contrast to many claims in the sensory feedback literature, prosthetic limbs are not an open-loop control. There are many sources of incidental feedback prosthesis users may rely on to understand what their prosthesis is doing. This concept is most apparent in body-powered prostheses, where users rely on cable tension to understand the aperture or applied force of a prosthetic hook. This perhaps helps to explain why sensory feedback frequently ranks among the top research priorities for myoelectric prosthesis users, but not for body-powered prostheses (Cordella *et al.*, 2016).

Myoelectric prostheses, too, have several sources of incidental feedback, notably the auditory cues from the motor and vibrations transmitted through the fitted socket (Biddiss and Chau, 2007). In addition, vision clearly plays a role in prosthesis use (Hebert *et al.*, 2019). There also exist differences in available incidental feedback between non-amputee and amputee subjects. Non-

amputee subjects performing isometric contractions will typically place their limb in a brace restricting their movement. However, they can use the resistive force of the brace as an indirect measure of their force generation, granting them a potential advantage. Thus, when these sources are ignored or omitted from studies, the results may not translate to clinical improvement (Antfolk *et al.*, 2013).

A central tenet of this dissertation was to consider incidental feedback and how it affects artificial feedback, and we paid particular attention to vision. However, as described above, our non-amputee subjects still had access to incidental feedback not available to amputee subjects. The braces used to allow isometric contraction exerted an opposing force which may have been felt via the mechanoreceptors in the hand and forearm. This force information provides another indirect estimate of muscle force, and thus joint speed – the exact information we provided via audio feedback. And indeed, our results suggest that there were differences in performance between non-amputee and amputee subjects, as well as differences in the conferred benefit of joint speed feedback.

These differences should be considered when developing and testing a sensory feedback system. From my experience gained during this thesis, I recommend that the following three questions be asked before starting research into sensory feedback:

1. What senses and incidental feedback are available to subjects during the real-world tasks this study is aiming to improve?
2. What senses and incidental feedback are available to subjects during the experimental tasks this study is founded on?

3. How can differences in the available feedback information between experimental and real-world tasks affect the potential for experimental outcomes to be translated to a clinical improvement in real-world tasks?

Answering these three questions may improve the quality of sensory feedback literature and address issue of lack-of-transfer of experimental outcomes to clinical benefit.

These results corroborate recent studies stating that the determinants of feedback benefit are multifaceted and complex (Markovic, Schweisfurth, Engels, Bentz, *et al.*, 2018), and build upon them by suggesting that the uncertainty of available feedback sources and their relevance to the task at hand also contribute to the degree of benefit gained from an artificial sensory feedback system.

5.3. Limitations

Unlike most adaptation studies which require subjects to control an endpoint with their biological limbs, this thesis involved adaptation studies combining positional and myoelectric control, or using myoelectric control exclusively. Myoelectric control can be difficult to use, more so when users have little time to complete a movement. However, many adaptation studies are conducted across short time scales, often employing ballistic movements which do not allow sensory feedback to influence a reach. As a result, the experiments conducted in **Chapters 3-4** had to make trade-offs between difficult control and protocol. Subjects made reaches with a hybrid positional-myoelectric controller. In this experiment, subjects had 500ms to complete a reach. This duration was very quick for myoelectric control, but even still exceeds the 200ms threshold of ballistic movement (Schmidt *et al.*, 1979). It is therefore possible that subjects were able to incorporate

some sensory feedback into their forward motor plan and make adjustments mid-reach, however this effect is likely minimal. Furthermore, shortening the reaching time any further may have increased reach variability, decreasing effect sizes and muddying statistical analyses.

In **Appendix A**, subjects made reaches with a simultaneous 2-DoF myoelectric controller. In this experiment, subjects had 1.5 second to complete a reach. This is a fairly typical speed for a prosthetic arm, but far exceeds the ballistic movement threshold. Subjects were clearly able to incorporate feedback into their feedforward plan and adjust to movement errors [**Figure 23a**]. As such, the trial-by-trial analyses conducted in **Chapter 3** could not be used. However, perturbation analyses could still be conducted to model reaching improvement over time, but the ability to adjust to errors mid-movement reduces the apparent effects of the perturbation.

Sensory feedback is a rapidly advancing research topic and has grown exponentially in the 21st century. Since starting in 2014, the total number of publications on sensory feedback for prosthetic limbs has nearly doubled [**Figure 4a**]. New feedback methods and testing protocols are proposed every year, and it is not always possible to implement new analyses with previously-collected data. This is a limitation that affected our analyses of **Chapters 3-4**. A 2018 study had showed that traditional trial-by-trial analysis methods were biased and did not provide an accurate estimate of adaptation rate, especially for noisy reaches (Blustein *et al.*, 2018). The study proposed a workaround to reduce this bias by removing non-steady-state trials, which was implemented in **Chapters 3** and **4**. However, a better method was not made available until after data collection was complete.

This method requires many trials towards the same target to generate an estimate of the true underlying adaptation rate; thus, our steady-state reaches towards changing targets could not be

analyzed using this method. Furthermore, amputee subjects completed 30 reaches in a row towards each of four targets; using this method, adaptation rate could only be calculated on these sets of 30 trials, which was fewer than recommended to generate an estimate. This method also has a chance to fail if used on non-adapting data. If non-adapting reaches are made towards a target with a positional value far from 0, it may either not compute, or compute an inflated estimate of adaptation rate. However, the calculation of control noise provided a way to verify the integrity of data, and served as an unintended secondary means of comparison.

Finding a model that could reliably fit to exponential decay data proved difficult. The first method developed, and the method used in **Chapter 4** and **Appendix A**, was to fit an exponential decay function to each subject and condition. This meant, however, that the model was being fit on a relatively small amount of data, and was critically dependent on the first few trials to drive the fit. I found that if the average value of the second trial was not noticeably higher than the average of the remaining trials, then the exponential decay fit would yield strange results; the model would pass through the average of the first trial, then immediately converge to the average of the remaining trials, resulting in an extremely high adaptation rate. One method which may mitigate this effect is to define the gain α and bias ε terms based on the initial and final errors, and only fit the decay rate λ to the data. However, this method may not help if data are too noisy. An extension of this method is to define a conservatively low bias ε, which helps to avoid extremely high adaptation rates. To do this, I developed a method to calculate the expected reaching error, given a distribution of reaches. To conservatively lower the bias, I shifted the distribution centroids to align with the target, giving an estimate of a best-case scenario of reaching errors, assuming reach variance did not change. This method is described in **Appendix B**.

Because of the relatively small amount of data models were being fit with, I investigated ways to combine data from all subjects and all conditions into a single model. The model I developed to do this is the hierarchical nonlinear mixed effects model described in **Section 3.3.6**. The hierarchical nature of this model meant I was able to fit all exponential decay parameters and model how they change between experimental conditions simultaneously, thereby exploiting the volume of data to tease out the exponential decay that is not easily discernable from individual trials or subjects. The limitation of this method is that it requires a large amount of data to fit the model; as a result, this method was not suitable for the reaches in **Appendix A**, nor the amputee subjects in **Chapter 4**.

One modeling option that we did not investigate was using a Bayesian statistical approach. Frequentist statistical approaches, especially those with small data pools or variable data, can be susceptible to overfitting or outlier bias; this was the issue the hierarchical model sought to address. However, a Bayesian statistical approach determines the effects of the conditions through likelihood estimation, which may result in more stable parameter estimates.

5.4. Future Directions

This thesis focused on developing an artificial feedback system by explicitly considering incidental feedback and aiming to supplement the information left uncertain by these residual feedback channels. Though successful in this endeavor, there remain several directions this research can take from here.

The first is to further investigate the impact of sensory feedback from a motor adaptation perspective. The model used in this study is a continuation of the hierarchical Kalman filter

proposed in (Reva E. Johnson *et al.*, 2017). This model includes explicit parameters by which important elements of trial-by-trial adaptation can be estimated, including control and sensory noise, Kalman gains, and internal model uncertainty. However, other adaptation models have been proposed which probe different aspects of adaptation like de-adaptation and savings. These models, including the two-rate model (McDougle, Bond and Taylor, 2015) and recently-proposed two-fast-triple-rate model (Forano and Franklin, 2019), may be used in conjunction with the CBI model used in this thesis to create a more complete picture of adaptation behavior.

These models all require rapid movements to quantify adaptation on a trial-by-trial basis. However, different adaptation analyses that can be used during longer reaches may permit study of how feedback is incorporated into real-time. This may be of particular importance for more complex myoelectric control, such as the 2-DoF control tested in **Appendix A**, which cannot easily be completed as quickly as is required for other trial-by-trial techniques. For example, the comparison between prosthesis trajectory and simulated optimal-energy paths (Farshchiansadegh *et al.*, 2016) may reveal movement strategies unique to prosthesis users.

The second direction this research can take is to pursue clinical implementation. This is not necessarily mutually exclusive with scientific inquiry; however, the formation of experiments to test each will differ. Rather than focus on simple and non-functional tasks for sake of repeat trials, clinical experiments will focus more on what situations feedback is necessary, or the information needed to complete activities of daily living. For example, the tasks associated with the Sensory-Motor Prosthetic Evaluation Suite may provide a broad understanding of the limitations of prosthetic sensory feedback systems. These clinical evaluations of prosthesis control may allow us to develop a better understanding of the complex and interconnecting factors that affect the

degree of benefit provided by sensory feedback (Markovic, Schweisfurth, Engels, Bentz, *et al.*, 2018).

These two research directions are not in isolation; even if a single study cannot accomplish both foci, lessons from one field can lead to advancements in the other. For example, a recent study suggested that the ability to accurately localize the end effector of a prosthesis differs between amputee and congenital limb different prosthesis users (Maimon-Mor, Faisal and Makin, 2019). This scientific knowledge might be useful in a clinical setting, suggesting that amputees may not need feedback on the location of the hand, but instead require different information to control their device. Furthermore, different types of prostheses may benefit differently from different sensory feedback systems. Those with body-powered or single-DoF myoelectric hands, and those who do heavy labor, may benefit most from discrete event-driven sensory feedback (Cipriani *et al.*, 2014), whereas those using multiarticulate limbs capable of simultaneous control may fully realize the benefits of proprioceptive and kinesthetic feedback.

A key perspective that should be considered for clinical implementation of artificial sensory feedback is user-centered design. Despite the technical superiority of multifunction myoelectric prostheses over body-powered or cosmetic prostheses, prosthetists will still prescribe these simpler devices to individuals with limb loss or difference. For some, these devices are more appropriate for the type of work they are doing, or are better suited to address the specific needs of the user. I envision a future for prosthetic care where the restored sense and modality of artificial sensory feedback are considered in the same way, where prosthetists are trained to mix-and-match devices and sensory feedback to create custom solutions for their patients. This approach to prosthetic care,

I believe, holds the greatest potential to restoring and improving prosthesis users' independence and quality of life.

6. **References**

Aboseria, M. *et al.* (2018) 'Discrete Vibro-Tactile Feedback Prevents Object Slippage in Hand Prostheses More Intuitively Than Other Modalities', *IEEE Transactions on Neural Systems and Rehabilitation Engineering*. IEEE, 26(8), pp. 1577–1584. doi: 10.1109/TNSRE.2018.2851617.

Antfolk, C. *et al.* (2013) 'Sensory feedback in upper limb prosthetics.', *Expert review of medical devices*, 10(1), pp. 45–54. doi: 10.1586/erd.12.68.

Asghari Oskoei, M. and Hu, H. (2007) 'Myoelectric control systems—A survey', *Biomedical Signal Processing and Control*, 2(4), pp. 275–294. doi: 10.1016/j.bspc.2007.07.009.

Atkins, D. J., Heard, D. C. Y. and Donovan, W. H. (1996) 'Epidemiologic Overview of Individuals with Upper-Limb Loss and Their Reported Research Priorities', *JPO Journal of Prosthetics and Orthotics*, 8(1), pp. 2–11. doi: 10.1097/00008526-199601000-00003.

Bastian, A. J. (2008) 'Understanding sensorimotor adaptation and learning for rehabilitation.', *Current opinion in neurology*, 21(6), pp. 628–33. doi: 10.1097/WCO.0b013e328315a293.

Battye, C. K., Nightingale, A. and Whillis, J. (1955) 'The use of myo-electric currents in the operation of prostheses.', *The Journal of bone and joint surgery. British volume*, 37-B(3), pp. 506–10. Available at: http://www.ncbi.nlm.nih.gov/pubmed/13252063.

Beeker, T. W., During, J. and Den Hertog, A. (1967) 'Artificial touch in a hand-prosthesis', *Medical and biological engineering*, 5(1), pp. 47–49. doi: 10.1007/BF02478841.

van Beers, R. J. *et al.* (2002) 'When Feeling Is More Important Than Seeing in Sensorimotor Adaptation', *Current Biology*, 12(10), pp. 834–837. doi: 10.1016/S0960-9822(02)00836-9.

Berger, N. and Huppert, C. R. (1952) 'The use of electrical and mechanical muscular forces for the control of an electrical prosthesis.', *The American journal of occupational therapy : official publication of the American Occupational Therapy Association*, 6(3), pp. 110–4. Available at: http://www.ncbi.nlm.nih.gov/pubmed/14923726.

Berniker, M. and Kording, K. (2008) 'Estimating the sources of motor errors for adaptation and generalization', *Nature Neuroscience*, 11(12), pp. 1454–1461. doi: 10.1038/nn.2229.

Berniker, M. and Kording, K. P. (2011) 'Estimating the relevance of world disturbances to explain savings, interference and long-term motor adaptation effects', *PLoS Computational Biology*, 7(10). doi: 10.1371/journal.pcbi.1002210.

Bernshteĭn, N. A. (1967) *The co-ordination and regulation of movements*. [1st Engli. Oxford, New York: Pergamon Press. Available at: https://search.library.northwestern.edu/permalink/f/1h5vb9e/01NWU_ALMA21388767170002441.

Biddiss, E. A. and Chau, T. T. (2007) 'Upper limb prosthesis use and abandonment: a survey of the last 25 years.', *Prosthetics and orthotics international*, 31(3), pp. 236–257. doi: 10.1080/03093640600994581.

Biddiss, E., Beaton, D. and Chau, T. (2007) 'Consumer design priorities for upper limb prosthetics.', *Disability and rehabilitation. Assistive technology*, 2(6), pp. 346–357. doi: 10.1080/17483100701714733.

Bilodeau, E. and Bilodeau, I. (1961) 'Motor-skills learning', *Annual review of psychology*, 12(12), pp. 243–280. doi: 10.1146/annurev.ps.12.020161.001331.

Blustein, D. *et al.* (2018) 'Conventional analysis of trial-by-trial adaptation is biased: Empirical and theoretical support using a Bayesian estimator', *PLOS Computational Biology*. Edited by M. A. Smith, 14(12), p. e1006501. doi: 10.1371/journal.pcbi.1006501.

Boenstrup, M. *et al.* (2019) 'A rapid form of offline consolidation in skill learning.', *Under Review*, pp. 1346–1351. doi: 10.1016/j.cub.2019.02.049.

Brown, J. D. *et al.* (2015) 'An exploration of grip force regulation with a low-impedance myoelectric prosthesis featuring referred haptic feedback', *Journal of NeuroEngineering and Rehabilitation*, 12(1), pp. 1–17. doi: 10.1186/s12984-015-0098-1.

Burge, J., Ernst, M. O. and Banks, M. S. (2008) 'The statistical determinants of adaptation rate in human reaching.', *Journal of vision*, 8(4), pp. 20.1–19. doi: 10.1167/8.4.20.

Burger, H., Maver, T. and Marinček, Č. (2007) 'Partial hand amputation and work', *Disabil Rehabil*, 29(17), pp. 1317–1321. doi: 10.1080/09638280701320763.

Canaveral, C. A. *et al.* (2017) 'Variance in exposed perturbations impairs retention of visuomotor adaptation', *Journal of Neurophysiology*, 118(5), pp. 2745–2754. doi: 10.1152/jn.00416.2017.

Chakraborty, A. K. and Chatterjee, M. (2013) 'On multivariate folded normal distribution', *Sankhya: The Indian Journal of Statistics*, 75 B, pp. 1–15. doi: 10.1007/s13571-013-0064-5.

Chen, Y. *et al.* (1998) 'Stimulus uncertainty affects velocity discrimination', *Vision Research*, 38(9), pp. 1265–1272. doi: 10.1016/S0042-6989(97)00282-4.

Childress, D. S. (1980) 'Closed-loop control in prosthetic systems: Historical perspective', *Annals of Biomedical Engineering*, 8(4–6), pp. 293–303. doi: 10.1007/BF02363433.

Cho, Y. *et al.* (2015) 'Vision is superior to touch in shape perception even with equivalent peripheral input', *Journal of Neurophysiology*, 115(1), pp. 92–99. doi: 10.1152/jn.00654.2015.

Christie, B. P. *et al.* (2019) 'Visual inputs and postural manipulations affect the location of somatosensory percepts elicited by electrical stimulation', *Scientific Reports*, 9(1), p. 11699. doi: 10.1038/s41598-019-47867-1.

Cipriani, C. *et al.* (2008) 'On the Shared Control of an EMG-Controlled Prosthetic Hand: Analysis of User-Prosthesis Interaction', *IEEE Transactions on Robotics*, 24(1), pp. 170–184. doi: 10.1109/TRO.2007.910708.

Cipriani, C. *et al.* (2014) 'Humans can integrate feedback of discrete events in their sensorimotor control of a robotic hand', *Experimental Brain Research*, 232(11), pp. 3421–3429. doi: 10.1007/s00221-014-4024-8.

Clemente, F. *et al.* (2015) 'Non-invasive, temporally discrete feedback of object contact and release improves grasp control of closed-loop myoelectric transradial prostheses', *IEEE Transactions on Neural Systems and Rehabilitation Engineering*, 4320(c), pp. 1–1. doi: 10.1109/TNSRE.2015.2500586.

Clites, T. R. *et al.* (2018) 'Proprioception from a Neurally-Controlled Bionic Prosthesis', *Science Translational Medicine*, 10(443), p. eaap8378. doi: 10.1126/scitranslmed.aap8373.

Cordella, F. *et al.* (2016) 'Literature review on needs of upper limb prosthesis users', *Frontiers in Neuroscience*, 10(MAY), pp. 1–14. doi: 10.3389/fnins.2016.00209.

D'Alonzo, M., Clemente, F. and Cipriani, C. (2015) 'Vibrotactile Stimulation Promotes Embodiment of an Alien Hand in Amputees With Phantom Sensations', *IEEE Transactions on Neural Systems and Rehabilitation Engineering*, 23(3), pp. 450–457. doi: 10.1109/TNSRE.2014.2337952.

Dhawale, A. K., Smith, M. A. and Ölveczky, B. P. (2017) 'The Role of Variability in Motor Learning', *Annual Review of Neuroscience*, 40(1), pp. 479–498. doi: 10.1146/annurev-neuro-072116-031548.

Dillingham, T. R., Pezzin, L. E. and MacKenzie, E. J. (2002) 'Limb amputation and limb deficiency: epidemiology and recent trends in the United States.', *The Southern medical journal*, 95(8), pp. 875–883. doi: 10.1097/00007611-200208000-00018.

Dosen, S. *et al.* (2015) 'Building an internal model of a myoelectric prosthesis via closed-loop control for consistent and routine grasping', *Experimental Brain Research*. doi: 10.1007/s00221-015-4257-1.

Earley, E. J. *et al.* (2017a) 'Joint-Based Velocity Feedback Improves Myoelectric Prosthesis Performance', in *Myoelectric Controls Symposium*. Available at: https://www.unb.ca/research/institutes/biomedical/mec/_resources/docs/MEC17-papers/earley-joint-based-velocity.pdf.

Earley, E. J. *et al.* (2017b) 'Joint-based velocity feedback to virtual limb dynamic perturbations', in *IEEE ... International Conference on Rehabilitation Robotics : [proceedings]*. United States, pp. 1313–1318. doi: 10.1109/ICORR.2017.8009430.

Earley, E. J. *et al.* (2018) 'Joint Speed Discrimination and Augmentation For Prosthesis Feedback', *Scientific Reports*, 8(1), p. 17752. doi: 10.1038/s41598-018-36126-4.

Earley, E. J. (2019) *Validation of Expected Reaching Error Calculation*. Available at: https://osf.io/nskhq/.

Earley, E. J. and Hargrove, L. J. (2019) 'Modeling Expected Reaching Error and Behaviors for Motor Adaptation', in *2019 41st Annual International Conference of the IEEE Engineering in Medicine and Biology Society (EMBC)*. IEEE, pp. 1534–1538. doi: 10.1109/EMBC.2019.8857562.

Earley, E.J. and Johnson, R. E. (2018) *Joint Speed Discrimination and Augmentation for Prosthesis Feedback*. Available at: https://osf.io/ahcpq/.

Earley, Eric J. and Johnson, R. E. (2018) *Joint Speed Discrimination Augmentation via Audio Feedback*. Available at: osf.io/q37hs.

Eibl-Eibesfeldt, I. (1973) 'The expressive behavior of the deaf-and-blind born', in Vine, I. (ed.) *Social Comm. and MOv.* 1st edn. London: Academic Press, pp. 163–193. Available at: http://hdl.handle.net/11858/00-001M-0000-0028-E817-1.

Englehart, K. and Hudgins, B. (2003) 'A robust, real-time control scheme for multifunction myoelectric control', *IEEE Trans Biomed Eng*, 50(7), pp. 848–854. doi: 10.1109/TBME.2003.813539.

Ernst, M. O. and Banks, M. S. (2002) 'Humans integrate visual and haptic information in a statistically optimal fashion.', *Nature*, 415(6870), pp. 429–433. doi: 10.1038/415429a.

Farshchiansadegh, A. *et al.* (2016) 'Sensory Agreement Guides Kinetic Energy Optimization of Arm Movements during Object Manipulation', *PLoS Computational Biology*, 12(4), pp. 1–9. doi: 10.1371/journal.pcbi.1004861.

Feeny, R. J. and Hagaeus, I. (1970) 'Evaluation of the EMG-controlled hand prosthesis', in *Proc. 3rd Int. Symp. on External Control of Human Extremities, ETAN*. Dubrovnik, Yugoslavia.

Fernandes, H. L. *et al.* (2014) 'The Generalization of Prior Uncertainty during Reaching', *Journal of Neuroscience*, 34(34), pp. 11470–11484. doi: 10.1523/JNEUROSCI.3882-13.2014.

Fernández, A., Isusi, I. and Gómez, M. (2000) 'Factors conditioning the return to work of upper limb amputees in Asturias, Spain.', *Prosthetics and orthotics international*, 24(2), pp. 143–7. doi: 10.1080/03093640008726537.

Fitts, P. M. (1954) 'The information capacity of the human motor system in controlling the amplitude of movement', *Journal of experimental psychology*, 47(6), pp. 381–391. Available at: http://www.ncbi.nlm.nih.gov/pubmed/1402698.

Forano, M. and Franklin, D. W. (2019) 'Timescales of motor memory formation in dual-adaptation', *bioRxiv*, p. 698167. doi: 10.1101/698167.

Franklin, D. W. *et al.* (2019) 'A Technique for Measuring Visuomotor Feedback Contributions to the Control of an Inverted Pendulum', pp. 1513–1516.

Gallagher, P. *et al.* (2011) 'Environmental barriers, activity limitations and participation restrictions experienced by people with major limb amputation.', *Prosthetics and orthotics international*, 35(3), pp. 278–84. doi: 10.1177/0309364611407108.

Ghahramani, Z., Wolpert, D. M. and Jordan, M. I. (1997) 'Computational models of sensorimotor integration', in *Self-Organization, computational maps and motor control*, pp. 117–147. doi: 10.1016/S0166-4115(97)80006-4.

Ghez, C. and Sainburg, R. (1995) 'Proprioceptive control of interjoint coordination', *Canadian Journal of Physiology and Pharmacology*, 73(2), pp. 273–284. doi: 10.1139/y95-038.

Graczyk, E. L., Resnik, L., *et al.* (2018) 'Home use of a neural-connected sensory prosthesis

provides the functional and psychosocial experience of having a hand again', *Scientific Reports*. Springer US, 8(1), pp. 1–17. doi: 10.1038/s41598-018-26952-x.

Graczyk, E. L., Delhaye, B. P., *et al.* (2018) 'Sensory adaptation to electrical stimulation of the somatosensory nerves', *Journal of Neural Engineering*, 15(4). doi: 10.1088/1741-2552/aab790.

Hadders-Algra, M. (2018) 'Early human motor development: From variation to the ability to vary and adapt', *Neuroscience and Biobehavioral Reviews*. Elsevier, 90(May), pp. 411–427. doi: 10.1016/j.neubiorev.2018.05.009.

Hahne, J. *et al.* (2014) 'Linear and non-linear regression techniques for simultaneous and proportional myoelectric control', *IEEE Transactions on Neural Systems and Rehabilitation Engineering*, 22(2), pp. 1–1. doi: 10.1109/TNSRE.2014.2305520.

Hardwick, R. M. *et al.* (2017) 'Motor Learning in Stroke: Trained Patients Are Not Equal to Untrained Patients With Less Impairment', *Neurorehabilitation and Neural Repair*, 31(2), pp. 178–189. doi: 10.1177/1545968316675432.

Hargrove, L. *et al.* (2007) 'A real-time pattern recognition based myoelectric control usability study implemented in a virtual environment', *Annual International Conference of the IEEE Engineering in Medicine and Biology - Proceedings*, pp. 4842–4845. doi: 10.1109/IEMBS.2007.4353424.

He, J. *et al.* (2015) 'User adaptation in long-term, open-loop myoelectric training: implications for EMG pattern recognition in prosthesis control.', *Journal of neural engineering*. IOP Publishing, 12(4), p. 046005. doi: 10.1088/1741-2560/12/4/046005.

Hebert, J. S. *et al.* (2019) 'Quantitative Eye Gaze and Movement Differences in Visuomotor Adaptations to Varying Task Demands Among Upper-Extremity Prosthesis Users', *JAMA Network Open*, 2(9), p. e1911197. doi: 10.1001/jamanetworkopen.2019.11197.

Hebert, J. S. and Burger, H. (2016) 'Return to Work Following Major Limb Loss', in Schulz, I. Z. and Gatchel, R. J. (eds) *Handbook of Return to Work*. 1st edn. Springer, pp. 505–517. doi: 10.1007/978-1-4899-7627-7.

Herberts, P. (1969) 'Myoelectric signals in control of prostheses', *Acta Ortop. Scand. (suppl)*, 40(124), p. 124.

Hillis, J. M. *et al.* (2002) 'Combining Sensory Information: Mandatory Fusion Within, but Not Between, Senses', *Science*, 298(5598), pp. 1627–1630. doi: 10.1126/science.1075396.

Huang, V. S. *et al.* (2011) 'Rethinking Motor Learning and Savings in Adaptation Paradigms: Model-Free Memory for Successful Actions Combines with Internal Models', *Neuron*. Elsevier Inc., 70(4), pp. 787–801. doi: 10.1016/j.neuron.2011.04.012.

Huang, V. S. and Shadmehr, R. (2007) 'Evolution of Motor Memory During the Seconds After Observation of Motor Error', pp. 3976–3985. doi: 10.1152/jn.01281.2006.

Hudgins, B., Parker, P. and Scott, R. N. (1993) 'A new strategy for multifunction myoelectric control', *IEEE Trans Biomed Eng*, 40(1), pp. 82–94. doi: 10.1109/10.204774.

Ison, M., Antuvan, C. W. and Artemiadis, P. (2014) 'Learning efficient control of robots using myoelectric interfaces', *Proceedings - IEEE International Conference on Robotics and Automation*, pp. 2880–2885. doi: 10.1109/ICRA.2014.6907273.

Jensen, J. L. W. V. (1906) 'Sur les fonctions convexes et les inégalités entre les valeurs moyennes', *Acta Mathematica*, 30, pp. 175–193. doi: 10.1007/BF02418571.

Jesteadt, W., Wier, C. C. and Green, D. M. (1977) 'Intensity discrimination as a function of frequency and sensation level', *The Journal of the Acoustical Society of America*, 61(1), pp. 169–177. doi: 10.1121/1.381278.

Johnson, R. E. *et al.* (2014) 'Does EMG control lead to distinct motor adaptation?', *Frontiers in Neuroscience*, 8(SEP), pp. 1–6. doi: 10.3389/fnins.2014.00302.

Johnson, R. E. (2015) *Motor Learning with Powered Upper Limb Prostheses : The Influence of EMG Control on Errors , Uncertainty , and Adaptation*. Northwestern University.

Johnson, Reva E. *et al.* (2017) 'Adaptation to random and systematic errors: Comparison of amputee and non-amputee control interfaces with varying levels of process noise', *PLoS ONE*, 12(3), pp. 1–19. doi: 10.1371/journal.pone.0170473.

Johnson, Reva E *et al.* (2017) 'EMG Versus Torque Control of Human–Machine Systems: Equalizing Control Signal Variability Does not Equalize Error or Uncertainty', *IEEE Transactions on Neural Systems and Rehabilitation Engineering*, 25(6), pp. 660–667. doi: 10.1109/TNSRE.2016.2598095.

Jones, L. A. (2000) 'Kinesthetic sensing', *Human and Machine Haptics*, pp. 1–10. doi: 10.1109/TMMS.1970.299971.

Kalman, R. E. (1960) 'A new approach to linear filtering and prediction problems', *Journal of basic Engineering*, 82(1), pp. 35–45. doi: 10.1115/1.3662552.

Kan, R. and Robotti, C. (2017) 'On Moments of Folded and Truncated Multivariate Normal Distributions', *Journal of Computational and Graphical Statistics*, 26(4), pp. 930–934. doi: 10.1080/10618600.2017.1322092.

Kawato, M. (1999) 'Internal models for motor control and trajectory planning', *Current Opinion in Neurobiology*, 9(6), pp. 718–727. doi: 10.1016/S0959-4388(99)00028-8.

Khushaba, R. N. *et al.* (2012) 'Toward improved control of prosthetic fingers using surface electromyogram (EMG) signals', *Expert Systems with Applications*. Elsevier Ltd, 39(12), pp. 10731–10738. doi: 10.1016/j.eswa.2012.02.192.

Klever, L. *et al.* (2019) 'Age effects on sensorimotor predictions: What drives increased tactile suppression during reaching?', *Journal of Vision*, 19(9), p. 9. doi: 10.1167/19.9.9.

Kluzik, J. *et al.* (2008) 'Reach Adaptation: What Determines Whether We Learn an Internal Model of the Tool or Adapt the Model of Our Arm?', *Journal of Neurophysiology*, 100(3), pp. 1455–1464. doi: 10.1152/jn.90334.2008.

Körding, K. P. and Wolpert, D. M. (2004) 'Bayesian integration in sensorimotor learning', *Nature*, 427(6971), pp. 244–247. doi: 10.1038/nature02169.

Krausz, N. E. and Hargrove, L. J. (2019) 'A survey of teleceptive sensing for wearable assistive robotic devices', *Sensors (Switzerland)*, 19(23), pp. 1–27. doi: 10.3390/s19235238.

Krueger, A. R. *et al.* (2017) 'Supplemental vibrotactile feedback control of stabilization and reaching actions of the arm using limb state and position error encodings', *Journal of NeuroEngineering and Rehabilitation*. Journal of NeuroEngineering and Rehabilitation, 14(1), pp. 1–23. doi: 10.1186/s12984-017-0248-8.

Kuiken, T. *et al.* (2016) 'A comparison of pattern recognition control and direct control of a multiple degree-of-freedom transradial prosthesis', *IEEE Journal of Translational Engineering in Health and Medicine*, 2372(c), pp. 1–1. doi: 10.1109/JTEHM.2016.2616123.

Kuiken, T. A. *et al.* (2009) 'Targeted muscle reinnervation for real-time myoelectric control of multifunction artificial arms.', *JAMA : the journal of the American Medical Association*, 301(6), pp. 619–628. doi: 10.1016/S0276-1092(09)79632-4.

Kuschel, M. *et al.* (2010) 'Combination and integration in the perception of visual-haptic compliance information', *IEEE Transactions on Haptics*, 3(4), pp. 234–244. doi: 10.1109/TOH.2010.9.

Kutner, M. H. (2005) *Applied Linear Statistical Models*. McGraw-Hill Irwin (McGrwa-Hill international edition).

Land, M., Mennie, N. and Rusted, J. (1999) 'The roles of vision and eye movements in the control of activities of daily living', *Perception*, 28(11), pp. 1311–1328. doi: 10.1068/p2935.

Leone, F. C., Nelson, L. S. and Nottingham, R. B. (1961) 'The Folded Normal Distribution', *Technometrics*, 3(4), pp. 543–550. doi: 10.1080/00401706.1961.10489974.

Li, G., Schultz, A. E. and Kuiken, T. A. (2010) 'Quantifying pattern recognition-based myoelectric control of multifunctional transradial prostheses', *IEEE Trans Neural Syst Rehabil Eng*, 18(2), pp. 185–192. doi: 10.1109/TNSRE.2009.2039619.

De Luca, C. J. (1979) 'Physiology and Mathematics of Myoelectric Signals', *Biomedical Engineering, IEEE Transactions on*, pp. 313–325. doi: 10.1109/TBME.1979.326534.

Maimon-Mor, R. O., Faisal, A. A. and Makin, T. R. (2019) 'Is visuo-motor integration innate? Evidence from a prosthesis reaching task with individuals born without a hand', in *2019 Society for Neuroscience Meeting*.

Marasco, P. D. *et al.* (2018) 'Illusory movement perception improves motor control for prosthetic hands', *Science Translational Medicine*, 10(432), p. eaao6990. doi: 10.1126/scitranslmed.aao6990.

Markovic, M. *et al.* (2017) 'GLIMPSE: Google Glass interface for sensory feedback in myoelectric hand prostheses', *Journal of Neural Engineering*. IOP Publishing, 14(3), p. 036007. doi: 10.1088/1741-2552/aa620a.

Markovic, M., Schweisfurth, M. A., Engels, L. F., Farina, D., *et al.* (2018) 'Myocontrol is closed-loop control: Incidental feedback is sufficient for scaling the prosthesis force in routine grasping', *Journal of NeuroEngineering and Rehabilitation*. Journal of NeuroEngineering and Rehabilitation, 15(1), pp. 1–11. doi: 10.1186/s12984-018-0422-7.

Markovic, M., Schweisfurth, M. A., Engels, L. F., Bentz, T., *et al.* (2018) 'The clinical relevance of advanced artificial feedback in the control of a multi-functional myoelectric prosthesis', *Journal of NeuroEngineering and Rehabilitation*. Journal of NeuroEngineering and Rehabilitation, 15(1), p. 28. doi: 10.1186/s12984-018-0371-1.

McCarty, M. E. *et al.* (2001) 'How Infants Use Vision for Grasping Objects', *Child Development*, 72(4), pp. 973–987. doi: 10.1111/1467-8624.00329.

McDougle, S. D., Bond, K. M. and Taylor, J. A. (2015) 'Explicit and implicit processes constitute the fast and slow processes of sensorimotor learning', *Journal of Neuroscience*, 35(26), pp. 9568–9579. doi: 10.1523/JNEUROSCI.5061-14.2015.

McDougle, S. D., Bond, K. M. and Taylor, J. A. (2017) 'Implications of plan-based generalization in sensorimotor adaptation', *Journal of Neurophysiology*, 118(1), pp. 383–393. doi: 10.1152/jn.00974.2016.

Miall, R. C. *et al.* (2018) 'Proprioceptive loss and the perception, control and learning of arm movements in humans: evidence from sensory neuronopathy', *Experimental Brain Research*. Springer Berlin Heidelberg, 236(8), pp. 2137–2155. doi: 10.1007/s00221-018-5289-0.

Mirelman, A. *et al.* (2011) 'Audio-biofeedback training for posture and balance in patients with Parkinson's disease', *Journal of NeuroEngineering and Rehabilitation*. BioMed Central Ltd, 8(1), p. 35. doi: 10.1186/1743-0003-8-35.

Murthy, G. S. R. (2015) 'A Note on Multivariate Folded Normal Distribution', *Sankhya B*, 77(1), pp. 108–113. doi: 10.1007/s13571-014-0092-9.

Newell, K. M. *et al.* (2006) 'Variability in Motor Output As Noise: A Default and Erroneous Proposition?', in Davids, K., Bennett, S., and Newell, K. (eds) *Movement System Variability*. Human Kinetics, pp. 3–23. Available at: https://books.google.com/books?id=IAamvxsVlGAC&lpg=PA3&ots=4XvsPSe8L1&dq=Motor output variability as noise%3A a default and erroneous proposition%3F&pg=PA3#v=onepage&q&f=false.

Ninu, A. *et al.* (2014) 'Closed-loop control of grasping with a myoelectric hand prosthesis: Which are the relevant feedback variables for force control?', *IEEE Transactions on Neural Systems and Rehabilitation Engineering*, 22(5), pp. 1041–1052. doi: 10.1109/TNSRE.2014.2318431.

De Nunzio, A. M. *et al.* (2017) 'Tactile feedback is an effective instrument for the training of grasping with a prosthesis at low- and medium-force levels', *Experimental Brain Research*. Springer Berlin Heidelberg, 235(8), pp. 2547–2559. doi: 10.1007/s00221-017-4991-7.

Papoulis, A. (1965) *Probability, Random Variables, and Stochastic Processes*. 1st edn. McGraw-Hill.

Parker, P. A. and Scott, R. N. (1986) 'Myoelectric control of prostheses', *Crit Rev Biomed Eng*, 13(4), pp. 283–310. Available at: http://www.ncbi.nlm.nih.gov/pubmed/3512166.

Pine, Z. M. *et al.* (1996) 'Learning of scaling factors and reference axes for reaching movements.', *Neuroreport*, 7(14), pp. 2357–61. doi: 10.1097/00001756-199610020-00016.

Poulet, J. F. A. and Hedwig, B. (2007) 'New insights into corollary discharges mediated by identified neural pathways', *Trends in Neurosciences*, 30(1), pp. 14–21. doi: 10.1016/j.tins.2006.11.005.

Prior, R. E. *et al.* (1976) 'Supplemental sensory feedback for the VA/NU myoelectric hand. Background and preliminary designs', *Bulletin of Prosthetics Research*, 10(26), pp. 170–191.

Psarakis, S. and Panaretos, J. (2000) 'On some bivariate extensions of the folded normal and the folded-t distributions', *J App Stat Sci*, 10(2), pp. 119–136.

Ranganathan, R. and Newell, K. M. (2010) 'Influence of motor learning on utilizing path redundancy', *Neuroscience Letters*, 469(3), pp. 416–420. doi: 10.1016/j.neulet.2009.12.041.

Raveh, E., Friedman, J. and Portnoy, S. (2018) 'Evaluation of the effects of adding vibrotactile feedback to myoelectric prosthesis users on performance and visual attention in a dual-task paradigm', *Clinical Rehabilitation*, 32(10), pp. 1308–1316. doi: 10.1177/0269215518774104.

Ross, H. E. (2003) 'Context effects in the scaling and discrimination of size', *Fechner Day 2003*, pp. 257–262.

Sainburg, R. L. *et al.* (1995) 'Control of limb dynamics in normal subjects and patients without proprioception.', *Journal of neurophysiology*, 73(2), pp. 820–835.

Sanders, A. F. (2013) *Elements of Human Performance*. Psychology Press. doi: 10.4324/9780203774250.

Saunders, I. and Vijayakumar, S. (2011) 'The role of feed-forward and feedback processes for closed-loop prosthesis control', *Journal of NeuroEngineering and Rehabilitation*, 8(1), p. 60. doi: 10.1186/1743-0003-8-60.

Scheidt, R. A. *et al.* (2005) 'Interaction of Visual and Proprioceptive Feedback During Adaptation of Human Reaching Movements', *Journal of Neurophysiology*, (January 2005), pp. 3200–3213. doi: 10.1152/jn.00947.2004.

Schiefer, M. *et al.* (2016) 'Sensory feedback by peripheral nerve stimulation improves task performance in individuals with upper limb loss using a myoelectric prosthesis.', *Journal of neural engineering*. IOP Publishing, 13(1), p. 016001. doi: 10.1088/1741-2560/13/1/016001.

Schiefer, M. A. *et al.* (2018) 'Artificial tactile and proprioceptive feedback improves performance and confidence on object identification tasks', *PLoS ONE*, 13(12), pp. 1–18. doi: 10.1371/journal.pone.0207659.

Schlesinger, G. (1919) 'Der mechanische Aufbau der künstlichen Glieder', in *Ersatzglieder und Arbeitshilfen*. Berlin, Heidelberg: Springer Berlin Heidelberg, pp. 321–661. doi: 10.1007/978-3-

662-33009-8_13.

Schmidt, R. A. *et al.* (1979) 'Motor-output variability: a theory for the accuracy of rapid motor acts.', *Psychological review*. American Psychological Association, 86(5), pp. 415–451. doi: 10.1037/0033-295X.86.5.415.

Schmitz, G. and Bock, O. L. (2017) 'Properties of intermodal transfer after dual visuo- and auditory-motor adaptation', *Human Movement Science*. Elsevier, 55(August), pp. 108–120. doi: 10.1016/j.humov.2017.08.006.

Schofield, J. S. *et al.* (2014) 'Applications of sensory feedback in motorized upper extremity prosthesis: A review', *Expert Review of Medical Devices*, 11(5), pp. 499–511. doi: 10.1586/17434440.2014.929496.

Shadmehr, R. and Mussa-Ivaldi, F. a (1994) 'Adaptive representation of dynamics during learning of a motor task', *The Journal of Neuroscience*, 14(5), pp. 3208–3224. doi: 8182467.

Shehata, Ahmed W., Scheme, E. J. and Sensinger, J. W. (2018) 'Audible Feedback Improves Internal Model Strength and Performance of Myoelectric Prosthesis Control', *Scientific Reports*, 8(1), p. 8541. doi: 10.1038/s41598-018-26810-w.

Shehata, Ahmed W, Scheme, E. J. and Sensinger, J. W. (2018) 'Evaluating Internal Model Strength and Performance of Myoelectric Prosthesis Control Strategies', *IEEE Transactions on Neural Systems and Rehabilitation Engineering*, 26(5), pp. 1046–1055. doi: 10.1109/TNSRE.2018.2826981.

Silcox, D. H. *et al.* (1993) 'Myoelectric prostheses. A long-term follow-up and a study of the use of alternate prostheses.', *The Journal of Bone & Joint Surgery*, 75(12), pp. 1781 LP – 1789. Available at: http://jbjs.org/content/75/12/1781.abstract.

Smyth, M. M. and Murray Marriott, A. (1982) 'Vision and proprioception in simple catching', *Journal of Motor Behavior*, 14(2), pp. 143–152. doi: 10.1080/00222895.1982.10735269.

Sober, S. J. and Sabes, P. N. (2005) 'Flexible strategies for sensory integration during motor planning', *Nature Neuroscience*, 8(4), pp. 490–497. doi: 10.1038/nn1427.

Sobuh, M. M. D. *et al.* (2014) 'Visuomotor behaviours when using a myoelectric prosthesis', *Journal of NeuroEngineering and Rehabilitation*, 11(1), pp. 1–11. doi: 10.1186/1743-0003-11-72.

Stanley, A. A. and Kuchenbecker, K. J. (2012) 'Evaluation of tactile feedback methods for wrist rotation guidance', *IEEE Transactions on Haptics*, 5(3), pp. 240–251. doi: 10.1109/TOH.2012.33.

Stephens-Fripp, B., Alici, G. and Mutlu, R. (2018) 'A review of non-invasive sensory feedback methods for transradial prosthetic hands', *IEEE Access*, 3536(c), pp. 1–1. doi: 10.1109/ACCESS.2018.2791583.

Sternad, D. (2018) 'It's not (only) the mean that matters: variability, noise and exploration in skill learning', *Current Opinion in Behavioral Sciences*. Elsevier Ltd, 20, pp. 183–195. doi: 10.1016/j.cobeha.2018.01.004.

Stocker, A. A. and Simoncelli, E. P. (2006) 'Noise characteristics and prior expectations in human visual speed perception.', *Nature neuroscience*, 9(4), pp. 578–585. doi: 10.1038/nn1669.

Tan, D. W. *et al.* (2014) 'A neural interface provides long-term stable natural touch perception', *Science Translational Medicine*, 6(257). doi: 10.1126/scitranslmed.3008669.

Thelen, E., Bradshaw, G. and Ward, J. A. (1981) 'Spontaneous kicking in month-old infants: Manifestation of a human central locomotor program', *Behavioral and Neural Biology*, 32(1), pp. 45–53. doi: 10.1016/S0163-1047(81)90257-0.

Walker, M. P. *et al.* (2002) 'Practice with Sleep Makes Perfect', *Neuron*, 35(1), pp. 205–211. doi: 10.1016/S0896-6273(02)00746-8.

Wei, K. and Körding, K. (2010) 'Uncertainty of feedback and state estimation determines the speed of motor adaptation', *Frontiers in computational neuroscience*, 4(May), p. 11. doi: 10.3389/fncom.2010.00011.

van der Wel, R. P. R. D. *et al.* (2007) 'Hand path priming in manual obstacle avoidance: Evidence for abstract spatiotemporal forms in human motor control.', *Journal of Experimental Psychology: Human Perception and Performance*, 33(5), pp. 1117–1126. doi: 10.1037/0096-1523.33.5.1117.

Welford, A. T. (1980) *Reaction Times*. Edited by A. T. Welford and J. M. T. Brebner. Academic Press.

Wier, C. C., Jesteadt, W. and Green, D. M. (1977) 'Frequency discrimination as a function of frequency and sensation level', *The Journal of the Acoustical Society of America*, 61(1), pp. 178–184. doi: 10.1121/1.381251.

Witteveen, H. J. B. *et al.* (2012) 'Vibro- and electrotactile user feedback on hand opening for myoelectric forearm prostheses', *IEEE Transactions on Biomedical Engineering*, 59(8), pp. 2219–2226. doi: 10.1109/TBME.2012.2200678.

Witteveen, H. J. B., Rietman, H. S. and Veltink, P. H. (2015) 'Vibrotactile grasping force and hand aperture feedback for myoelectric forearm prosthesis users', *Prosthetics and Orthotics International*, 39(3), pp. 204–212. doi: 10.1177/0309364614522260.

Wolpert, D. M., Ghahramani, Z. and Flanagan, J. R. (2001) 'Perspectives and problems in motor learning', *Trends in Cognitive Sciences*, 5(11), pp. 487–494. doi: 10.1016/S1364-6613(00)01773-3.

Wolpert, D. M., Ghahramani, Z. and Jordan, M. I. (1995) 'An internal model for sensorimotor integration', *Science-AAAS-Weekly Paper Edition*, 269(5232), pp. 1880–1882. doi: 10.1126/science.7569931.

Wolpert, D. M. and Kawato, M. (1998) 'Multiple paired forward and inverse models for motor control', *Neural Networks*, 11(7–8), pp. 1317–1329. doi: 10.1016/S0893-6080(98)00066-5.

Yamada, M., Niwa, N. and Uchiyama, A. (1983) 'Evaluation of a multifunctional hand prosthesis system using EMG controlled animation', *IEEE Trans Biomed Eng*, 30(11), pp. 759–763. Available at: http://www.ncbi.nlm.nih.gov/pubmed/6662533.

Yin, C. *et al.* (2019) 'Sensorimotor priors are effector dependent', *Journal of Neurophysiology*, 122(1), pp. 389–397. doi: 10.1152/jn.00228.2018.

Young, A. J. *et al.* (2013) 'Classification of simultaneous movements using surface EMG pattern recognition', *IEEE Transactions on Biomedical Engineering*, 60(5), pp. 1250–1258. doi: 10.1109/TBME.2012.2232293.

Ziegler-Graham, K. *et al.* (2008) 'Estimating the prevalence of limb loss in the United States: 2005 to 2050', *Arch Phys Med Rehabil*, 89(3), pp. 422–429. doi: 10.1016/j.apmr.2007.11.005.

Appendix A. Joint-Based Velocity Feedback to Virtual Limb Dynamic Perturbations

Authors: Eric J. Earley, Kyle J. Kaveny, Reva E. Johnson, Levi J. Hargrove, Jon W. Sensinger

A.1. Abstract

Despite significant research developing myoelectric prosthesis controllers, many amputees have difficulty controlling their devices due in part to reduced sensory feedback. Many attempts at providing supplemental sensory feedback have not significantly aided control. We hypothesize this is because the feedback provided contains redundant information already provided by vision. However, whereas vision provides egocentric, position-based feedback, sensory feedback tied to joint coordinates may provide information complementary to vision. In this study, we tested if providing audio feedback of joint velocities can improve performance and adaptation to dynamic perturbations while controlling a virtual limb. While subjects performed time-controlled center-out reaches, we perturbed the dynamics of the system and measured the rate subjects adapted to this change. Our results suggest that initial speed errors upon perturbation were reduced in the presence of audio feedback, and we theorize this is due to subjects identifying the perturbed limb dynamics sooner. We also noted other possible benefits including improved muscle activation detection. However, we saw no conclusive differences for transhumeral amputee subjects controlling the same system.

A.2. Introduction

For many upper-limb amputees, myoelectric prosthetic devices represent the current standard of restoring functionality. Recent studies have focused on extending myoelectric control to simultaneous movements of multiple degrees of freedom (DoFs) through pattern recognition or regression algorithms (Young *et al.*, 2013; Hahne *et al.*, 2014). However, these controllers are

initially difficult to use and require a period to learn how to control the device (Kuiken *et al.*, 2016). Part of this learning is associated with making repeatable contractions (He *et al.*, 2015); however, it is likely that this learning is also partly attributed to the users recognizing the dynamical properties of the device. Reduced sensory feedback due to missing or damaged sensory organs (e.g. proprioceptors, mechanoreceptors, nociceptors) may contribute to this difficulty (Childress, 1980).

There have been several attempts to provide feedback via sensory substitution to improve performance, though few were successful in doing so with vision feedback present (Antfolk *et al.*, 2013). For example, Ninu et al. showed that grasping force, commonly studied in sensory substitution, can be estimated with vision alone by watching the velocity of the closing prosthesis (Ninu *et al.*, 2014). Successful studies are able to improve performance by providing complementary sensory information not provided by vision, such as tactile information (Schiefer *et al.*, 2016). Additionally, studies suggest that providing feedback in a discrete fashion may be more beneficial for some tasks, confirming completion of a task more clearly than continuous feedback (Cipriani *et al.*, 2014). Effective sensory substitution requires not just providing a stimulus, but also consideration of how it will be interpreted by the user. For example, it is important for stimuli provided for one task to allow users to generalize their performance to other tasks (Shadmehr and Mussa-Ivaldi, 1994). Sensory substitution should also provide information not available to, or with similar or lesser variance than, the other intact senses, most notably vision (Ernst and Banks, 2002).

Vision can be an extremely precise feedback modality, and is the most relied upon modality for amputees performing tasks (Sobuh *et al.*, 2014). Vision provides feedback in a global, egocentric

reference frame (Scheidt *et al.*, 2005); therefore, less precise sensory substitutions providing feedback in the same global reference frame do not significantly improve control. However, the same sensory substitution providing feedback in a local, joint-based reference frame may provide information complementary to vision; one study suggests that joint-based velocity information is more relevant when users are less certain about control of their bodies than about the external environment (Berniker and Kording, 2008). Additionally, vision provides more precise feedback with position information (Ross, 2003), but is less precise with velocity information (Stocker and Simoncelli, 2006); thus, sensory substitution encoding velocity information may also complement existing visual feedback.

The purpose of this study is to determine if continuous, local reference frame-based velocity feedback improves performance even in the presence of vision. This study is in contrast to prior works that have used discrete feedback or provided sensory substitution in global reference frames (Antfolk *et al.*, 2013). Our hypothesis was tested using a continuous joint-based, velocity-based feedback paradigm when controlling a 2-DoF myoelectric interface with control perturbations. The virtual limb was inspired by the control of a trans-humeral prosthesis consisting of an elbow and wrist. Subjects performed time- constrained center-out reaches (Schmidt *et al.*, 1979) with and without audio feedback, during which the dynamics of the virtual limb were perturbed at discrete intervals. We tested the hypothesis that providing joint- and velocity-based audio feedback during these reaches would improve the rate of adaptation to perturbations to the virtual limb dynamics, and that this improved adaptation would generalize to multiple target locations.

A.3. Methods

A.3.1. Subjects

Twenty right hand-dominant, non-amputee subjects and two transhumeral amputee subjects [**Table IV**] were recruited for this study, which was approved by the Northwestern University Institutional Review Board. All subjects provided informed consent before starting the study. Transhumeral amputee participants had previously undergone targeted muscle reinnervation (TMR), giving them four independent muscle activation sites for prosthesis control (Kuiken *et al.*, 2009).

Table IV. Transhumeral Amputee Subject Demographics

Subject ID	Sex	Age	Side of Amputation	Years since Amputation	Cause of Amputation
TH1	M	39	R	9	Trauma
TH2	F	44	R	2	Infection

A.3.2. Experimental Protocol

Subjects participated in two experimental sessions, separated by at least one day: one session with no audio feedback, and one session with joint- and velocity-based audio feedback provided. The order of these sessions was randomized across subjects using balanced block randomization.

Subjects were seated in front of a computer monitor with their right arm placed in a rigid forearm brace clamped to a table, affixing the elbow and wrist positions. Four Delsys Bagnoli electromyographic (EMG) sensors were placed on the subject's arm: over the biceps and triceps on the upper arm, and over the flexor and extensor compartments of the forearm. Reference

electrodes were placed over the olecranon, and the electrode sites were wrapped with an elastic cohesive bandage [**Figure 22a**].

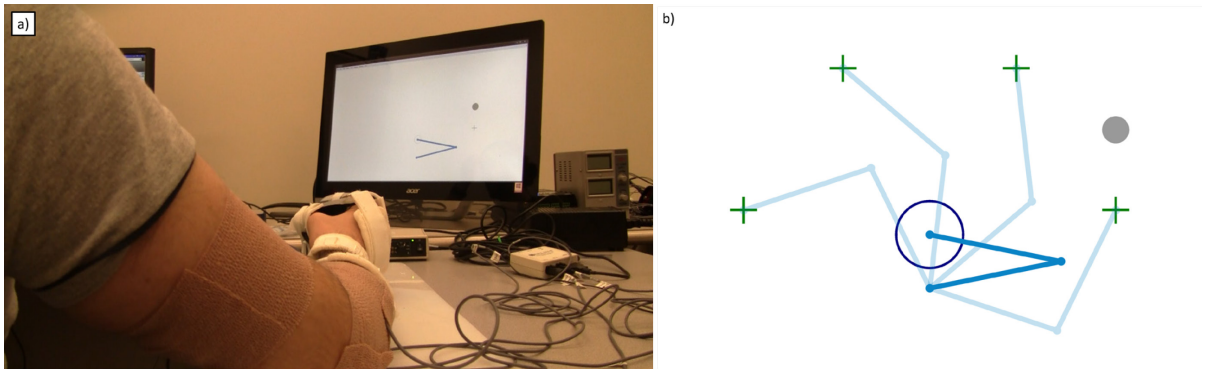

Figure 22. Pilot Experimental Layout.

(a) Non-amputee experiment setup. The hand was immobilized in a forearm brace. EMG Electrodes placed over the upper arm and forearm controlled the virtual arm displayed on the screen. (b) Virtual environment. The cursor of the virtual arm would begin each trial at the home position (blue circle). One of four random targets would appear (green +), and subject would reach for the target (faded blue). During familiarization trials and the testing blocks, a ball (grey circle) would appear above the target; once the arm cursor left the home circle, the ball would drop, aligning with the target 1.5 seconds after dropping.

Subjects used arm and forearm EMG from isometric muscle contractions to control a virtual two-link arm. EMG from elbow flexion applied a counter-clockwise torque to the proximal linkage; EMG from elbow extension, clockwise torque. EMG from wrist flexion applied a counter-clockwise torque to the distal linkage; EMG from wrist extension, clockwise. Links were simulated with a length of 10 cm, a mass of 5 kg, and a damping coefficient of 1.5 Ns/m.

During the audio feedback session, subjects wore a pair of noise-canceling headphones (Bose Corporation, Framingham, MA). Audio feedback consisted of two pitches whose volumes were proportional to the speed of the two virtual linkages; the speed of the proximal linkage determined

the amplitude of a 200 Hz pitch, and the speed of the distal linkage determined the amplitude of a 300 Hz pitch.

Subjects completed the following experimental tasks [**Table V**]:

Table V. Pilot Experimental Tasks.

Experimental Protocol	Free Training	Familiarization	Testing Blocks				
			Baseline	***No perturbation***	***Perturbation***	***Left generalization***	***Right generalization***
Time-Constrained	No	Yes	Yes				
Trials	100 (random targets)	100-200 (random targets)	40 (random targets)	20 (far-right target)	20 (far-right target)	20 (top-left target)	20 (top-right target)
Perturbation	No	No	No	No	Yes	Yes	Yes

A.3.2.1. System Tuning

EMG gains and dead zones were tuned during a free exploration session lasting only a few minutes, where subjects were permitted to control the virtual arm and explore the workspace with no objective, allowing users to become familiar with the dynamics of the system.

A.3.2.2. Free Training

Subjects completed 100 free training trials; during free training, subjects performed center-out reaches towards one of four 2 cm diameter targets located 14 cm from the home position (25

reaches towards each target, in randomized order) [**Figure 22b**]. When the cursor of the arm stopped within the target, the arm was reset to the starting position and a new target was presented.

A.3.2.3. Familiarization

Subjects completed 100 familiarization trials introducing them to the protocol of the testing blocks. The protocol was similar to free training (25 reaches towards each of four targets); however, subjects were instructed to reach the target at 1.5 seconds after leaving the 5 cm diameter home circle (Schmidt *et al.*, 1979). This time-constrained task was used to ensure similar movement profiles across trials. A ball was shown above each target, and began dropping at a constant speed when the cursor left the home circle [**Figure 22b**]. This ball would align concentrically with the target at 1.5 seconds, thus indicating when the subject was to reach the target. If the subject moved for longer than 2 seconds, the trial was marked as timed out. Subjects were also instructed to complete the reach in a single fluid movement; if the cursor speed dropped below 1 cm/s, the trial ended, the arm was reset to the starting position, and a new target was presented. After completing 100 familiarization trials, if subjects did not stop within a ±0.25 second time window for at least 40% of the trials, or if they desired additional practice, they completed a second set of 100 familiarization trials.

A.3.2.4. Testing Blocks

Subjects performed 40 baseline reaches towards the four targets (10 reaches towards each target, in randomized order) to provide a baseline performance, before making 20 reaches towards the far-right target (*no perturbation* trials). The dynamic properties of the simulated arm were then perturbed by reducing the damping coefficient of each linkage to 0.5 Ns/m; this perturbation was used to promote adaptation to an intrinsic disturbance (Berniker and Kording, 2008). Subjects

performed 20 additional reaches towards the far-right target with the new dynamics (*perturbation* trials). Following this, subjects performed 20 reaches towards the top-left target (*left generalization*) and 20 reaches towards the top-right target (*right generalization*), for 120 total trials.

A.3.3. Performance Metrics

Two performance metrics were calculated for each trial: Euclidean distance between the cursor and the target at 1.5 seconds (when the timing ball was concentrically aligned with the targets), and the average cursor speed during the 1.5 seconds of movement. Both metrics were adjusted by subtracting the average from the baseline trials to account for varying accuracy and speeds to different targets. From these performance metrics, adaptation during *perturbation*, *left generalization*, and *right generalization* trials were calculated for each subject by fitting the data to an exponential decay function:

$$\alpha e^{-\lambda t} + \varepsilon \tag{15}$$

where α, the exponential decay gain, represents the overall magnitude of error upon perturbation, λ, the exponential decay rate, represents the adaptation rate, and ε, the exponential decay offset, represents the difference between the perturbation error at convergence and the steady-state error without perturbation. Additionally, experiments were video- and screen captured, allowing for subsequent observation of subject performance.

A.4. Results

Sample data from a representative non-amputee subject are shown in **Figure 23**. Reaches towards the far-right target during *no perturbation* trials (black) are consistent and accurate. However,

when movement dynamics are perturbed (grey), movement becomes more erratic [**Figure 23a**]. This can be seen in the increase in distance from the target and average movement speed immediately after trial 60 [**Figure 23b**]. However, subjects typically adapted quickly to this change and improved their performance closer to baseline levels. Furthermore, while we expected to see an increase in error during initial reaches towards both generalization targets, these initial reaches were often near baseline performance.

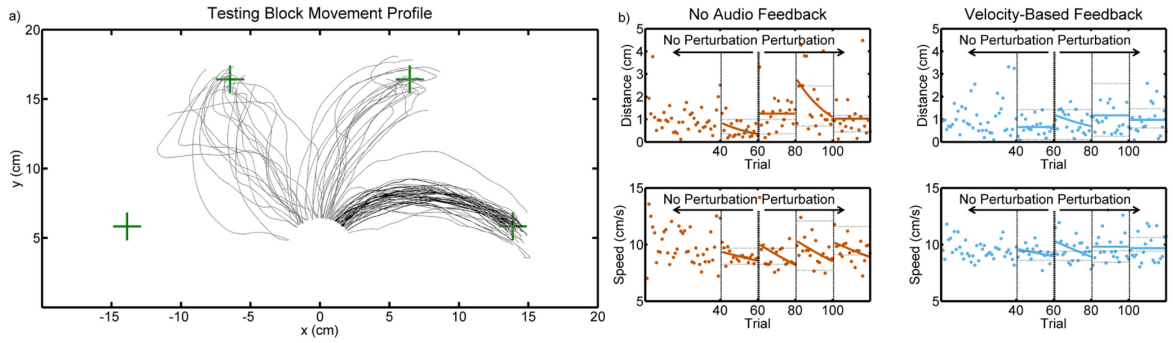

Figure 23. Sample Pilot Data from Representative Subject.

(a) Individual subject movement profiles during testing block, starting at trial 41. Subject was provided audio feedback in this testing block. Trace colors represent no perturbation (black), perturbation, left generalization, and right generalization (grey) trials. (b) Individual subject performance during testing blocks. Vertical dashed lines separate between testing block subsections. Horizontal dashed lines indicate mean ± standard deviation for the corresponding target during baseline trials. Example exponential decay curves are fit to the data.

A.4.1. Non-Amputee Adaptation

During *no perturbation* trials, Euclidean distance was unchanged from the baseline trials, as expected [**Figure 24a**]. After the system dynamics were perturbed, there was a trend to an increase in Euclidean distance error during the first few perturbed trials, which did not differ between feedback conditions. Even after many trials, errors did not converge back to baseline values. There

were no clear trends during either of the generalization blocks, which may indicate that subjects were capable of adapting their control over the entire movement space.

As with Euclidean distance, during *no perturbation* trials the average cursor speed was unchanged from baseline trials [**Figure 24b**]. After the system dynamics were perturbed, cursor speed increased due to the reduced damping term in the dynamics of the limb. This speed increase appears to be greater in the absence of audio feedback, as shown both in the figure and in the increased exponential fit gains. Similar to Euclidean distance error, these increases lessened over time, generally returning to baseline levels after a few trials. There appeared to be a second spike in cursor speed during initial reaches towards the *left generalization* target, with similar adaptation profiles as subjects adjusted their movements; furthermore, this error spike appears smaller during audio feedback blocks. There was no clear increase in speed during *right generalization* trials.

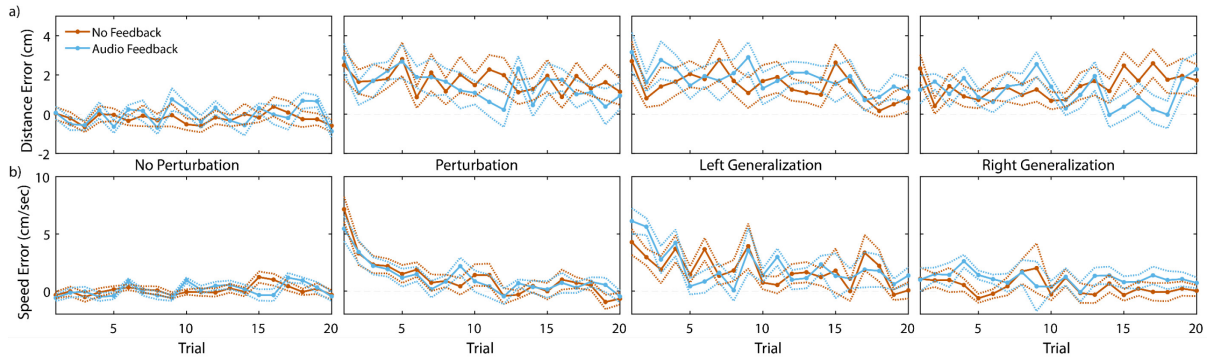

Figure 24. Pilot Baseline-Adjusted Non-Amputee Performance during Testing Blocks.

Baseline values are subtracted from raw metrics. Bold lines represent trial mean and dashed lines represent trial standard error, averaged across subjects. No perturbation and perturbation trials are reaches towards the far-right target. Left and right generalization trials are reaches towards the top-left and top-right target, respectively. (a) Baseline-adjusted Euclidean distance during testing blocks. (b) Baseline-adjusted cursor speed during testing blocks.

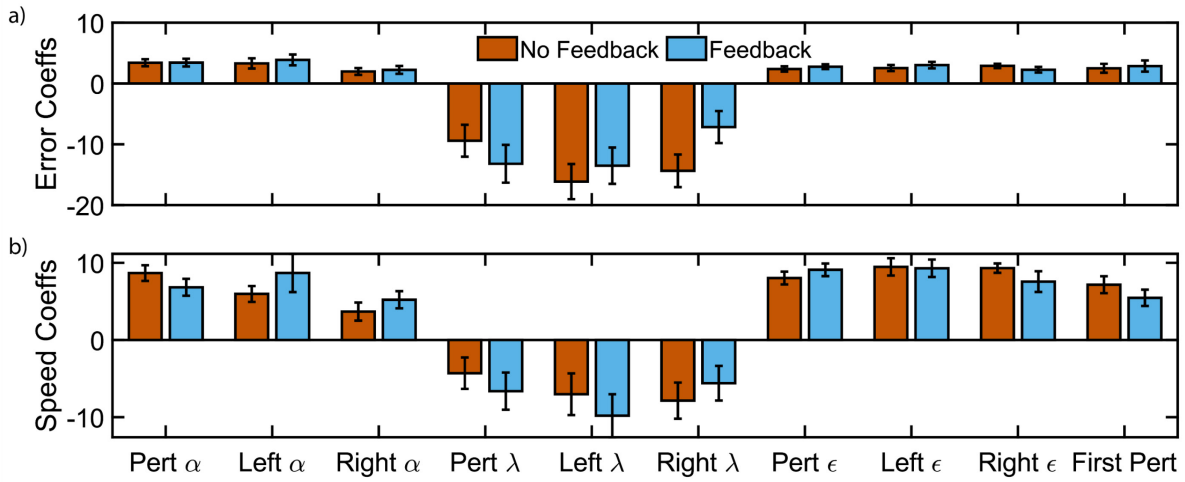

Figure 25. Pilot Non-Amputee Adaptation Coefficients and Perturbation Response.

Average exponential decay coefficients for gain (α), decay rate (λ), and offset (ε), as well as the values for the first perturbation trial, are shown. Error bars show standard error. (a) Coefficients and initial value for Euclidean distance error. (b) Coefficients and initial value for average speed.

A.4.2. Transhumeral Amputee Performance

Errors were generally more variable for transhumeral amputee subject than for non-amputee subjects [**Figure 26a**]. An increase in error was still visible after system dynamics are perturbed, however no clear adaptation trends appear.

Transhumeral amputee subjects also showed stable cursor speed during *no perturbation* trials [**Figure 26b**]. However, unlike non-amputee subjects, transhumeral amputee subjects showed no clear adaptation behavior following perturbation.

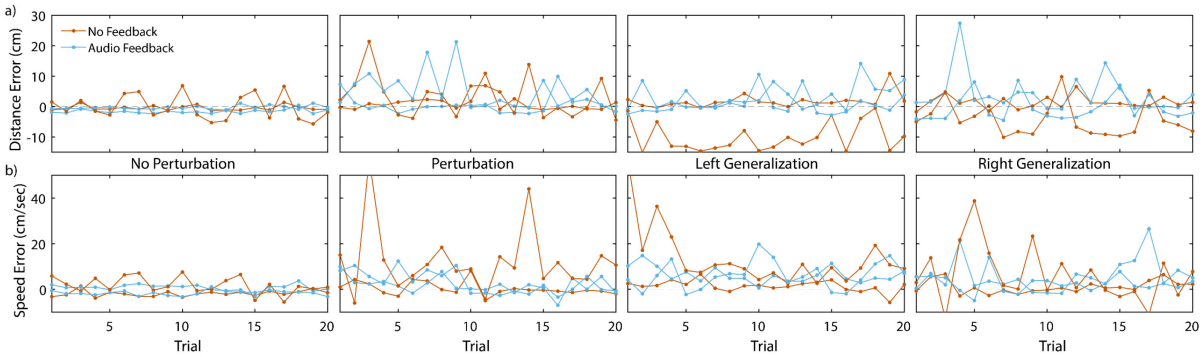

Figure 26. Pilot Transhumeral Amputee Baseline-Adjusted Performance during testing.

Baseline values are subtracted from raw metrics. Each line represents error from one transhumeral amputee subject. No perturbation and perturbation trials are reaches towards the far-right target. Left and right generalization trials are reaches towards the top-left and top-right target, respectively. (a) Baseline-adjusted Euclidean distance during testing blocks. (b) Baseline-adjusted cursor speed during testing blocks.

Figure 27 below shows the exponential decay coefficients fit to the perturbed trials for transhumeral amputee subjects. Only two subjects were recruited for this pilot study, so no statistical analyses were run. The variability of the reaches themselves extend to the variability of the exponential decay coefficients. Aside from these coefficients, no consistent differences were seen in the initial increase in error upon perturbation.

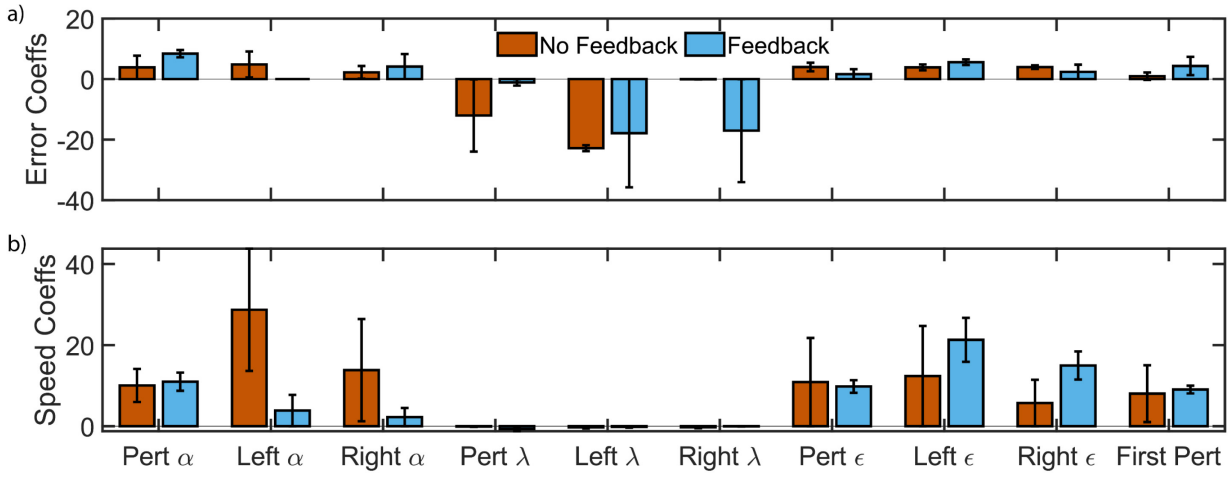

Figure 27. Pilot Transhumeral Amputee Adaptation Coefficients and Perturbation Response

Average exponential decay coefficients for gain (α), decay rate (λ), and offset (ε), as well as the values for the first perturbation trial, are shown. Error bars show standard error. (a) Coefficients and initial value for Euclidean distance error. (b) Coefficients and initial value for average speed.

A.5. Discussion

Two of the most desirable features of trans-humeral prostheses are the simultaneous and proportional control of multiple joints to perform coordinated movements, and a reduction in visual attention required to perform certain functions (Atkins, Heard and Donovan, 1996). Sensory feedback and proprioception of the prosthetic limb are key components to addressing these limitations, but restoring these senses remains a major challenge facing myoelectric prostheses (Childress, 1980). Closed-loop control for prosthetic devices is a vital part of correcting for errors, and plays an even greater role in learning unintuitive or arbitrary control mappings (Ison, Antuvan and Artemiadis, 2014). If sensory feedback provides the same information as intact senses (such as vision) but with greater uncertainty, this redundant feedback has little effect on the final state estimate (Körding and Wolpert, 2004).

In this study, we investigated a joint- and velocity-based feedback paradigm's effect on subjects' myoelectric control of a 2-DoF virtual limb to determine if sensory feedback provided in a local reference frame complemented visual feedback provided in a global reference frame. The dynamics of the virtual limb were perturbed during use to calculate performance impact and adaptation to the new dynamics (*perturbation* trials), and to determine if this adaptation was in a local or global frame (*generalization* trials).

These preliminary results suggest that, while subjects were able to adapt both their movement errors and movement speed to the perturbed dynamics of the virtual limb over time and return to baseline performance, initial speed increases upon perturbation were smaller when audio feedback was present. We theorize that this reduction is because the feedback was providing joint-based and velocity-based, rather than Cartesian-based, information continuously throughout the movement, allowing subjects to identify earlier within the trial that the dynamics were perturbed and facilitated earlier adaptation. This hypothesis is supported by the increase in average speed over the first few *perturbation* trials; because vision is relatively imprecise in determining speed (Stocker and Simoncelli, 2006) compared to position (Ross, 2003), providing separate channel of feedback encoding the velocity of the virtual limb should improve subjects' control over limb velocity. Providing continuous joint- and velocity-based feedback also serves to provide, in essence, an efference copy of control inputs resulting in limb movements. By directly providing this efference copy through a different sensory modality, our feedback paradigm enables subjects to develop a better feedforward model of the prosthesis control (Kawato, 1999), ultimately resulting in an improved ability to adapt to perturbations and to generalize this improvement across the entire workspace.

In our experiment with transhumeral amputee subjects, however, the larger variability in reaching error obfuscates general trends that might otherwise have been uncovered. This variability may be due to large control uncertainty, the complexity of the task, or a combination of these factors.

When asked to provide subjective feedback, several subjects commented that the audio feedback helped them to recognize when they were unintentionally contracting their muscles, allowing them to relax their muscles to prevent the virtual arm from making unintended movements, particularly between trials while waiting for the target to appear. These comments appear to support the results of (Cipriani *et al.*, 2014), who found that humans are capable of integrating feedback of discrete events, such as finger contact with grasped objects, into their sensorimotor control. One can argue that the binary state of muscle activation (below- or above movement threshold), and the corresponding continuous audio feedback (below- or above hearing threshold) are discrete events, and thus subjects may have been incorporating these discrete events in their control of the virtual limb during this study. In addition to the tested hypothesis, there are several other possible benefits of sensory feedback that were not investigated during this study. One such benefit is prosthesis embodiment. Studies have shown that providing sensory feedback with prosthesis use, regardless of modality, can improve the user's embodiment of the prosthesis and make them feel more connected to the device (D'Alonzo, Clemente and Cipriani, 2015; Dosen *et al.*, 2015; Schiefer *et al.*, 2016).

We originally expected that the perturbation would influence the generalization trial performances more than what was observed. We believe that this was likely due to our choice of perturbation. The change in damping uniformly affected the workspace. If we were to have implemented a curl field or other external perturbation (Shadmehr and Mussa-Ivaldi, 1994), we may have found

greater differences at the generalization targets. We also did not expect that subjects would adapt before the first trial was completed. However, upon examining video capture of subjects performing the task, the within trial adaption was apparent.

Sensory feedback remains an expansive field of study with many challenges yet to be overcome. However, addressing these challenges will give us an improved understanding of how humans incorporate multiple sources of sensory inputs, ultimately leading to improved prosthetic devices capable to restoring greater functionality and quality of life.

Appendix B. Modeling Expected Reaching Error and Behaviors from Distribution

Authors: Eric J. Earley, Levi J. Hargrove

B.1. Abstract

Motor adaptation studies can provide insight into how the brain handles ascending and descending neural signals during motor tasks, revealing how neural pathologies affect the capacity to learn and adapt to movement errors. Such studies often involve reaches towards prompted target locations, with adaptation and learning quantified according to Euclidean distance between reach endpoint and target location. This paper describes methods to calculate steady-state error using knowledge of the distribution of univariate, bivariate, and multivariate steady-state reaches. Additionally, in cases where steady-state error is known or estimated, it does not fully describe underlying reach distributions that could be observed at steady-state. Thus, this paper also investigates methods to describe univariate, bivariate, and multivariate steady-state reaching behavior using knowledge of the estimated steady-state error. These methods may yield a clearer understanding of adaptation and steady-state reaching behavior, allowing greater opportunities for inter-study comparison and modeling.

B.2. Introduction

Motor adaptation is the process by which motor errors are gradually reduced over time via modifications of movements on a trial-by-trial basis (Bastian, 2008). This process is critical for learning new tasks, as well as dexterously performing learned tasks. Numerous studies investigate motor adaptation to understand how learning is affected by neural pathologies (Hardwick *et al.*, 2017), sensory feedback (Wei and Körding, 2010; Earley *et al.*, 2017b; Schmitz and Bock, 2017;

Ahmed W. Shehata, Scheme and Sensinger, 2018), and brain-computer interfaces (Reva E. Johnson *et al.*, 2017).

To quantify adaptation, many studies utilize reaching paradigms including side-to-side (Fitts, 1954) and center-out reaches (Fernandes *et al.*, 2014; McDougle, Bond and Taylor, 2017). Subjects typically move a cursor towards a target, attempting to land as close to the target as possible. Errors are calculated as the Euclidean distance between the final cursor position and the target location.

Though error gradually decreases over repeated trials, inherent variability in reaches guarantees errors never converge to zero. Instead, as reach behavior becomes more consistent, errors converge to some positive value. This steady-state error can be estimated from the distribution of cursor positions, defined simply by their mean and (co)variance. This method allows for direct calculation of steady-state error based on steady-state reach behavior in similar studies, or reach behavior as predicted by motor learning models.

The purpose of this paper is to detail methods of calculating the steady-state level of reaching errors during adaptation studies using the distribution of steady-state reaches. These methods provide an alternative to using Monte Carlo methods to approximate steady-state reaching behavior.

Some studies, such as those investigating models of motor learning, simulate reaching task errors over time for different conditions (Huang *et al.*, 2011). In these cases, steady-state error remains a somewhat arbitrary metric and does not describe all aspects of reaching behavior; however, it is possible to use steady-state error to estimate the mean and (co)variance of steady-state reaches.

In this paper we also explore the inverse process of describing the expected reaching behavior at convergence using steady-state error. Both processes are described in three categories of reaching tasks: univariate reaches, bivariate reaches, and generalized multivariate reaches.

B.3. Methods

B.3.1. Univariate Normal Reaches

We start with the simplest reaching tasks: univariate, or 1-dimensional reaching tasks. These include experimental protocol such as oscillating side-to-side reaches (Fitts, 1954) and cursor movement along a circular track (Reva E. Johnson *et al.*, 2017). In these tasks, error (ε) is defined as the absolute value of the distance between the cursor and the target, and steady-state error (ε_∞) is defined as the average error achieved when the distribution of reaches has stabilized (Blustein *et al.*, 2018). Even if this distribution is centered over the target, the average error cannot be zero unless variance is also zero.

Errors for univariate reaches are described by the folded normal distribution (Leone, Nelson and Nottingham, 1961). Given a univariate normal distribution $X \sim N(\mu, \sigma^2)$ with probability density function (PDF) $f(x|\mu, \sigma^2)$, the PDF of the folded normal distribution is defined as:

$$f_f(x|\mu, \sigma^2) = \frac{1}{\sigma\sqrt{2\pi}}\left(e^{-\frac{(x-\mu)^2}{2\sigma^2}} + e^{-\frac{(x+\mu)^2}{2\sigma^2}}\right), x \geq 0 \tag{16}$$

where μ and σ^2 are the mean and variance of the underlying normal distribution, respectively. Simply, the likelihood of negative values is added to the likelihood of their corresponding positive values.

Figure 28 shows the relationship between the normal PDF and the folded normal PDF. Importantly, it shows that the mean of the folded normal distribution is always greater than that of the underlying distribution. This mean is calculated as:

$$\mu_f = \varepsilon_\infty = \sigma\sqrt{\frac{2}{\pi}}e^{\frac{-\mu^2}{2\sigma^2}} + \mu\left(1 - 2\Phi\left(\frac{-\mu}{\sigma}\right)\right) \tag{17}$$

where $\Phi(x)$ is the standard normal cumulative density function (CDF) $F(x|0,1)$ (Leone, Nelson and Nottingham, 1961). This mean represents the average error of reaches following the underlying distribution. In other words, it is the same as the expected steady-state error. Likewise, the variance of steady-state errors is calculated as:

$${\sigma_f}^2 = \mu^2 + \sigma^2 - {\mu_f}^2 \tag{18}$$

In summary, given a mean and variance of steady-state reaches, the mean and variance of reach errors can be explicitly calculated.

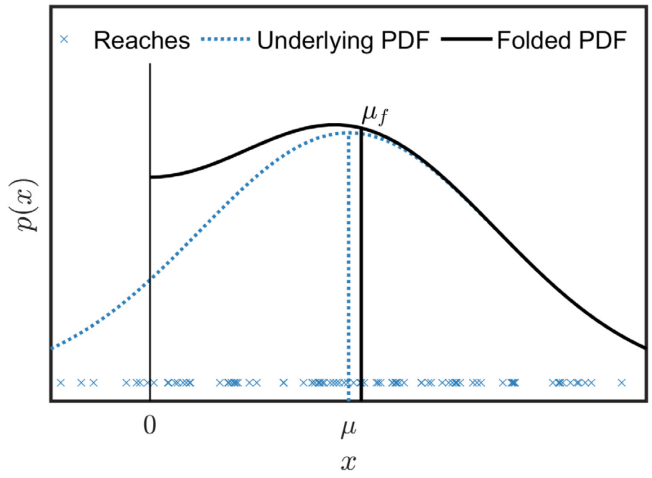

Figure 28. Univariate Folded Normal PDF.

1D reaches (blue x) are normally distributed (blue line), but the absolute error is distributed according to a folded normal PDF (black line). As a result, $\mu < \mu_f$

A special case of the folded normal distribution, known as the half-normal distribution, arises when the mean of steady-state reaches is also the position of the target (Leone, Nelson and Nottingham, 1961). Solving (16) for $\mu = 0$, the PDF of the half-normal distribution is defined as:

$$f_h(x) = \frac{\sqrt{2}}{\sigma\sqrt{\pi}} e^{-\frac{x^2}{2\sigma^2}}, x \geq 0 \tag{19}$$

Solving (17) and (18) for $\mu = 0$, the steady-state error for reaches centered over the target is calculated as:

$$\mu_h = \varepsilon_\infty = \sigma\sqrt{\frac{2}{\pi}} \tag{20}$$

and the variance of these errors is calculated as:

$$\sigma_h{}^2 = \sigma^2\left(1 - \frac{2}{\pi}\right) \tag{21}$$

This distribution can be used to describe a potential best-case scenario, where reaching errors are solely attributed to inherent variability in reaches.

Rearranging (20) to solve for σ^2 yields an explicit calculation of variance of steady-state reaches, given an estimated steady-state error ε_∞ and assuming $\mu = 0$:

$$\sigma^2 = \frac{\pi}{2}\varepsilon_\infty{}^2 \tag{22}$$

Though (20) and (21) provide explicit formulae to describe steady-state behavior, (17) and (18) cannot be rearranged in provide an analytical solution for reach behavior at steady-state. However, numerical solutions can reveal the valid combinations of μ and σ^2 for a given ε_∞ or $\sigma_f{}^2$. Some possible solutions are detailed in **Section B.4.1**.

B.3.2. Bivariate Normal Reaches

Having discussed the simplest reaching tasks, we now move to perhaps the most common task in testing motor adaptation – the center-out reaching task (Fernandes *et al.*, 2014; McDougle, Bond and Taylor, 2017). Like univariate reaches, errors in reach are calculated as the Euclidean distance between the cursor and the target. If bivariate reaches are distributed according to a bivariate normal distribution $X \sim N_2(\mu, \Sigma)$ with PDF $f(x|\mu, \Sigma)$, defined by mean μ and covariance matrix Σ, the PDF of absolute reach locations can be calculated using a bivariate folded normal distribution (Psarakis and Panaretos, 2000), as can the mean reach location (Kan and Robotti, 2017). **Figure 29** shows the relationship between the bivariate normal PDF and the bivariate folded normal PDF.

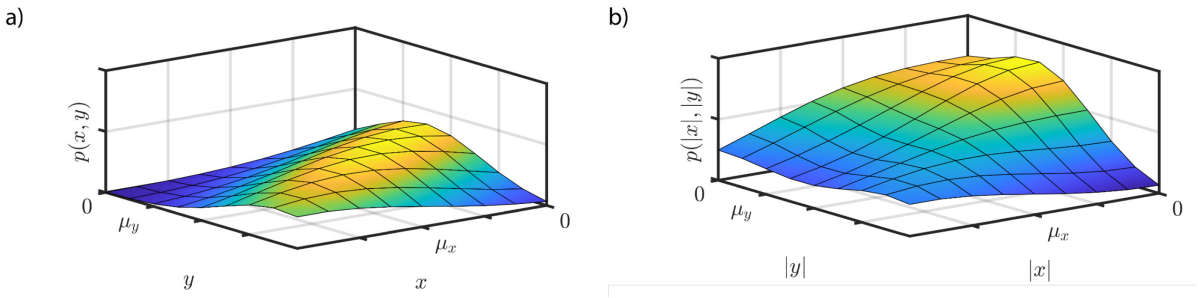

Figure 29. Bivariate Folded Normal PDF.

(a) 2D reaches are bivariate normally distributed. (b) The absolute positions of 2D reaches are distributed according to a bivariate folded normal PDF.

Here, reaching errors are quantified via the Euclidean distance, which is constrained to positive values. However, although we can calculate the mean reach of a bivariate folded normal PDF, calculating the Euclidean distance between the origin and the mean reach underestimates the mean error of all reaches, as demonstrated by Jensen's inequality (Jensen, 1906):

$$\sqrt{E[X_1]^2 + E[X_2]^2} \leq E\left[\sqrt{{X_1}^2 + {X_2}^2}\right] \tag{23}$$

$E[X]$ is the expected value of bivariate random variable $X \sim N_2(\mu, \Sigma)$, defined as:

$$E[X] = \int_{-\infty}^{\infty} xF(x|\mu, \Sigma)\, dx \tag{24}$$

where $F(x|\mu, \Sigma)$ is the CDF of X. It is thus necessary to directly calculate the expected value of the Euclidean distance from the bivariate normal PDF, requiring the following theorem (Papoulis, 1965):

$$E[g(X)] = \int_{-\infty}^{\infty} g(x) f(x|\mu, \Sigma)\, dx \tag{25}$$

Applying (25) to Euclidean distance yields the expected error:

$$E\left[\sqrt{{X_1}^2 + {X_2}^2}\right] = \int_{-\infty}^{\infty} \int_{-\infty}^{\infty} \sqrt{{x_1}^2 + {x_2}^2} f(x|\mu, \Sigma)\, dx_2\, dx_1 \tag{26}$$

Furthermore, the expected variance of X is defined as (Papoulis, 1965):

$$Var(X) = E[X^2] - E[X]^2 \tag{27}$$

Applying (25) to (27) yields the expected variance of reaching errors:

$$Var\left(\sqrt{{X_1}^2 + {X_2}^2}\right) = E\left[{X_1}^2 + {X_2}^2\right] - E\left[\sqrt{{X_1}^2 + {X_2}^2}\right]^2 \tag{28}$$

$$E\left[{X_1}^2 + {X_2}^2\right] = \int_{-\infty}^{\infty} \int_{-\infty}^{\infty} ({x_1}^2 + {x_2}^2) f(x|\mu, \Sigma)\, dx_2\, dx_1 \tag{29}$$

Numerical integration allows for calculation of the expected mean and variance of Euclidean distance reaching errors following any arbitrary mean and covariance. However, solutions for reach behavior given an estimated steady-state error are not unique. Some possible solutions assuming independent random variables are detailed in **Section B.4.2**.

B.3.3. Multivariate Normal Reaches

Multivariate reaching tasks may involve endpoint reaching in three dimensions, endpoint or joint orientation, end effector state, or some combination thereof. Like the bivariate case, formulae have been proposed for the multivariate folded normal distribution (Chakraborty and Chatterjee, 2013; Murthy, 2015) and their mean (Kan and Robotti, 2017). Also like the bivariate case, the folded normal distribution cannot be used to calculate expected error, and it is necessary to directly calculate the expected error from the multivariate PDF.

The derivation of expected error is simply the multivariate extension of (26). Given a k-dimensional multivariate normal distribution $X \sim N_k(\mu, \Sigma)$, the expected error is calculated from the multivariate normal PDF $f(x|\mu, \Sigma)$ as follows:

$$E\left[\sqrt{\sum_{i=1}^{k} {X_i}^2}\right] = \int_{-\infty}^{\infty} \dots \int_{-\infty}^{\infty} \sqrt{\sum_{i=1}^{k} {x_i}^2}\, f(x|\mu, \Sigma)\, dx_k \dots dx_1 \tag{30}$$

And the expected variance of errors is calculated as:

$$Var\left(\sqrt{\sum_{i=1}^{k} {X_i}^2}\right) = E\left[\sum_{i=1}^{k} {X_i}^2\right] - E\left[\sqrt{\sum_{i=1}^{k} {X_i}^2}\right]^2 \tag{31}$$

$$E\left[\sum_{i=1}^{k} {X_i}^2\right] = \int_{-\infty}^{\infty} \dots \int_{-\infty}^{\infty} \left(\sum_{i=1}^{k} {x_i}^2\right) f(x|\mu, \Sigma)\, dx_k \dots dx_1 \tag{32}$$

As with the bivariate case, solutions for reach behavior given an estimated steady-state error are not unique.

B.3.4. Validation

To validate the approaches presented in this paper to calculate expected reach error, given arbitrary reach distributions, proposed solutions were compared to solutions estimated via Monte Carlo methods. MATLAB code validating these methods are freely available for download on the Open Science Framework (Earley, 2019).

For univariate validation, 10,000 conditions were tested, consisting of 100 values for μ evenly distributed between 0 and 10, and 100 values for σ evenly distributed between 0.25 and 10. For each condition, 1,000,000 data were drawn from a univariate normal distribution $X \sim N(\mu, \sigma^2)$. The mean and variance of the error between generated data and the origin were calculated, and the difference between the Monte Carlo solution and those obtained from equations (17) and (18) were normalized by the mean error of the simulated data.

For bivariate validation, 160,000 conditions were tested, consisting of 20 values each for μ_x and μ_y evenly distributed between 0 and 10, 20 values for σ_x evenly distributed between 0.25 and 10, and 20 values for the ratio $\frac{\sigma_y}{\sigma_x}$ between 1 and 10. For each condition, 1,000,000 data were drawn from a bivariate normal distribution $X \sim N_2(\mu, \Sigma)$. The mean and variance of the Euclidean distance error between generated data and the origin were calculated, and the difference between the Monte Carlo solutions and those obtained from equations (26) and (28) were normalized by the mean error of the simulated data. Validation results are presented in **Section B.4.3**.

B.4. Results

This section covers some numerical solutions of the univariate and bivariate reaches as detailed in **Sections B.3.1** and **B.3.2**, as well as the validations detailed in **Section B.3.4**.

B.4.1. Univariate Normal Reaches

There are two conditions for which steady-state reach behavior can be determined analytically. If the mean of reaches is 0 (i.e. centered over the target), the variance of the underlying distribution given an estimated steady-state reaching error is calculated using (22). Alternatively, if the variance of reaches is 0, the mean of the underlying distribution is the same as the estimated reaching error. However, solving (17) for parameters of the underlying distribution requires numerical methods. **Figure 30** shows the valid combinations of μ and σ^2 for a given ε_∞. Importantly, it shows that a linear increase in ε_∞ results in an equivalent linear increase in maximum μ, but an exponential increase in maximum σ^2.

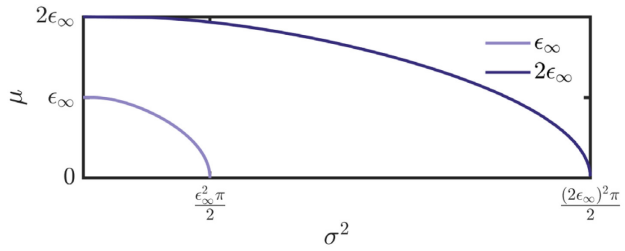

Figure 30. Visualization of Possible Univariate Reaching Behaviors.

Plot shows valid means and variances of the underlying normal distribution resulting in an estimated steady-state error (light), as well as how these valid combinations change when steady-state error is doubled (dark).

B.4.2. Bivariate Normal Reaches

For bivariate steady-state reaches, (26) contains 6 parameters which can affect estimated error: μ_x, μ_y, σ_{xx}, σ_{yy}, σ_{xy}, and σ_{yx}. Rotating the basis vectors to align with the eigenvectors of the underlying distribution sets $\sigma_{xy} = 0$ and $\sigma_{yx} = 0$ and removes redundant solutions for these two parameters, reducing the possibility space to 4 parameters. For a given ε_∞, **Figure 31a** shows

possible distribution means with defined variances, while **Figure 31b** shows possible distribution variances with defined means. Importantly, the dashed black lines show maximum possible values corresponding to zero variance (**Figure 31a**) and zero mean (**Figure 31b**). **Figure 31** also shows diagonal symmetry when variances or means are constrained to be equivalent, but asymmetry otherwise.

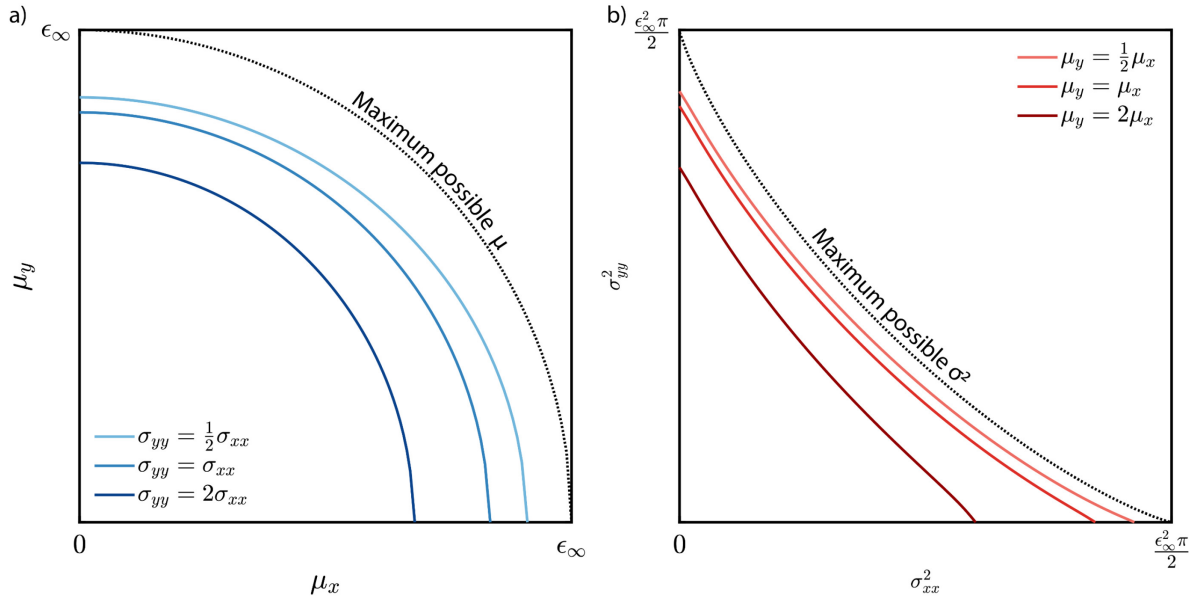

Figure 31. Visualization of Possible Bivariate Reaching Behaviors.

Some common assumptions are proposed to visualize valid mean and variance combinations (a) Valid means of the underlying normal distribution resulting in an estimated steady-state error for ${\sigma_{xx}}^2 = \frac{\varepsilon_\infty}{4}$. The maximum possible means are achieved when ${\sigma_{xx}}^2 = {\sigma_{yy}}^2 = 0$ (b) Valid variances of the underlying normal distribution resulting in an estimated steady-state error for $\mu_x = \frac{\varepsilon_\infty}{4}$. The maximum possible variances are achieved when ${\mu_x}^2 = {\mu_y}^2 = 0$.

B.4.3. Validation

For univariate reaches, the mean error for data generated via Monte Carlo methods was within 0.062% of that calculated by equation (17), and the variance of error was within 0.457% of that calculated by equation (18).

For bivariate reaches, the mean error for data generated via Monte Carlo methods was within 0.040% of that calculated by equation (26), and the variance of error was within 0.260% of that calculated by equation (28).

Taken together, reaching error and variance estimates procured via Monte Carlo methods closely matched those obtained by the methods proposed in this paper.

B.5. Discussion

In this paper, we explore methods for estimating steady-state error during univariate, bivariate, and multivariate reaching tasks using the distribution of steady-state reaches. We also describe the inverse process, providing guidelines for estimating steady-state reaching behavior given an estimated steady-state error. Together, these may yield a clearer picture of adaptation and steady-state reaching behavior.

The methods presented in this paper can also be modified based on predicted changes in reach behavior. For example, it is possible to calculate how errors will change if the distribution means shift, or if the covariance of reaches changes. Furthermore, applying various assumptions to reaching behavior can reveal the maxima of means or covariances, given a particular reaching error. This may provide insight into how changes in reaching error (for example, as a result of a visuomotor rotation) impacts reaching behavior.

The proposed methods are demonstrated and validated assuming normally-distributed reaching behavior. However, these methods are generalizable to any probability distribution with a known PDF. Thus, they are versatile for use in studies and simulations which do not constrain reaching behavior to normal distributions.

In addition to the methods presented here, existing distributions may be valid in specific cases. For example, the Rayleigh distribution requires two independent random variables with zero mean and equal variance, as does its parent Chi-squared distribution. However, these do not generalize to arbitrary distribution means and covariances, whereas the methods described in this paper can handle reach distributions of any size, orientation, and dimensionality.

It is possible to estimate steady-state error through direct calculation of previously-collected steady-state data, or by using Monte Carlo methods. However, applicable steady-state data may not be available for the specific study at hand. Although Monte Carlo methods are viable for estimating steady-state error, inverting them to provide insight into steady-state reaching behavior given estimated steady-state error may be difficult.

The methods described in this paper provide a mathematical solution to estimating steady-state error of reaches given their probability distribution, and vice versa. Solutions derived from these methods provide an alternative to Monte Carlo methods. Furthermore, they may be used to gain a clearer understanding of adaptation and steady-state reaching behavior, ultimately allowing greater opportunities for inter-study comparison and modeling.

Appendix C. Hierarchical Kalman Filter Model

C.1. Introduction

The Control Bottleneck Index (CBI) was developed through the Defense Advanced Research Projects Agency (DARPA)'s Hand Proprioception and Touch Interfaces (HAPTIX) program by Drs. Dan Blustein and Jon Sensinger. The method seeks to model adaptation by understanding corrupting noise from motor control and sensory feedback, and identifying bottlenecks in the control loop.

C.2. Methods

The CBI method assumes a hierarchical Kalman model of trial-by-trial adaptation (Reva E. Johnson *et al.*, 2017).

C.2.1. Nomenclature

To ensure clarity in notation, the following nomenclature will be used:

- Discrete trials are indicated by superscript indexes (x^k)
- Estimates are denoted by hats ($\hat{B}$)
- Priors are denoted by bars ($\bar{P}$)
- Prior estimates are denoted by a bar and a hat ($\hat{\bar{x}}$)

C.2.2. Variables

Table VI describes each variable in the hierarchical Kalman model and provides example units for a theoretical force (*N*)-to-position (*cm*) reaching task.

Table VI. Hierarchical Kalman Model Variables.

Variable	Description	Example Units
x	State	*cm*
B	Internal model	*cm/N*
x_T	Target	*cm*
u^k	Motor command	*N*
P^k	Internal model uncertainty	cm^2
Q	Control uncertainty	cm^2
R	Sensory uncertainty	cm^2
K^k	Kalman gain	-
${P_p}^k$	Internal model uncertainty	cm^2/N^2
Q_p	Internal model noise	cm^2/N^2
${K_p}^k$	Internal model Kalman gain	*1/N*
H_p	Internal model sensitivity	*N*
${R_p}^k$	Internal model sensory uncertainty	cm^2

C.2.3. Hierarchical Models

The first model describes state control and estimation:

$$\hat{\bar{x}}^k = \hat{B}^k u^k = x_T \tag{33}$$

$$\bar{P}^k = {H_p}^2 {P_p}^k + Q \tag{34}$$

$${x_u}^k = B u^k \tag{35}$$

$${x_m}^k = {x_u}^k + \epsilon(0, Q) \tag{36}$$

$${x_s}^k = {x_m}^k + \epsilon(0, R) \tag{37}$$

$${x_\varepsilon}^k = {x_s}^k - \hat{\bar{x}}^k \tag{38}$$

$$K^k = \frac{\bar{P}^k}{\bar{P}^k + R} \tag{39}$$

$$\hat{x}^k = \hat{\bar{x}}^k + K^k(x_\varepsilon{}^k) \tag{40}$$

$$P^k = \bar{P}^k(I - K^k) \tag{41}$$

The second model describes parameter estimation, or the update of the internal model:

$$\bar{P}_p{}^{k+1} = P_p{}^k + Q_p \tag{42}$$

$$R_p{}^{k+1} = Q + P^k \tag{43}$$

$$K_p{}^{k+1} = \frac{\bar{P}_p{}^{k+1} H_p}{H_p{}^2 \bar{P}_p{}^{k+1} + R_p{}^{k+1}} \tag{44}$$

$$\hat{B}^{k+1} = \hat{B}^k + K^k K_p{}^{k+1}(x_\varepsilon{}^k) \tag{45}$$

$$P_p{}^k = \bar{P}_p{}^{k+1}(I - H_p K^k K_p{}^{k+1}) \tag{46}$$

C.3. Adaptation Calculation

Control uncertainty (Q) is time invariant, thus this can be estimated from reach data by fitting a regression between data and its time-shifted copy.

The estimated internal model adaptation rate ($\widehat{H_p K K_p}$) can be estimated via the following equation:

$$\widehat{H_p K K_p} = \frac{H_p ff B_{x_T} \sqrt{2var(x_{m0}) - 2Q\left(1 + \widehat{H_p K K_p}\right) - 2cov(x_{m0}, x_{m1})}}{[x^4 \widehat{_{m0}x^2}_{m1}] - 2x_T[x^3 \widehat{_{m0}x^2}_{m1}] + x^2{}_T[x^2 \widehat{_{m0}x^2}_{m1}] - \left([x^2 \widehat{_{m0}x}_{m1}] - x_T[\widehat{x_{m0}x_{m1}}]\right)} \tag{47}$$

where ff is assumed to have a Gaussian form factor $\sqrt{2/\pi}$ and $\widehat{H_p K K_p}$ can be iterated via a grid search to find the adaptation rate prior estimate that results in the smallest error between the prior and posterior estimates.

C.4. Effect of free variables

In this model, there are three free variables: Q (control uncertainty), R (sensory uncertainty), and ${Q_p}^*$ (minimum internal model noise). I wanted to determine how increasing each variable would affect internal model uncertainty (${P_p}^k$), Kalman gain (K), internal model Kalman gain (K_p), and adaptation ($\widehat{H_p K K_p}$). To do this, I simulated 1000 trials, defining trial 100 as the cutoff for steady-state. The position of the target was 30 cm, and the true internal model gain was 30 cm/N. The initial internal model estimate and uncertainty were 28 cm/N and 10 cm^2/N^2, respectively. The nominal values for each variable was 0.001.

To determine the effect of changing a variable, I ran the model three sets of times:

1. Variable at nominal value
2. Variable at ¼ nominal value
3. Variable at 4x nominal value

For each condition, I tweaked the values of the other two variables to cover a variable space of 1/5 to 5x the nominal value. This created a grid for which I could calculate the outcome of interest. To determine the effects of each variable, I subtracted the outcome of interest for conditions (2) and (3) from that of condition (1) and plotted the resulting surface.

Figure 32 shows the effects of changing control uncertainty Q. An increase in control uncertainty resulted in the following changes:

- Increased internal model uncertainty ${P_p}^k$
- Increased Kalman gain K

- Decreased internal model Kalman gain K_p
- Decreased adaptation rate $\widehat{H_pKK_p}$

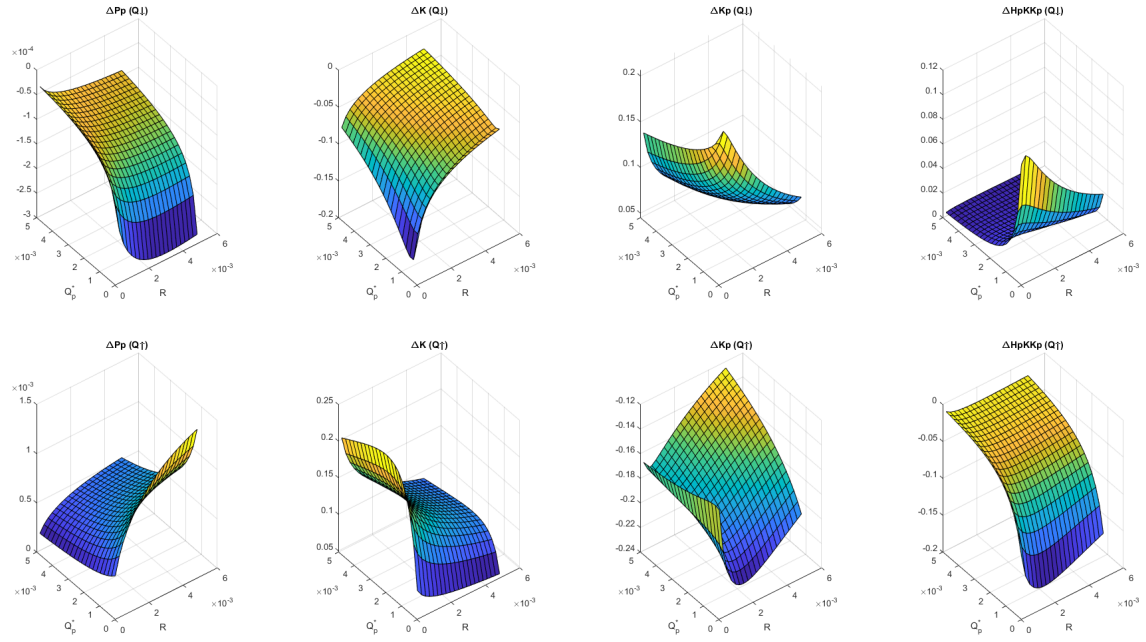

Figure 32. Effect of Control Uncertainty on CBI Outcomes.

Top and bottom rows show the change in outcomes when Q changes from 0.001 to 0.00025 (top) and 0.004 (bottom). R ranges from 0.0002 to 0.005. $Q_p{}^*$ ranges from 0.0002 to 0.005.

Figure 33 shows the effects of changing sensory uncertainty R. An increase in sensory uncertainty resulted in the following changes:

- Increased internal model uncertainty $P_p{}^k$
- Decreased Kalman gain K
- Decreased internal model Kalman gain K_p
- Decreased adaptation rate $\widehat{H_pKK_p}$

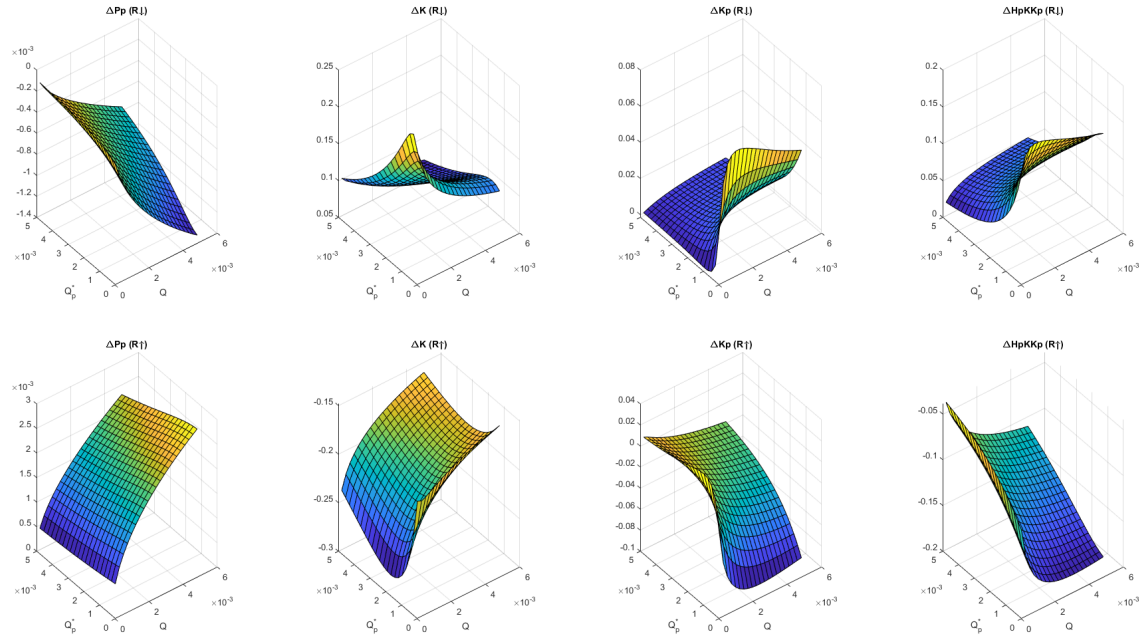

Figure 33. Effect of Sensory Uncertainty on CBI Outcomes.

Top and bottom rows show the change in outcomes when R changes from 0.001 to 0.00025 (top) and 0.004 (bottom). Q ranges from 0.0002 to 0.005. ${Q_p}^*$ ranges from 0.0002 to 0.005.

Figure 34 shows the effects of changing minimum internal model noise ${Q_p}^*$. An increase in minimum internal model noise resulted in the following changes:

- Increased internal model uncertainty ${P_p}^k$
- Increased Kalman gain K
- Increased internal model Kalman gain K_p
- Increased adaptation rate $\widehat{H_p K K_p}$

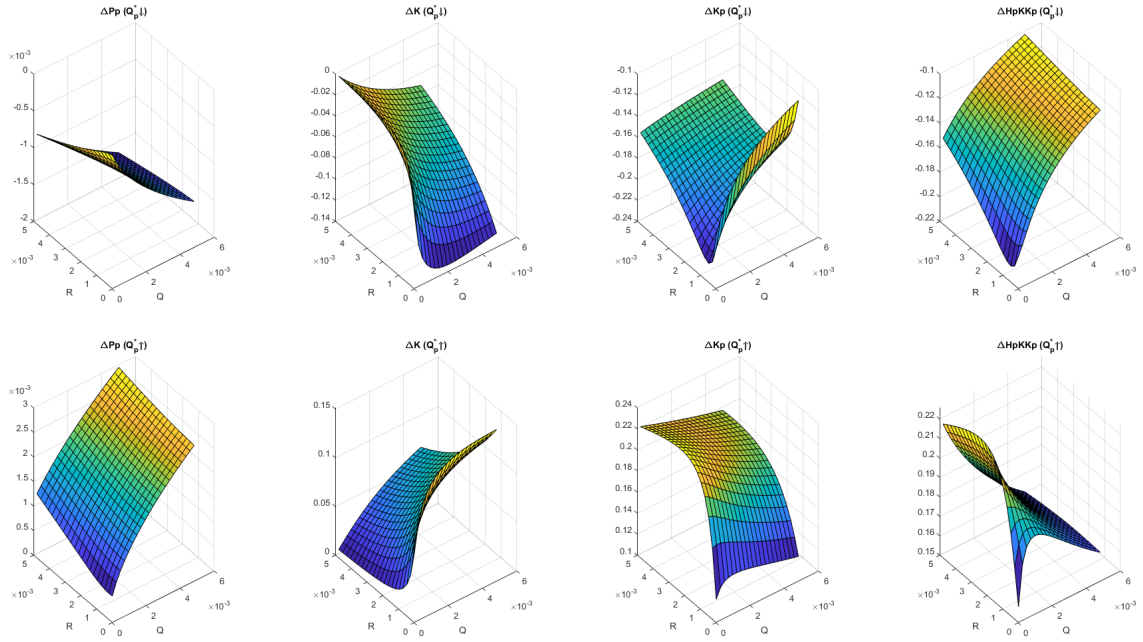

Figure 34. Effect of Minimum Internal Model Noise on CBI Outcomes.

Top and bottom rows show the change in outcomes when $Q_p{}^*$ changes from 0.001 to 0.00025 (top) and 0.004 (bottom). Q ranges from 0.0002 to 0.005. R ranges from 0.0002 to 0.005.

These simulations demonstrate that internal model adaptation rate is negatively correlated with both control and sensory uncertainty.